PART 8

Climate, Environment and Dating

'Star Carr lies in the Danelaw, the area of eastern England historically settled by the Vikings. "Star Carr" apparently derives from the Danish star kjær, "Sedge Fen", as Godwin also noted.'
(Rowley-Conwy 2010, 77)

CHAPTER 17

Dating the Archaeology and Environment of the Star Carr Embayment

Alex Bayliss, Barry Taylor, Christopher Bronk Ramsey, Elaine Dunbar, Bernd Kromer, Michael Bamforth, Chantal Conneller, Ben Elliot, Becky Knight and Nicky Milner

Introduction

Chronology has always been a key issue in the interpretation of Star Carr, both in terms of the age of the site and the period of time over which it was occupied. The ways in which this issue has been addressed have varied in the years since Clark's initial excavations, as subsequent researchers have taken advantage of methodological and interpretive advances in radiocarbon dating. However, all researchers have been faced with a similar set of problems. Firstly, that the bulk of the material record from the site was rendered un-datable by the conservation treatment used by Clark, and secondly, that the relationship between this material and the stratigraphy of the site could never be properly demonstrated.

The new excavations at Star Carr have provided an opportunity to address both of these issues by collecting a large number of new dating samples of known stratigraphic provenance. This enables us to date newly excavated material (thus avoiding the issue of past conservation treatments) and to combine the calibrated radiocarbon dates with the stratigraphic sequence in a formal Bayesian statistical model. The analysis of this new data has enabled us to construct a more precise chronology for human activity and the local environment at Star Carr.

This chapter focuses on the construction of the chronicle of what happened when around the Star Carr embayment during the early centuries of the Mesolithic. It does not attempt to untangle the web of causality, connections and consequence that creates narrative from the mere sequence and tempo of beads on the string (Ingold 1993, 187). This is undertaken in Chapter 9.

Previous dating

The first attempts to establish a chronology for Star Carr drew upon a broad range of methods to determine both the age of the site and the duration of occupation. With radiocarbon dating still in its infancy, Clark relied largely on

Figure 17 (page 31): Bulrush and willow, Christleton, Cheshire (Copyright Barry Taylor, CC BY-NC 4.0).

How to cite this book chapter:
Bayliss, A., Taylor, B., Ramsey, C. B., Dunbar, E., Kromer, B., Bamforth, M., Conneller, C., Elliot, B., Knight, B. and Milner, N. 2018. Dating the Archaeology and Environment of the Star Carr Embayment. In: Milner, N., Conneller, C. and Taylor, B. (eds.) *Star Carr Volume 2: Studies in Technology, Subsistence and Environment*, pp. 33–112. York: White Rose University Press. DOI: https://doi.org/10.22599/book2.c. Licence: CC BY-NC 4.0

the more-established method of pollen zonation to date the site in relation to the known sequence of vegetation succession across Northern Europe after the end of the Last Glacial Maximum. Based on Walker and Godwin's pollen analysis, this placed the occupation of Star Carr at the end of the Preboreal (Godwin's pollen Zone IV), making it earlier than typologically similar sites in Northern Europe (Clark 1954, 179). This was supported by two of the first radiocarbon measurements ever undertaken on British archaeological materials, on pieces of the brushwood platform recorded during the excavations, which fell within the known ages of the European Preboreal (Clark 1954, 12).

Different approaches were taken to establish the duration of activity at the site. Here, Clark drew upon the vertical distribution of artefacts and charcoal layers in the peat, and typological differences in the form of the barbed points to argue that the site had been occupied at least twice (Clark 1954, 9), whilst the estimated calorific value of the animal remains suggested a total duration of no more than six and a half years.

Although the application of radiocarbon dating become more widespread in succeeding decades, attempts to use it to establish a more precise chronology for Star Carr were hampered by the conservation methods used by Clark, which had contaminated the artefact and faunal assemblages to such an extent that they could not be dated (Dark et al. 2006, 186). However, new excavations and associated palaeoenvironmental investigations carried out by the Vale of Pickering Research Trust provided an opportunity to establish an absolute chronology, both for the human occupation of the site and its environmental history. In 1985, the Trust carried out excavations to the east of Clark's trenches in order to investigate the environmental setting of the site, during the course of which they recorded a small assemblage of faunal material and part of a wooden platform (Cloutman and Smith 1988). As this material had never been conserved, it provided the first opportunity to date directly material culture from Star Carr. To this end, AMS dates were also obtained on two pieces of bone and antler, a fragment of charcoal, and a sample from the timber platform, along with conventional dates on the sediments from around these and several other artefacts (Cloutman and Smith 1988, 42). Bulk samples of peat and a piece of charcoal from a series of four pollen profiles were also dated, and the results brought together to establish the chronology for the changing environments at the site and the episodes of human occupation (Cloutman and Smith 1988).

Unfortunately, as Cloutman and Smith noted, the results of their dating programme were problematic (Cloutman and Smith 1988, 54). To begin with, the samples taken from the base of the pollen profiles appeared to be erroneously old, which Cloutman suggested resulted from the reworking of older material into the basal sediments (Cloutman and Smith 1988, 45). What is more, the timber platform was several centuries younger than the other artefacts, even though they had been recorded from a similar level, and some of the artefacts were older than the sediment surrounding them (Cloutman and Smith 1988). Whilst Cloutman and Smith argued that may have been caused by the artefacts moving in the peat or that they were already old when they were deposited, the net result was that they were unable to provide a convincing date for occupation at the site or its duration (Cloutman and Smith 1988, 54–55).

In the following years it became clear that a number of methodological issues lay behind these problems. Principal among these was the dating of bulk samples of sediment, which could be contaminated through the inclusion of intrusive, younger material particularly in the form of rootlets (Mellars 1990, 839), or older reworked material (Cloutman and Smith 1988, 45), or the presence of aquatic plant material containing 'old' carbon derived from lake water rather than the atmosphere (Day 1996a, 10–11).

In the absence of a radiocarbon calibration curve covering the Early Holocene, Cloutman and Smith (1988) perforce worked in a 'timescale' of uncalibrated radiocarbon measurements. However, from the late 1980s, it was increasingly apparent that Star Carr dated to a time when measured radiocarbon ages showed no detectable change over a period of several centuries, making it difficult to distinguish different episodes of activity within this 'plateau' (Mellars 1990). High-precision tree-ring calibration was first proposed for this period in 1993 (Kromer and Becker 1993).

In the early 1990s a new programme of palaeoenvironmental investigations provided an opportunity to address these issues (Dark 1998a; Mellars and Dark 1998). Again, dating was undertaken on a vertical sequence of samples from one of the environmental profiles from VP85A (Profile M1), as well as at a lower resolution on a profile taken close to Clark's cutting II (referred to as the Clark Site profile) (Dark 1998a, 142). But this time AMS dates were obtained on terrestrial macrofossils to avoid potential contamination, and 'wiggle matching' was used to overcome the difficulties caused by the plateau in the calibration curve (Dark 1998a). As well as supporting the palaeoenvironmental analysis, these dates provided the backbone for the first reliable calendar chronology for the site.

To begin with, Mellars compared the vertical distribution of the artefacts in VP85A with the dated peat stratigraphy from the environmental sequence and suggested that the assemblage in that trench had been

deposited between c. 8700 and c. 8400 cal BC (Mellars and Dark 1998, 210). This was refined further by the work of Dark, who used evidence for episodes of burning, represented by inputs of micro- and macro-charcoal in the environmental profiles, as a proxy for human activity at the site. As these profiles had been dated, it was possible to estimate the chronological range of these episodes, both by dating the levels in the monolith where they started and ended and by estimating their duration by calculating the sedimentation rate of the deposits from which the charcoal had been recorded (Day and Mellars 1994; Dark 1998a; Dark 2000).

This programme of radiocarbon dating was pioneering, clearly recognising the need to utilise the archaeological or sedimentary sequence of deposits to overcome the emerging issues of radiocarbon calibration in the Early Holocene and addressing complex technical issues in dating the sediments from the Vale of Pickering accurately. However, the initial results were swiftly overtaken by developments in the methods employed. Firstly, the initial calibration data proposed for this period were swiftly revised (Spurk et al. 1998; Kromer and Spurk 1998; Stuiver et al. 1998), which led to substantial revisions to the chronology for Star Carr than had been originally proposed (Dark 2000). Secondly, the statistical methods for age-depth modelling available in the mid-1990s were primitive, either visual fitting of the uncalibrated sequence of radiocarbon measurements to the calibration curve (Day and Mellars 1994, 420–1; Dark 1998b, 119) or a simple Bayesian model incorporating only the relative sequence of dated samples (Dark 1998b, figure 10.3). Although the first formal mathematical approaches for modelling age-depth sequences through sediments were appearing at this time (Christen et al. 1995; Kilian et al. 2000), freely available software allowing the application of these approaches was in the future (Blaauw and Christen 2005; Bronk Ramsey 2008; Haslett and Parnell 2008).

The chronology proposed in the 1990s was refined further by the integration of archaeological material from Clark's excavations. During the 1990s direct dates had been obtained on a number of artefacts that had not been contaminated by the conservation techniques employed by Clark. The most significant of these was the Tot Lord collection, a small assemblage of material that had been collected from the baulks of two of Clark's trenches after the 1950 excavation season (Dark et al. 2006, 192). Four of these artefacts were dated by the Oxford Radiocarbon Accelerator Unit, two of which were subsequently re-dated using a different pre-treatment method (Dark et al. 2006, 193–4). In addition to these, a date was obtained on a 'resin cake', a piece of birch resin that had been recorded by Clark but not conserved (Roberts et al. 1998). Dark et al. (2006, 190) also attempted to correlate the deposition of artefacts in Clark's trenches with the phases of burning, by comparing the heights of the barbed points with the vertical distribution of the macro charcoal in the adjacent environmental profile.

Bringing this material together with the two AMS dates on artefacts from VP85A, Dark et al. (2006, figure 2) proposed the first detailed chronology for human activity at Star Carr, estimating both the initial date of occupation and its duration. Dark's (2000) analysis of the dating of the charcoal record suggested that the first phase of burning recorded in VP85A began at 8970 cal BC and lasted c. 80 years, with a contemporary though slightly longer episode in Clark's Site profile. This seemed to correspond with the majority of the artefacts recorded by Clark and in trench VP85A, and with the direct dates on artefacts made by AMS (Dark 2000, 197–8). Following a brief hiatus, a second phase of activity was represented by burning recorded in VP85A, which started at 8790 cal BC and lasted c. 130 years, and a later episode in the Clark Site profile. This seemed to correspond with a lower quantity of material culture and was thought to reflect a change in either the character or location of activity (Dark 2000, 198).

Subsequent work has challenged aspects of this interpretation, particularly the suggestion that the different episodes of burning may have reflected differences in forms of activity at the site. Excavations in trench SC22 in 2006 recorded two pieces of worked antler in a trench to the east of the area investigated by Clark. Dating of this material (OxA-16809–10) suggested that it was contemporary with the second phase of burning recorded in Dark's Clark Site profile, indicating that comparable forms of activity and deposition may have occurred in both phases at the site (Conneller et al. 2009, 89). Despite this, the chronology proposed by Dark et al. (2006), and in particular the two dated phases of occupation, have continued to structure the way the site has been discussed (e.g. Mellars 2009).

The aims of current dating programme

Whilst Dark et al.'s (2006) chronology for Star Carr was well established by the time the current fieldwork began, the new excavations quickly showed that occupation at the site was far more complex than had previously been thought. Structures were recorded on both the wetland and dryland areas as well as numerous

episodes of artefact deposition representing a range of different activities (e.g. Taylor 2007; Conneller et al. 2009; Conneller et al. 2012). What is more, this material occurred at different levels within the peat stratigraphy suggesting numerous phases of occupation. As the existing chronology only dated two phases of activity, a new programme of dating was required in order to establish the timing and duration of different episodes of human occupation at the site more precisely.

Initially the dating programme focused on providing sufficient information on the scale, condition and importance of the surviving archaeological remains on the site to inform the designation of Star Carr as a Scheduled Monument (which occurred in November 2011). Following the agreement of the management strategy (Milner 2011), the radiocarbon and chronological modelling programme was extended to include material from the European Research Council (ERC) and English Heritage/Historic England funded excavations (2013–2015) and to address the wider research objectives of that project. A partnership approach was adopted, with English Heritage/Historic England supporting the dating of the archaeological remains and environmental sequence around the Star Carr embayment reported in this chapter, and the ERC supporting the more extensive environmental and climatic research programme around Lake Flixton (Chapter 18).

This new dating programme had three aims.

First, to construct a human-scale narrative for Star Carr by:

- untangling the order of episodes of activity that cannot be related by direct stratigraphy,
- determining the duration and intensity of different episodes of activity,
- understanding the temporal relationships between different episodes of human activity and identifying any hiatus in occupation.

Second, to establish the chronological relationships between different forms of human activity at Star Carr and the contemporary environment and climate by:

- relating different types of human activity to the changing character of the wetland environments at the lake edge,
- relating the human occupation at Star Carr with changes in climate over time,
- relating the occupation at Star Carr with changes occurring to the landscape and environment at other points around the lake and the wider Vale.

Third, to compare human activity at Star Carr with contemporary activity at other sites in Britain (Conneller et al. 2016).

Bayesian chronological modelling

The application of Bayesian statistics for the interpretation of radiocarbon dates allows chronologies that are precise within a scale of human lifetimes and generations to be constructed routinely (Bayliss 2009). This makes fuzzy prehistory, a space where past agents and individuals float timelessly in a kind of pseudo-ethnographic present, a choice rather than a necessity and opens up new avenues of interpretation for archaeologists (Bayliss and Whittle 2007; Whittle et al. 2011; Bayliss and Whittle 2015).

The basic idea behind the Bayesian approach to the interpretation of data is encapsulated by Bayes' theorem (Bayes 1763; Figure 17.1). This simply means that we analyse the new data we have collected about a problem ('the standardised likelihoods') in the context of our existing experience and knowledge about that problem (our 'prior beliefs'). This enables us to arrive at a new understanding of the problem which incorporates both our previously existing knowledge and our new data (our 'posterior belief'). We do this by the use of formal probability theory, where all three elements of our model (that is, existing beliefs, new information, and revised interpretations) are expressed as probability density functions. These give us a quantitative measure of our state of knowledge of each component of the model. Bayesian models are thus interpretative constructions which rely on multiple lines of evidence (Buck et al. 1996). An accessible general introduction to the principles of Bayesian statistics is provided by Lindley (1985), and to its history by Bertsch McGrayne (2011).

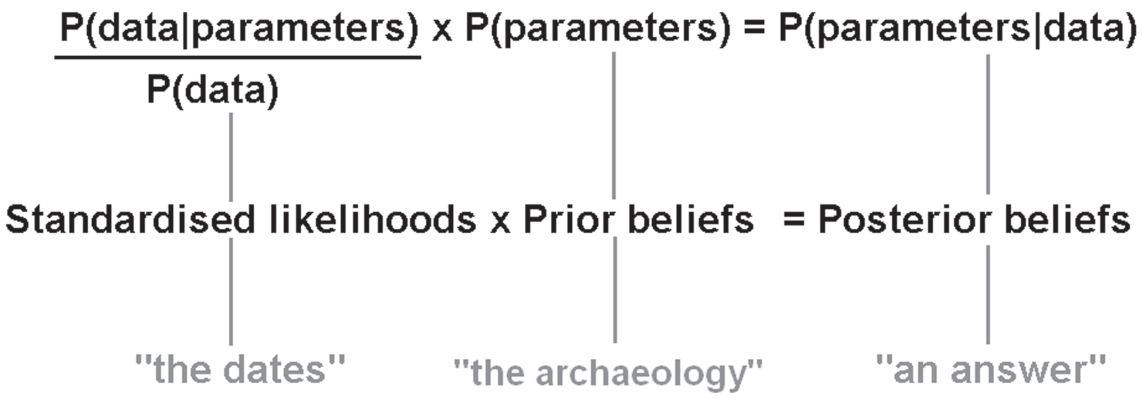

Figure 17.1: Bayes' theorem (Copyright Historic England, CC BY-NC 4.0).

Alison Wylie (2002, 162–3) has suggested that 'scientific arguments are more like cables than chains'. In this view, individual lines of argument that are insufficient on their own can make a cumulatively persuasive case when woven together, although the strands that make up a cable of comparative, evaluative argument may conflict with one another and thus may require dynamic judgements and revisions. In the construction of archaeological chronologies, Bayesian statistics provide a formal and explicit methodology for weaving together different strands of evidence to form the cable. The approach combines calibrated radiocarbon dates with knowledge of the character and sequence of deposits from which they are derived to produce a series of formal, probabilistic date estimates. Stringent demands are made of both the radiocarbon dates and our archaeological understanding of stratigraphy, associations, sample taphonomy and context in general, but the combined chronology should be more reliable than its individual components, since it is reliant on multiple strands of reinforcing evidence. To return to Wylie's metaphor, the resultant cable should be both stronger (more robust) and tighter (more precise).

Our models incorporate archaeological prior beliefs of various kinds. We need to be clear about the basis of these beliefs. Some may be comparatively unequivocal—the stratigraphic succession of a sequence of plant macrofossils in a monolith, for example. In other cases the stratigraphic sequence may be open to alternative interpretations, or there may be doubt about the taphonomy of the dated material. The fundamental point is that Bayesian statistics, being a formal methodology, force archaeologists to be explicit about their strands of reasoning.

In theory, once the model has been defined, the posterior beliefs can be calculated using Bayes' theorem. However, in practice almost all chronological models have so many independent parameters that the number of possible outcomes to consider at a useful resolution makes such a calculation impractical. For this reason, Markov Chain Monte Carlo (MCMC) methods are used to provide a possible solution set of all of the parameters of the model. The algorithm 'samples' the prior probability distributions (i.e. usually calibrated radiocarbon dates), and then attempts to reconcile these distributions with the prior beliefs included in the model (such as relative dating from stratigraphy), by repeatedly sampling each distribution to build up a set of solutions consistent with the model structure. The probability of a particular solution appearing in the MCMC analysis should be directly proportional to its probability as defined by the posterior probability density.

In most cases a reasonably representative solution can be generated by this method. If there are too few iterations in the analysis, the resulting probability distributions will usually be noisy and will vary from run to run. The degree to which a truly representative solution set has been generated is called 'convergence'. The verification of convergence in models which employ MCMC sampling is not straightforward and a number of diagnostic tools have been proposed: that employed in OxCal is described by Bronk Ramsey (1995, 429). This convergence integral has a critical value of 95%, and models which fail to pass this threshold may be unstable and their outputs should be regarded with the utmost caution (Bronk Ramsey 1998, 469). The program attempts to produce stable models by increasing the number of passes the MCMC sampler calculates each time

the convergence value falls below 95%. In an attempt to ensure stable outcomes all models reported in this volume have been calculated using a minimum of 20 million passes.

Stability of the model outputs is not the only criterion by which models can be validated. We also need to consider whether the two components input into the model, the 'prior beliefs' and the 'standardized likelihoods', are compatible. There are four main reasons why radiocarbon dates may conflict with the archaeological information included in a model:

1. Erroneous prior beliefs—situations where the overall form of the model is incorrect (for example, unidentified episodes of truncation interrupting continuous sedimentation). These must be identified and more plausible alternative prior beliefs implemented.
2. Statistical outliers—the 1 in 20 radiocarbon results whose true age lies outside the 95% range. These must be retained in the model as their exclusion would statistically bias the model outputs.
3. Misfits—dates which do not fit in the expected stratigraphic position, or which are inaccurate for some technical reason. Generally, samples which prove to be residual can be used as *termini post quos* for their contexts, but intrusive samples or inaccurate dates need to be excluded from the analysis. Sometimes it may be possible to reinterpret the stratigraphy.
4. Offsets—measurements that are systematically offset from the calibration data (most commonly, reservoir effects). Confusingly, categories 3 and 4 are both known in the statistical literature as 'systematic offsets' although archaeologically they are very different.

We clearly have the potential for all four situations in our assemblage of radiocarbon dates and chronological models from Star Carr.

There are two possible approaches to this issue.

The first approach is to identify problems manually using our archaeological judgement about the character of particular samples and deposits and the agreement indices provided by OxCal (Bronk Ramsey 1995, 429; Bronk Ramsey 2009a, 356–7), and then to decide how to include each date in the model depending on its specific characteristics. The major advantage of this approach is that it allows us to account for all the information we have about the character of particular samples or deposits; the disadvantage is that the indices of agreement provided by OxCal are not derived from a formal statistical approach (although they have proven robust in a wide range of applications).

The second approach is formal, statistical outlier detection. This assumes that we can never really be sure whether any particular measurement is an outlier, and so weights each sample according to how likely it is to be correct using a model averaging approach. The advantage of this method is that it is an explicit statistical process; the disadvantage is that it may not take account of the archaeological information we may have about the relative strengths and weaknesses of particular samples or deposits. Since we are hoping to identify misfits that are outliers on the calendar scale (samples that are residual or intrusive at the depth at which they were found), the general outlier model proposed by Bronk Ramsey (2009b, 1028) would be appropriate for this application.

These diagnostic statistical tools aid us in ensuring internal consistency within our cable (see also Wylie 2002, 176–7).

The chronological model presented in this chapter has been constructed using the program OxCal v4.2 (Bronk Ramsey 2009a; Bronk Ramsey 2009b; Bronk Ramsey and Lee 2013) and the atmospheric calibration curve for the northern hemisphere published by Reimer et al. (2013). The model is defined exactly by the OxCal CQL2 code provided in Appendix 17.1 (with additional parameters calculated using the code provided in Appendix 17.2). In the Figures, the posterior density estimates output by the model are shown in black, with the unconstrained calibrated radiocarbon dates shown in outline. The other distributions correspond to aspects of the model. For example, '*start Star Carr*' is the estimated date when Mesolithic activity at Star Carr began (Figure 17.2). In the text and Tables, the Highest Posterior Density intervals of the posterior density estimates are given in *italics*. So, for example, the model presented in this chapter estimates that Mesolithic activity at Star Carr began in *9385–9260 cal BC* (*95% probability*; *start Star Carr*; Figure 17.2), probably in *9335–9275 cal BC* (*68% probability*). Where unmodelled radiocarbon dates are given, they have been calibrated using the probability method (Stuiver and Reimer 1993) and IntCal 13. All ranges have been rounded outwards to the nearest five years.

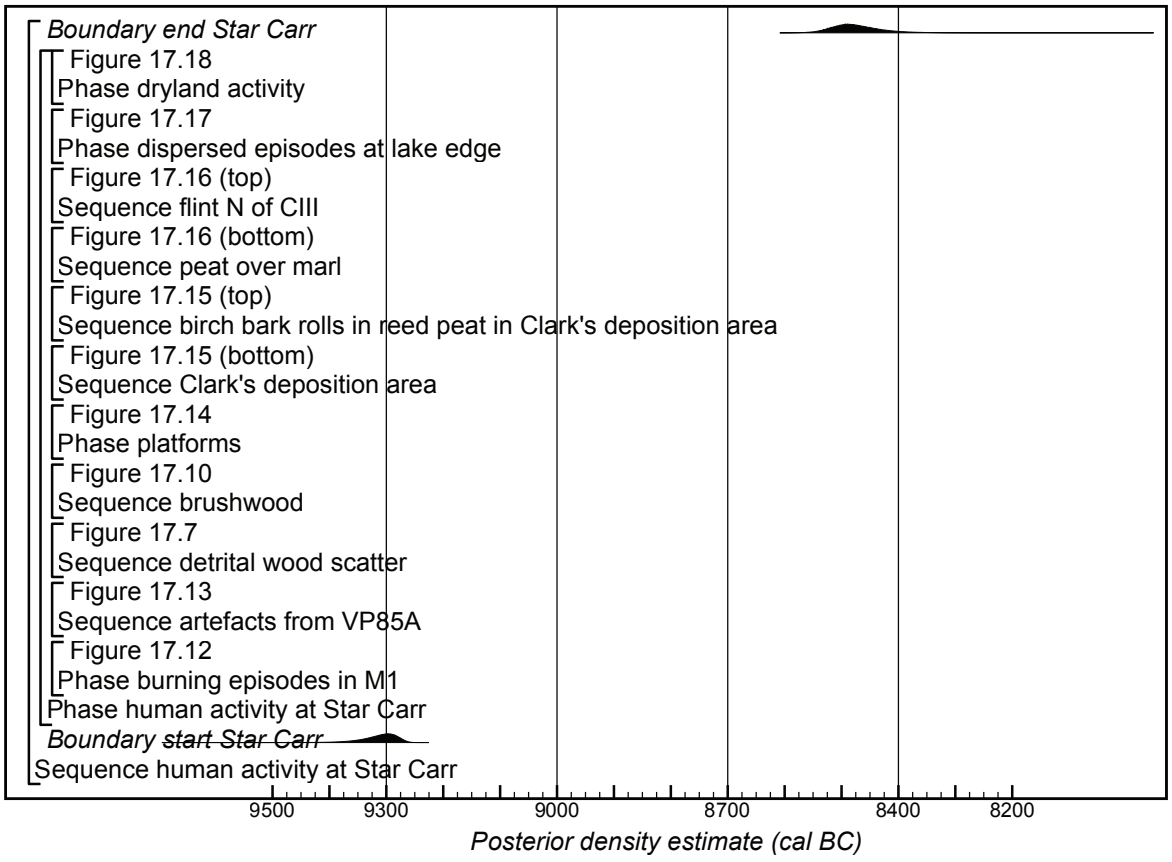

Figure 17.2: Diagram showing the overall form of the model for human activity along the lake edge at Star Carr, components are illustrated in the Figures indicated (but the model is only exactly defined by the CQL2 code in Appendix 17.I) (Copyright Historic England, CC BY-NC 4.0).

Sampling strategy

The dating programme followed the reflexive approach to implementing Bayesian chronological modelling in archaeology that has been developed by English Heritage/Historic England over the past twenty years (Bayliss 2009, figure 9). A sequential sampling strategy was thus devised using a series of simulation models which combined the available archaeological and environmental information with simulated radiocarbon dates from the available pool of potential suitable datable samples and the large suite of existing radiocarbon dates (Tables 17.1 and 17.2).

Sampling was also informed by a series of pragmatic considerations:

First, the objectives of the dating programme developed during the course of the project. Initially sampling focused on the trenches along the lake edge excavated between 2004 and 2010 as part of a programme of research to assess the extent of the site and the quality of its preservation (Milner 2011). Once the excavation of the site had been agreed, the dating programme was extended to cover material from the dryland and newly excavated areas and the range of academic objectives described above.

Second, sampling was informed by technical difficulties in dating some sample types. Bone and antler artefacts recovered by Grahame Clark in the 1950s were vacuum impregnated with a chemical consolidant (Clark 1954, plate IIIA), and we were not confident that this could be completely removed and accurate radiocarbon measurements obtained. In 2007, two severely degraded antler samples were dated from trench SC22 (OxA-16809–10; Table 17.1). These produced radiocarbon ages which are clearly anomalously recent in relation

Laboratory number	Sample and context description	Radiocarbon age (BP)	$\delta^{13}C_{IRMS}$ (‰)	$\delta^{15}N$ (‰)	C:N	References
Clark's Site Legacy						
KIA-307034	*Canis familiaris* subadult cranium (no. 58.11.15.3) from unknown location in Clark's excavation	9342±41	−21.1±0.1	9.0±0.2	3.5	Schulting and Richards 2009
OxA-V-994-33	*Canis familiaris* adult left femur (no.58.11.15.4) from unknown location in Clark's excavation	9680±55	−19.0±0.2	11.2±0.3	3.5	Schulting and Richards 2009
OxA-2343	Unconserved inner fragment of resin 'cake' from unknown location in Clark's excavation	9350±90	−29.1			Hedges *et al* 1994; Roberts *et al* 1998
Q-14	Waterlogged wood, *Betula* sp., from 'brush platform' in Clark's excavation	9557±210	nm			Godwin and Willis 1959; Clark 1954
C-353	Replicate of Q-14	9488±350	nm			Arnold and Libby 1951; Clark 1954
Mean	T'=0.0; T'(5%)=3.8; ν=1	9539±181				
Clark Site Legacy (Lord Collection)						
OxA-4451	The lower (proximal) portion of an anciently broken *Cervus elaphus* antler barbed point (no. 463) from unknown location in Clark's excavation	9120±150	−22.9±0.2			Dark *et al* 2006; Mellars and Dark 1998
OxA-21236	Replicate of OxA-4451	9561±38	−21.3±0.2			Jacobi pers comm
OxA-10808	Replicate of OxA-4451	9505±60	−22.3±0.2	1.9±0.3	3.2	Dark *et al* 2006
Mean	T'=**7.9**; T'(5%)=6.0; ν=2					
OxA-4450	Anciently broken *Cervus elaphus* antler splinter (no. 460) from unknown location in Clark's excavation	9060±220	−23.1±0.2			Dark *et al* 2006; Mellars and Dark 1998
OxA-10809	Replicate of OxA-4450	9530±55	−21.4±0.2	+2.2±0.3	3.2	Dark *et al* 2006
OxA-21237	Replicate of OxA-4450	9585±39	−22.2±0.2			Jacobi pers comm
Mean	T'=5.6; T'(5%)=6.0; ν=2	9567±32				
OxA-4577	*Cervus elaphus* antler crown splinter (no. 461) from unknown location in Clark's excavation	9670±100	−20.8±0.2			Dark *et al* 2006; Mellars and Dark 1998
OxA-21238	Replicate of OxA-4577	9485±38	−22.7±0.2			Jacobi pers comm
Mean	T'=3.0; T'(5%)=3.8; ν=1	9509±36				
OxA-4578	Fragment of *Cervus elaphus* antler tine (no. 465) from unknown location in Clark's excavation. This fragment may originate from the crown dated by OxA-4577	9590 ±90	−20.2±0.2			Dark *et al* 2006; Mellars and Dark 1998

OxA-21239	Replicate of OxA-4578	9468±38	−22.6			Jacobi pers comm
Mean	T'=1.6; T'(5%)=3.8; ν=1	9487±36				
VP85A Legacy						
CAR-921	Bulk sample of coarse detritus mud from around antler tine (no. 130) dated by OxA-1154, context 223, Trench VP85A	9360±110	nm			Cloutman and Smith 1988, figure 3
CAR-922	Bulk sample of coarse wood peat from around antler (no.216), context 223, Trench VP85A	9250±80	nm			Cloutman and Smith 1988, figure 3
CAR-925	Bulk sample of medium detritus mud from around barbed point (no.245), context 223, Trench VP85A	9260±100	nm			Cloutman and Smith 1988, figure 3
OxA-1154	*Cervus elaphus* antler tine (no. 130) (wrongly described as an antler frontlet in Cloutman & Smith 1988) from context 223, Trench VP85A (See CAR-921)	9500±120	nm			Hedges *et al* 1989; Cloutman and Smith 1988; Mellars 1990
CAR-923	Bulk sample of coarse reed peat from around *Bos primigenius* metatarsal (no. 56) dated by OxA-1176, context 225, Trench VP85A	9030±100	nm			Hedges *et al* 1989; Cloutman and Smith 1988; Mellars 1990
OxA-1176	*Bos primigenius* metatarsal (no. 56), context 225, Trench VP85A (See CAR-923)	9700±160	nm			Hedges *et al* 1989; Cloutman and Smith 1988; Mellars 1990
CAR-920	Bulk sample of coarse detritus mud around worked antler (no.141), base of context 225, Trench VP85A	9400±110	nm			Cloutman and Smith 1988, figure 3
CAR-924	Bulk sample of coarse reed peat from around *Bos primigenius* skull (no.150), context 225, Trench VP85A	9320±80	nm			Cloutman and Smith 1988, figure 3
CAR-930	Bulk sample of coarse reed peat from around charcoal (no.153), base of context 225, Trench VP85A	9660±110	nm			Cloutman and Smith 1988, figure 3; Mellars 1990
CAR-928	Unidentified charcoal from beneath the central platform dated by CAR-926, probably context 226, Trench VP85A	9670±120	nm			Cloutman and Smith 1988, figure 3; Mellars 1990
CAR-919	Bulk sample of fine detritus mud from around antler point blank (no.222) from top of context 228, Trench VP85A	9510±80	nm			Cloutman and Smith 1988, figure 3
CAR-926	Unidentified waterlogged wood from central platform, probably from the base of context 225, Trench VP85A	9240±90	nm			Cloutman and Smith 1988, figure 3
CAR-927	Bulk sample of coarse reed from around central platform (See CAR-926)	9800±80	nm			Cloutman and Smith 1988, figure 3

Table 17.1: Radiocarbon and stable isotopic measurements on archaeological samples made before 2006 (* indicates stable isotopic ratio measured by AMS; nm indicates stable isotopic ratio not determined).

to stratigraphically associated samples of waterlogged wood and plant macrofossils, and so dating bone was generally avoided until better preserved material was recovered from deeper deposits in 2013.

Third, our attempts to date artefacts recovered from the 1980s excavation of VP85A were frustrated. The waterlogged timbers, which had remained in cold storage at the English Heritage/Historic England laboratory facility at Fort Cumberland, Portsmouth, had degraded to the point where neither species identification nor ring counting was possible. Furthermore, all but two of the bone artefacts, which had been considered too precious for sampling in the 1980s (Cloutman and Smith 1988, 42), could not be located.

In 2011–12, samples of waterlogged wood and plant macrofossils were dated from sequences of deposits in trenches SC22, SC24 and the 2010 extensions of cutting II and VP85A extension. These were selected to bracket stratigraphically key archaeological events, such as the construction of the central platform in VP85A, thus providing dating for the archaeological deposits within the sediments. Preliminary modelling of these results indicated that it was possible to obtain coherent sequences of radiocarbon dates from the available material, although some inaccurate results on waterlogged wood could be identified using the sequence of stratigraphic relationships between the dated samples and the programme of inter-laboratory replication. It also indicated that key horizons in the hydroseral succession at Star Carr—the onset of organic sedimentation, the onset of seasonal flooding, and possibly the onset of fen/carr—might be sufficiently close in date along the lake edge to enable them to be used as marker horizons to tie the stratigraphic sequences in separate trenches together.

Early in 2015, once excavations had been extended into deeper deposits farther away from the lake shore, a series of bone and antler samples were submitted for dating from within the detrital wood scatter (see Chapters 6 and 7). Each bone or antler was dated by two laboratories and was inter-stratified between waterlogged timbers that were also dated. Other samples submitted at this time were on humanly modified waterlogged wood, to assess the span of human activity on the site. All three pairs of replicate measurements on the bone and antler samples were statistically consistent (OxA-32061–3 and SUERC-59180, -59184–5; Table 17.3) and, with one exception, the dates on the bones were compatible with those on the stratigraphically related samples of waterlogged wood. For this reason, in 2015–16, a larger series of samples from archaeological activity around the lake edge at Star Carr were dated, including worked waterlogged wood, worked bone and antler (including a selection of artefacts), and charred birch bark rolls. Different areas of activity were dated, including materials from Clark's area, the brushwood area, the eastern and western timber platforms, an area where stone beads were manufactured (north of Clark's area) and further material from within the detrital wood scatter. Particular efforts were made to locate datable material from areas of human activity within the wood peat, to ensure that a representative sample was obtained of later episodes of occupation.

Further preliminary chronological models were constructed during this sampling programme, as each set of results was reported. This raised the question of how far the key horizons in the environmental profiles, which had been highlighted as potentially marker horizons in 2012, could be considered contemporaneous away from the shoreline. To investigate this question, a further series of samples were dated from an environmental profile at the southern end of the site in 2015 (Profile 3178; see Chapter 19), although in the event half the samples that were submitted for dating from this sequence failed during laboratory processing.

Finally, early in 2016 a series of samples was submitted from the three dryland structures (Chapter 5). All were single fragments of short-lived charcoal, recovered either from postholes of the structure or from the central hollow. In all cases, there was very little datable material of sufficient size even for dating by Accelerator Mass Spectrometry and so there are fewer radiocarbon dates than the simulation models suggested would be ideal.

Overall, the sampling strategy for Star Carr was constructed on the basis of a pragmatic mix of archaeological, scientific and statistical criteria.

Radiocarbon dating

A total of 223 radiocarbon measurements are now available from archaeological and palaeoenvironmental deposits around the Star Carr embayment, of which 76 were obtained by previous researchers (Tables 17.1 and 17.2) and 147 have been obtained as part of the current project (Table 17.3). All but the two measurements

made in the early 1950s (C-353 and Q-14), which were not corrected for fractionation, are conventional radiocarbon ages (Stuiver and Polach 1977).

A pair of statistically consistent measurements was obtained in the early years of radiocarbon dating on a waterlogged birch timber from the 'platform' in Clark's trench (C-353 and Q-14; see Table 17.1). The measurement made in Chicago (C-) was undertaken using screen-wall counting of elemental carbon as described by Libby (1952), that made at Cambridge (Q-) was dated by gas proportional counting of carbon dioxide as described by Godwin and Willis (1959).

A total of 42 measurements were undertaken at Cardiff University (CAR-) in the mid 1980s using gas proportional counting of methane (Dresser 1985). All but two of these samples were of bulk organic sediment, the acid- and alkali-insoluble fraction being selected for dating. Ten samples of waterlogged wood were dated by gas proportional counting of carbon dioxide at the Universität Heidelberg (Hd-) in 2011–12 using methods outlined by Münnich (1957), Dörr et al. (1989) and Schoch et al. (1980).

The 98 radiocarbon results reported by the Oxford Radiocarbon Accelerator Unit have been produced using a variety of methods over the past 30 years. Two samples of bone and antler submitted in 1986 (OxA-1154, -1176; Table 17.1) were pre-treated using the ion-exchange protocol, graphitised and dated by accelerator mass spectrometry (AMS) as described by Hedges et al. (1989). Four samples of bone and antler from artefacts recovered by Tot Lord from Clark's section in 1950 (and thus not consolidated; OxA-4450–1 and OxA-4577–8; Table 17.1) submitted in 1995 were similarly processed using the ion-exchange protocol, but combusted to carbon dioxide and dated by AMS (Hedges 1981; Gillespie *et al.* 1983; Hedges et al. 1992). A sample of resin 'cake' recovered in Clark's excavations and submitted for dating in 1990 (OxA-2343; Table 17.1) was not pretreated, but simply combusted and dated using the same methods. In 1991–4, a series of waterlogged plant macrofossil and charcoal samples were dated from two environmental profiles (OxA-3342–51, OxA-4376–7, and OxA-4797–8; Table 17.2). The samples from VP85A M1 were pretreated using variations of the acid-base-acid protocol (Brock et al. 2010, Table 17.1) and those from Dark's Clark Site Core were pretreated using acid washes only (Brock et al. 2010, 108). Both series of samples were then combusted and dated by AMS (Hedges 1981; Gillespie et al. 1983; Hedges et al. 1992).

Two of the antler samples were re-dated in 2001 using the original ultrafiltration protocol at Oxford (Bronk Ramsey *et al.* 2000; OxA-10808–9; Table 17.1), graphitised (Dee and Bronk Ramsey 2000) and dated by AMS using the hybrid ion source (Bronk Ramsey and Hedges 1997). This pretreatment protocol was subsequently found on occasion to produce measurements that were slightly too old (Bronk Ramsey et al. 2004a), and in 2009 new samples from all four previously dated artefacts recovered by Tot Lord were processed using the revised ultrafiltration protocol (Bronk Ramsey et al. 2004a), graphitised and dated by AMS as described by Bronk Ramsey et al. (2004b). At this time two further radiocarbon measurements were obtained on dog remains recovered in Clark's excavations. OxA-V-994-33 had been treated by PVA and was subject to an acetone pretreatment (Moore et al. 1989) followed by collagen extraction and ultrafiltration (Brown et al. 1988) at the Max Planck Institute in Leipzig. This sample was then combusted, graphitised and dated at Oxford (Dee and Bronk Ramsey 2000; Bronk Ramsey et al. 2004b). A further unconsolidated sample from a different, sub-adult dog was similarly gelatinised and ultrafiltered in Leipzig (Brown et al. 1988) but combusted, graphitised and dated by AMS at the Christian-Albrechts Universität, Kiel (KIA-) as described by Nadeau et al. (1997; 1998).

In 2006, two samples of antler were dated from excavations undertaken earlier that year (OxA-16809–10; Table 17.3). These samples were gelatinised, ultrafiltered, combusted, graphitised and dated by AMS as described by Bronk Ramsey et al. (2004a; 2004b). In 2011–16, a further 67 samples were dated at Oxford, using methods described by Brock et al. (2010) and Bronk Ramsey et al. (2004b). At this time a total of 68 samples were also dated by AMS at the Scottish Universities Environmental Research Centre (SUERC-) using methods described in Dunbar et al. (2016). In 2011, two samples which had been submitted for gas proportional counting at the Universität Heidelberg failed to produce sufficient carbon dioxide for conventional measurement. Consequently, the carbon dioxide was sub-sampled, graphitised, and dated by AMS at the Curt-Engelhorn-Zentrum Archäometrie, Mannheim (MAMS-) as described by Kromer et al. (2013).

All the radiocarbon laboratories that have produced measurements for Star Carr maintain continual programmes of quality assurance procedures, in addition to participation in international inter-comparison exercises. Even in the 1950s groups of radiocarbon laboratories were exchanging and dating known-age materials (Willis et al. 1960), and inter-comparisons are available that are relevant to all the measurements that

Laboratory number	Sample and context description	Radiocarbon age (BP)	$\delta^{13}C$(‰)	References
Dark's Clark Site Core				
OxA-4799	*Phragmites australis* charcoal picked from a slice of sediment 2cm thick at 23.52–23.54m OD in Dark's Clark Site Core. Probably equivalent to the base of context 242 in Trench CII	9500±75	−26.1	Mellars and Dark 1998, 142; Dark *et al* 2006
OxA-4797	*Phragmites australis* charcoal picked from a slice of sediment 2cm thick at 23.75–23.77m OD in Dark's Clark Site Core. Probably equivalent to the middle of context 242 in Trench CII	9385±80	−27.7	Mellars and Dark 1998, 142; Dark *et al* 2006
OxA-4798	*Phragmites australis* charcoal picked from a slice of sediment 2cm thick at 23.59–23.61m OD in Dark's Clark Site Core. Probably equivalent to context 241 in Trench CII	9260±100	−27.6	Mellars and Dark 1998, 142; Dark *et al* 2006
Legacy Sequences Star Carr Environs				
CAR-884	A 2cm slice from bulk of oxidised coarse detritus mud at 25.00m OD from Transect NC-Sample 25	8430±100	nm	Cloutman 1988, Table 1
CAR-885	A 2cm slice from bulk of coarse reed rich detritus mud at 24.00m OD from Transect NC-Sample 24	9510±100	nm	Cloutman 1988, Table 1
CAR-886	A 2cm slice from bulk *Phragmites* peat at 23.00m OD from Transect NC-Sample 23	10100±80	nm	Cloutman 1988, Table 1
CAR-864	A 2cm slice from bulk oxidised peat over calcareous sand at 25.00m OD from Transect SCP-Sample 25	8830±100	nm	Cloutman 1988, Table 1
CAR-866	A 2cm slice from bulk oxidised peat over sand with chalk pebbles at 24.00m OD from Transect SCP-Sample 24	8950±90	nm	Cloutman 1988, Table 1
CAR-867	A 2cm slice from bulk *Phragmites* peat over coarse grey sand at 23.00m OD from Transect SCP-Sample 23	10150±110	nm	Cloutman 1988, Table 1
CAR-868	A 2cm slice from bulk oxidised peat (possible plough damage) at 25.00m OD from Transect SCS-Sample 25	6200±90	nm	Cloutman 1988, Table 1
CAR-869	A 2cm slice from bulk oxidised reed peat at 24.00m OD from Transect SCS-Sample 24	9280±80	nm	Cloutman 1988, Table 1
CAR-870	A 2cm slice from bulk *Phragmites* peat at 23.00m OD from Transect SCS-Sample 23	9710±110	nm	Cloutman 1988, Table 1
VP85A Monolith M1				
OxA-3342	Miscellaneous waterlogged terrestrial plant detritus from a 0.5cm thick sample at 23.755–23.76m OD, the lower part of context 223 from Monolith M1 from the east-facing section of VP85A	9390±70	−29.2	Day 1993; Day and Mellars 1994; Mellars and Dark 1998
OxA-3343	Miscellaneous waterlogged terrestrial plant detritus from a 0.5cm thick sample at 23.705–23.71m OD, the base of context 223 from Monolith M1 from the east-facing section of VP85A	9420±70	−28.4	Day and Mellars 1994; Mellars and Dark 1998
OxA-4376	Unidentified waterlogged wood from a 2cm thick sample of coarse wood peat at 23.81–23.83m OD, from the middle of context 223 from Monolith M1 from the east-facing section of VP85A	9385±115	−28.5	Day and Mellars 1994; Mellars and Dark 1998
OxA-4377	Unidentified waterlogged wood from a 2cm thick sample of coarse wood peat at 23.93–23.95m OD, from the top of context 223 from Monolith M1 from the east-facing section of VP85A	8940±90	−28.5	Day and Mellars 1994; Mellars and Dark 1998

OxA-3344	Miscellaneous waterlogged terrestrial plant detritus from a 0.5cm thick sample of peat at 23.65–23.655m OD, from the middle of context 224 from Monolith M1 from the east-facing section of VP85A	9360±70	−28.1	Day and Mellars 1994; Mellars and Dark 1998
OxA-3345	Carbonised reed fragment from a 0.5cm thick sample of peat at 23.595–23.60m OD, from the top of context 225 from Monolith M1 from the east-facing section of VP85A	9580±70	−26.3	Day 1993; Day and Mellars 1994; Mellars and Dark 1998
OxA-3346	Unidentified waterlogged wood from a 1cm thick sample of coarse reed peat at 23.55–23.56m OD, from the middle of context 225 from Monolith M1 from the east-facing section of VP85A	9560±70	−27.3	Day and Mellars 1994; Mellars and Dark 1998
OxA-3347	Unidentified waterlogged wood from a 0.5cm thick sample of coarse reed peat at 23.505–23.51m OD, from the lower part of context 225 from Monolith M1from the east-facing section of VP85A	9680±70	−28.7	Day and Mellars 1994; Mellars and Dark 1998
OxA-3348	Carbonised reed from a coarse reed peat from a 0.5cm thick sample at 23.45–23.455m OD, from the top of context 226 from Monolith M1 from the east-facing section of VP85A	9700±70	−25.7	Day and Mellars 1994; Mellars and Dark 1998
OxA-3349	Unidentified waterlogged wood from a 0.5cm thick sample of coarse reed peat at 23.415–23.42m OD, from the middle of context 226 from Monolith M1 from the east-facing section of VP85A	9640±70	−26.6	Day 1993; Day and Mellars 1994; Mellars and Dark 1998
OxA-3350	Waterlogged *Populus tremula* and *Betula* sp. fruits, bud- and catkin-scales from a 1cm thick sample of coarse reed peat at 23.36–23.37m OD, from the base of context 226 from Monolith M1 from the east-facing section of VP85A	9500±70	−27.4	Day and Mellars 1994; Mellars and Dark 1998
OxA-3351	Waterlogged *Populus tremula* and *Betula* sp. fruits, bud- and catkin-scales from a 1cm thick sample of fine detrital mud at 23.30–23.31m OD, from the base of context 228 from the east-facing section Monolith M1 of VP85A	9630±100	−27.2	Day 1993; Day and Mellars 1994; Mellars and Dark 1998
VP85A/1 Cloutman pollen sequence				
CAR-1047	A 2cm slice of coarse wood peat at 23.87–23.89m OD, probably from the bottom of context 223 from Column 1 from the west-facing section of VP85A	9690±110	nm	Mellars 1990; Cloutman & Smith 1988
CAR-1048	A 2cm slice of coarse wood peat at 24.19–24.21m OD, probably from the upper part of context 223 from Column 1 from the west-facing section of VP85A	8810±100	nm	Mellars 1990; Cloutman & Smith 1988
CAR-1049	A 2cm slice of coarse wood peat at 24.13–24.15m OD, probably from the upper part of context 223 from Column 1 from the west-facing section of VP85A	9240±110	nm	Mellars 1990; Cloutman & Smith 1988
CAR-1050	A 2cm slice of coarse wood peat at 23.97–23.99m OD, probably from the lower part of context 223 from Column 1 from the west-facing section of VP85A	9310±80	nm	Mellars 1990; Cloutman & Smith 1988
CAR-1051	A 2cm slice of coarse wood peat at 23.83–23.85m OD, probably from the base of context 223 from Column 1 from the west-facing section of VP85A	10010±80	nm	Mellars 1990; Cloutman & Smith 1988
VP85A/2 Cloutman pollen sequence				
CAR-1017	A 1cm slice of coarse reed peat at 23.76–23.77m OD, probably from the top of context 224 from Column 2 from the west-facing section of VP85A	8580±90	nm	Mellars 1990; Cloutman & Smith 1988
CAR-1018	A 1cm slice of coarse reed peat at 23.52–23.53m OD, probably from the base of context 225 (above timber platform) from Column 2 from the west-facing section of VP85A	9410±110	nm	Mellars 1990; Cloutman & Smith 1988

Table 17.2: *Continued*

Laboratory number	Sample and context description	Radiocarbon age (BP)	$\delta^{13}C$(‰)	References
CAR-1020	A 1cm slice of fine detrital mud at 23.36–23.37m OD, probably from the top of context 228 from Column 2 from the west-facing section of VP85A	9720±80	nm	Mellars 1990; Cloutman & Smith 1988
CAR-1021	A 1cm slice of coarse sand with fine detrital mud at 23.33–23.34m OD, probably from the coarse sand (229) from Column 2 from the west-facing section of VP85A	11010±120	nm	Mellars 1990; Cloutman & Smith 1988
CAR-1019	A 1cm slice of coarse reed peat at 23.39–23.40m OD, probably from the base of context 226 from Column 2 from the west-facing section of VP85A	9410±110	nm	Mellars 1990; Cloutman & Smith 1988
VP85A/3 Cloutman pollen sequence				
CAR-1022	A 1cm slice of wood peat at 221. 23.94–23.95 m OD, probably from the base of context 221 from Column 3 from the west-facing section of VP85A	8670±90	nm	Mellars 1990; Cloutman & Smith 1988; Mellars & Dark 1998
CAR-1023	A 1cm slice of coarse reed peat at 23.65–23.66m OD, probably from the upper part of context 225 from Column 3 from the west-facing section of VP85A	9290±60	nm	Mellars 1990; Cloutman & Smith 1988; Mellars & Dark 1998
CAR-1024	A 1cm slice of coarse reed peat at 23.41–23.42m OD, probably from the upper part of context 226 from Column 3 from the west-facing section of VP85A	9540±110	nm	Mellars 1990; Cloutman & Smith 1988; Mellars & Dark 1998
CAR-1025	A 1cm slice of coarse reed peat at 23.35–23.36m OD, probably from the middle of context 226 from Column 3 from the west-facing section of VP85A	9480±100	nm	Mellars 1990; Cloutman & Smith 1988; Mellars & Dark 1998
CAR-1026	A 1cm slice of fine detrital mud at 23.25–23.26m OD, probably from the middle of context 288 from Column 3 from the west-facing section of VP85A	9680±110	nm	Mellars 1990; Cloutman & Smith 1988; Mellars & Dark 1998
CAR-1027	A 1cm slice of coarse sand with fine detrital mud at 23.14–23.15m OD, probably from the base of context 229 from Column 3 from the west-facing section of VP85A	10950±90	nm	Mellars 1990; Cloutman & Smith 1988; Mellars & Dark 1998
VP85B Cloutman Pollen Sequence				
CAR-1028	A 1cm slice of coarse detritus mud containing many reeds including *Phragmites* at 23.74–23.75m OD, at the top of the monolith from the north-facing section of VP85B	8620±100	nm	Cloutman & Smith 1988
CAR-1030	A 1cm slice of coarse *Cladium* peat at 23.26–23.27m OD, from the monolith from the north-facing section of VP85B	9160±100	nm	Cloutman & Smith 1988
CAR-1031	A 1cm slice of fine detrital mud at 23.10–23.11m OD, from the monolith from the north-facing section of VP85B	9760±100	nm	Cloutman & Smith 1988
CAR-1032	A 1cm slice of marl at 22.96–22.97m OD, from the top of the marl in the monolith from the north-facing section of VP85B	10710±90	nm	Cloutman & Smith 1988
CAR-1033	A 2cm slice of marl at 22.82–22.84m OD, from the base of the marl in the monolith from the north-facing section of VP85B	10520±90	nm	Cloutman & Smith 1988
CAR-1029	A 1cm slice of coarse *Cladium* peat at 23.50–23.51m OD, from the monolith from the north-facing section of VP85B	8830±100	nm	Cloutman & Smith 1988

Table 17.2: Radiocarbon and stable isotopic measurements on environmental samples made before 2006 (* indicates stable isotopic ratio measured by AMS).

have subsequently been made on materials from the site (Otlet et al. 1980; Scott et al. 1990; Rozanski 1991; Rozanski et al. 1992; Bronk Ramsey et al. 2002, Table 17.1; Scott 2003; Scott et al. 2007; Scott et al. 2010a; Scott et al. 2010b).

Replicate radiocarbon measurements are available on 27 samples: 19 samples have two measurements, seven samples have three measurements, and one has four (Tables 17.1 and 17.3). Nineteen of the 27 replicate groups are statistically consistent at 95% confidence (Ward and Wilson 1978), with three more consistent at the 99% level but not the 95% level. This scatter is more than would be expected simply from the statistical spread of replicate radiocarbon measurements. It is clear that samples of waterlogged wood have proven particularly problematic, as seven of the thirteen replicate groups are inconsistent. In contrast, only one of the nine replicate groups on animal bone or antler is statistically inconsistent (Table 17.1), probably reflecting our caution in only attempting to date bone from the deeper parts of the site where preservation was better.

Examination of the statistically inconsistent groups of measurements reveals that, in almost all cases, one measurement in the group is a clear misfit (e.g. OxA-4451 is clearly much more recent than the other two measurements on barbed point no.463; Table 17.1). This suggests that the issue is with the chemical pretreatment of certain samples, which did not adequately remove all exogenous carbon. Since all the participating laboratories produced some misfits, it is unlikely that the observed replication arises from laboratory error, rather some samples seem to have been degraded to the point where accurate dating was difficult (if not impossible). Overall, perhaps 9 or 10 of the 63 measurements in the replicate groups are incorrect (*c.* 15%). However, this is probably not a true reflection of the overall accuracy of the dataset as replicate measurements were not always selected randomly; rather, they were obtained on a number of samples when the initial result seemed problematic.

Five pairs of replicate $\delta^{13}C$ and $\delta^{15}N$ values are available, all of which are statistically consistent at 95% confidence (Ward and Wilson 1978; Table 17.3).

Statistically consistent replicate groups on radiocarbon measurements have been combined by taking a weighted mean before calibration and inclusion in the chronological model (Tables 17.1 and 17.3). The accuracy of each measurement in the statistically inconsistent groups has been assessed from the replicate group itself, from any notes made during its laboratory processing and from the agreement between the date and related dates within the model. The accuracy of measurements that have not been replicated has also been judged on this basis. Results that we consider inaccurate for technical reasons have been excluded from the model described below.

Modelling Star Carr

This is a complex model defined by the OxCal CQL2 code provided in Appendix 17.1 (with additional parameters calculated using the code provided in Appendix 17.2). The basic principle behind it is that stratigraphic relationships between radiocarbon dates associated with human activity and dates associated with environmental sequences and events are implemented together, and then cross reference is made to these constrained distributions in considering the chronologies of the human activity and lake edge environment respectively. For example, the dates on artefacts from the detrital wood scatter from trench SC34 were recovered from fine detrital mud that must post-date the start of organic sedimentation in the adjacent environmental profile 3178. However, this date estimate also provides information on when environmental Zone 1 began in a specific part of the lake edge. The parameter *onset organics 3178,* which is shown in the age-depth model in Figure 17.6, therefore cross-refers to both the archaeological and environmental parts of the model and is constrained by relationships of both types.

Human activity

The overall form of the model for human activity around the lake at Star Carr is illustrated in Figure 17.2. Human activity at Star Carr during the Mesolithic is assumed to comprise a relatively continuous period of possibly episodic but regular activity. Within this overall phase of use we have modelled separate phases for episodes of human occupation where we have four or more effective likelihoods (i.e. radiocarbon dates or calculated parameters) relating to that activity. This ensures that episodes of potentially short duration that have a

Laboratory number	Sample and context description	Radiocarbon age (BP)	$\delta^{13}C$ (‰)	$\delta^{15}N$ (‰)	C:N
110553					
OxA-32056	Waterlogged *Salix/Populus* sp. radially 1/3 split timber (Find no 110553), context 320	10010±40	−28.1±0.2		
SUERC-65242	Replicate of OxA-32056	9977±30	−28.3±0.2		
Mean	T'=0.4; T'(5%)=3.8; ν=1	9989±25			
Bead manufacturing area north of CIII					
OxA-33664	Carbonised *Betula* sp. bark roll (Find no 114968), context 310 to the north of Clark's trenches	9660±45	−30.0±0.2		
SUERC-66043	Carbonised *Betula* sp. bark roll (Find no 113409), context 310 to the north of Clark's trenches	9448±27	−27.3±0.2		
OxA-33663	Carbonised *Betula* sp. bark roll (Find no 115499), context 312 to the north of Clark's trenches	9550±40	−28.7±0.2		
SUERC-66039	Carbonised *Betula* sp. bark roll (Find no 115037), context 312 to the north of Clark's trenches	9552±30	−27.5±0.2		
Birch Bark Rolls in Clark's deposition area					
OxA-33667	Carbonised *Betula* sp. bark roll (Find no 116553), context 312 to the south of Clark's trenches	9580±45	−29.2±0.2		
OxA-33669	Carbonised *Betula* sp. bark roll (Find no 115195), context 312 to the south of Clark's trenches	9465±45	−29.8±0.2		
OxA-33670	Replicate of OxA-33669	9490±45	−29.1±0.2		
Mean	T'=0.2; T'(5%)=3.8; ν=1	9478±32			
SUERC-66048	Carbonised *Betula* sp. bark roll (Find no 115014), context 312 to the south of Clark's trenches	9600±28	−28.1±0.2		
SUERC-66049	Carbonised *Betula* sp. bark roll (Find no 115185), context 312 to the south of Clark's trenches	9389±29	−28.0±0.2		
Birch Bark Rolls to North of CII					
OxA-33665	Carbonised *Betula* sp. bark roll (Find no 94084), context 310 at the north end of Trench 34	9500±45	−30.8±0.2		
SUERC-66045	Carbonised *Betula* sp. bark roll (Find no 95934), context 310 at the north end of Trench 34	9519±29	−28.3±0.2		

Clark's deposition area					
OxA-33674	Groove and splintered *Cervus elaphus* antler beam from a frontlet/headdress (Find no 115876), the middle of context 312 from the baulk between cuttings I and II	9345±50	−21.0±0.2	+2.4±0.3	3.2
SUERC-66177	Replicate of OxA-33674	9431±32	−20.9±0.2	+3.0±0.3	3.3
Mean	T'=2.1; T'(5%)=3.8; ν=1	9406±27			
OxA-33676	Worked piece of *Bos primigenius* (Find no 117546), context 312 from the baulk between cuttings I and II	9560±45	−22.6±0.2	+3.7±0.3	3.1
OxA-33677	Worked piece of *Cervus elaphus* tibia (Find no 115872), context 312 from the baulk between cuttings I and II	9490±45	−20.3±0.2	+7.0±0.3	3.1
SUERC-66178	*Cervus elaphus* pedicle fragment from a frontlet/headdress (find no 114937), context 312 to the south of Clark's cutting I	9529±35	−22.5±0.2	+2.4±0.3	3.3
SUERC-66187	Worked piece of *Cervus elaphus* right ulna (Find no 117267), context 312 to the south of Clark's cutting I	9479±35	−21.6±0.2	+3.4±0.3	3.3
OxA-33675	Worked piece of *Cervus elaphus* radius (Find no 116803), context 317 from the baulk between cuttings I and II	9465±45	−22.4±0.2	+3.6±0.3	3.2
SUERC-66182	Worked piece of *Cervus elaphus* humerus (Find no 117900), context 317 to the south of Clark's cutting III.	9531±35	−22.4±0.2	+4.5±0.3	3.3
SUERC-66186	Worked piece of *Cervus elaphus* 3rd phalanx (Find no 116896), context 317 from the baulk between cuttings I and II	9518±35	−22.7±0.2	+3.1±0.3	3.3
Southern end of Clark's excavation area					
OxA-25240	Waterlogged *Salix* sp. bow with 5 rings (Find no 92684), context 234, cutting II extension. Rest of the artefact was excavated in 2015 (Find no 113300), Trench 34	9470 ±45	−26.1±0.2		
SUERC-66047	Carbonised *Betula* sp. bark roll (Find no 114814), context 312 south of Clark's excavation area, Trench 34	9518±29	−28.4±0.2		
Brushwood					
OxA-32059	Waterlogged *Salix/Populus* sp. tangentially split possible wood working debris (Find no 98016), context 312, brushwood spit 2	9580±40	−24.7±0.2		
OxA-32060	Waterlogged *Populus* sp. radial 1/3 split roundwood debris (Find no 94032), context 312, brushwood spit 1	9696±40	−27.9±0.2		
OxA-32320	Waterlogged cf *Salix/Populus* sp. radially half split roundwood debris (Find no 98031), context 312, brushwood spit 2	9615±45	−27.5±0.2		
SUERC-59170	Waterlogged *Salix* sp, tangentially split and possibly hewn timber (Find no 98009), context 312, brushwood spit 2	9465±31	−27.7±0.2		

Table 17.3: *Continued*

Laboratory number	Sample and context description	Radiocarbon age (BP)	$\delta^{13}C$ (‰)	$\delta^{15}N$ (‰)	C:N
OxA-32055	Waterlogged cf *Salix/Populus* sp. *or Betula, Alnus/Corylus* sp., radially half split roundwood debris (Find no 98862), context 317, brushwood spit 7	9766±39	−26.1±0.2		
SUERC-59174	Waterlogged worked cf *Salix/Populus* sp., tangentially split roundwood debris (Find no 98792), context 317, brushwood spit 3	9471±31	−27.8±0.2		
SUERC-59175	Waterlogged worked *Betula/Alnus* sp., radially half split round wood (Find no 98865), context 317, brushwood spit 6	9547±31	−28.9±0.2		
SUERC-59176	Waterlogged worked cf *Salix/Populus* sp., radially half split roundwood debris (Find no 99210), context 317, brushwood spit 7	9670±31	−28.4±0.2		
OxA-32319	Waterlogged worked cf *Salix/Populus* sp., tangentially aligned outer split timber (Find no 103196), context 320, base of brushwood spit 9	9540±50	−29.1±0.2		
Central Platform					
OxA-25247	Waterlogged *Betula* sp. twig (Sample no 381A.3), picked from a bulk sample 4cm thick at 23.86–23.90m OD, context 223, Trench VP85A	8865±40	−29.9±0.2		
OxA-26561	Waterlogged *Salix* sp. twig (Sample no 246B), context 224, Trench VP85A	9305 ±45	−28.3±0.2		
SUERC-40160	Replicate of OxA-26561	9415 ±30	−29.8±0.2		
Mean	T'=4.1; T'(5%)=3.8; ν=1	9382±25			
OxA-25246	Waterlogged cf *Betula* sp. bark (Sample 300), context 225, Trench VP85A	9515±40	−27.4±0.2		
SUERC-36338	Waterlogged *Populus* sp. roundwood (Sample 244), context 225, Trench VP85A	9555 ±35	−28.9±0.2		
SUERC-36339	Waterlogged *Salix* sp. twig (Sample no 381M.2) picked from a bulk sample 2.5cm thick at 23.435–23.46m OD from macrofossil profile VP85a/2010, context 226, Trench VP85A	9600 ±35	−27.2±0.2		
OxA-33570	Carbonised *Salix/Populus* sp. roundwood fragment with 3 years growth and pith but no bark (Sample 1909A), context 318, Trench 34	9580 ±50	−29.5±0.2		
SUERC-65241	Carbonised *Salix/Populus* sp. roundwood fragment with 8 years growth, close to the pith (Sample no 1909B), context 318, Trench 34	9606 ±30	−24.2±0.2		
OxA-32146	Waterlogged sapwood from unconverted timber of diffuse/semi ring porous species (Find no 99738) from the upper layer of central platform, context 312, Trench 34	9660±45	−28.0±0.2		
SUERC-59169	Replicate of OxA-32146	9702±45	−29.0±0.2		
Mean	T'=0.4; T'(5%)=3.8; ν=1	9681±32			
OxA-32318	Waterlogged *salix/populus* or *betula/alnus/corylus* sapwood from unconverted timber (Find no 99726) from the upper layer of central platform, context 312, Trench 34	9460±65	−28.2±0.2		
SUERC-59168	Replicate of SUERC-59168	9650±31	−29.2±0.2		

Mean	T'=**6.9**; T'(5%)=3.8; ν=1				
OxA-33574	Waterlogged *Salix Populus* sp. tangentially split timber (Find no 103111), from the middle layer of the central platform, context 312, Trench 34	9735±45	−29.5±0.2		
OxA-33731	Waterlogged *Salix Populus* sp. tangentially split timber (Find no 103288), from the central platform, context 312, Trench 34	9675±45	−27.2±0.2		
SUERC-65243	Waterlogged *Salix Populus* sp. tangentially outer split timber (Find no 103290) from the lower layer of the central platform, context 312, Trench 34	9663±31	−26.8±0.2		
SUERC-65247	Waterlogged *Salix Populus* sp. tangentially split timber (Find no 103254) from the middle layer of central platform, context 312, Trench 34	9629±30	−27.4±0.2		
Cutting II 2010					
OxA-25238	Waterlogged *Salix* sp. stem (Sample no 450L.1) picked from bulk sample 5cm thick at 23.47–23.52m OD from macrofossil profile CII/2010, context 235, cutting II	9735±40	−27.6±0.2		
SUERC-36348	Waterlogged *Salix* sp. stem, (Sample no 450L.2) picked from bulk sample 5cm at 23.47–23.52m OD, from macrofossil profile CII/2010, context 235, cutting II	9710±35	−25.9±0.2		
OxA-25242	Waterlogged *Betula* sp twig (Sample no 450A.4) picked from bulk sample 5cm thick at 24.03–24.08 m OD, from macrofossil profile CII/2010, context 243/231, cutting II	8810 ±40	−28.4±0.2		
SUERC-36354	Waterlogged *Betula* sp twig (Sample no 450A.1) picked from bulk sample 5cm thick at 24.03–24.08 m OD, from macrofossil profile CII/2010, context 243/231, cutting II	8845 ±35	−28.1±0.2		
OxA-25239	Waterlogged *Salix* sp twig (Sample no 450H.1) picked from bulk sample 5cm thick at 23.67–23.72m OD, from macrofossil profile CII/2010, context 244, cutting II	9400 ±40	−27.7±0.2		
Detrital Wood Scatter					
OxA-33668	Carbonised *Betula* sp. bark roll (Find no 107756) associated with a partial wooden stick (possible torch), from context 312, Trench 34	9570±45	−28.2±0.2		
OxA-33672	*Cervus elaphus* pedicile from a frontlet/headdress (Find no 99528), from context 312, Trench 34	9545±45	−22.1±0.2	+1.5±0.3	3.2
SUERC-66179	Replicate of OxA-33672	9538±35	−22.1±0.2	+1.8±0.3	3.3
Mean	T'=0.0; T'(5%)=3.8; ν=1	9541±28			
SUERC-66180	*Bos primigenius* left femur head (Find no 99484), from context 312, Trench 34	9553±33	−22.8±0.2	+4.9±0.3	3.2
OxA-32061	*Alces alces* antler (Find no 108966), from context 317, Trench 34	9680±45	−20.9±0.2	+1.5±0.3	3.4

Table 17.3: *Continued*

Laboratory number	Sample and context description	Radiocarbon age (BP)	$\delta^{13}C$ (‰)	$\delta^{15}N$ (‰)	C:N
SUERC-59180	Replicate of OxA-32061	9608±39	−21.1±0.2	+1.5±0.3	3.3
Mean	T'=1.5; T'(5%)=3.8; ν=1	9639±30			
OxA-32062	Unshed *Curvus elephus* antler (Find no 108967), from context 317, Trench 34	9645±45	−20.5±0.2	+3.5±0.3	3.4
SUERC-59184	Replicate of OxA-32062	9611±37	−20.5±0.2	+3.2±0.3	3.2
Mean	T'=0.3; T'(5%)=3.8; ν=1	9625±29			
OxA-32063	*Alces alces* cranium (Find no 108941), from context 317, Trench 34	9820±45	−21.4±0.2	+2.4±0.3	3.4
SUERC-59185	Replicate of OxA-32063	9779±40	−21.6±0.2	+2.3±0.3	3.3
Mean	T'=0.5; T'(5%)=3.8; ν=1	9797±30			
SUERC-59178	Waterlogged cf. *Salix/Populus* sp. radial 1/3 split timber (Find no 109559), from context 317, Trench 34	9723±31	−28.6±0.2		
SUERC-59179	Waterlogged *Salix/Populus* sp. unworked timber (Find no 109030), from context 317, Trench 34	9743±31	−28.9±0.2		
OxA-33673	*Cervus elaphus* antler beam from a frontlet/headdress (Find no 103625), context 317, Trench 34	9585±45	−21.0±0.2	+1.9±0.3	3.2
SUERC-66181	*Cervus elaphus* left tibia (Finds no 103639), from context 317, Trench 34	9780±32	−22.0±0.2	+3.5±0.3	3.2
OxA-33671	*Cervus elaphus* worked right metatarsal (Find no 103650), from context 317, Trench 34	9520±45	−21.7±0.2	+2.8±0.3	3.2
Eastern Platform					
OxA-33662	Waterlogged *Salix/Populus* sp. timber of unknown conversion 10–12 years growth (Find no 113252), part of the eastern platform, context 312, Trench 34 (Outer rings sampled).	9525±45	−27.9±0.2		
OxA-33713	Waterlogged *Prunus padus* seed picked from a 5cm thick layer of reed peat (Sample S3404A&B), from above tree (113251), context 312, Trench 34	9320±50	−29.0±0.2		
SUERC-66037	Waterlogged *Betula* sp. fruits and catkin scales from a 5 cm thick slice of fine detrital mud (Sample S3404E) below timber 113252, context 317, Trench 34	9762±29	−28.2±0.2		
SUERC-66036	Waterlogged *Salix/Populus* sp. tree 5–7 years of growth (Find no 113251), context 312, Trench 34. (Outer rings sampled).	9512±29	−29.1±0.2		
Peat over marl in the area south of the western platform					
OxA-25241	Waterlogged *Betula* sp. twig (Sample 446B.1) picked from a bulk sample 5cm thick from the top of context 233, cutting II extension	8883±39	−29.7±0.2		
SUERC-36353	Waterlogged *Betula* sp. twig (Sample 446B.2) picked from a bulk sample 5cm thick., from the top of context 233, cutting II extension	8890±35	−28.7±0.2		
SUERC-36349	Carbonised *Phragmites* reed fragment (Sample 446J.1) picked from a bulk sample 3cm thick, from the base of context 234, cutting II extension	9510±35	−25.0±0.2		

OxA-33666	Carbonised *Betula* sp. bark roll (Find no 108565) from context 310 to the south of the western platform, Trench 34	9640±40	−28.6±0.2		
SUERC-66046	Carbonised *Betula* sp. bark roll (Find no 108554), from context 310 to the south of the western platform, Trench 34	9577±28	−27.7±0.2		
SUERC-66044	Carbonised *Betula* sp. bark roll (Find no 108454), from context 310 to the south of the western platform, trench 34	9562±29	−26.3±0.2		
OxA-33678	*Canis familiaris* complete left canine (Find no 108574), from the semi-articulated skeleton of a dog, context 310, Trench 34	9680±50	−18.5±0.2	+13.0±0.3	3.3
SC14 Macrofossil column 3178					
SUERC-65223	Waterlogged rhizome/culm base of indeterminate species (Sample D2) picked from a 5cm thick slice of reed peat at 23.635–23.685m OD, top of context 312. From macrofossil column 3178, taken from the north facing section of Trench 34	9290±30	−28.8±0.2		
OxA-33698	Waterlogged *Betula* sp. fruits and catkin scales, *Populus tremula* budscales and *Carex* nutlets (Sample Q1), picked from a 2.5cm thick slice of reed peat at 23.235–23.26m OD, context 312. From macrofossil column 3178, taken from the north facing section of Trench 34	9555±55	−26.3±0.2		
SUERC-65227	Carbonised *Poaceae* sp. culm node (Sample Q2), picked from a 2.5cm thick slice of reed peat at 23.235–23.26m OD, context 312. From macrofossil column 3178, taken from the north facing section of Trench 34	9583±30	−27.2±0.2		
Mean	T'=0.2; T'(5%)=3.8; ν=1	9577±27			
OxA-33699	Waterlogged *Betula* sp. fruits (Sample R1) picked from a 2.5cm thick slice of reed peat at 23.21–23.234m OD, interface between contexts 312 & 317. From macrofossil column 3178, taken from the north facing section of Trench 34	9740±65	−25.6±0.2		
SUERC-65228	Waterlogged *Carex* nutlets, *Betula* catkin scales and *Populus tremula* budscales (Sample R3) picked from a 2.5cm thick slice of reed peat at 23.21–23.235m OD, interface between contexts 312 & 317. From macrofossil column 3178, taken from the north facing section of Trench 34	9559±31	−26.7±0.2		
Mean	T'=**6.4**; T'(5%)=3.8; ν=1	9593±28			
SUERC-65229	Unidentified waterlogged twig (Sample X2) picked from a 2.5cm thick slice of fine detrital mud at 23.06–23.085, context 317. From macrofossil column 3178, taken from the north facing section of Trench 34	10095±30	−29.7±0.2		
Eastern Dryland Structure					
SUERC-65237	Carbonised *Betula* sp. fragment of 20–25 years growth (Sample S156B), from the lower fill of the hollow of the eastern structure	9556±30	−27.2±0.2		

Table 17.3: *Continued*

Laboratory number	Sample and context description	Radiocarbon age (BP)	$\delta^{13}C$ (‰)	$\delta^{15}N$ (‰)	C:N
OxA-33700	Carbonised cf *Salix/Populus* sp. fragment (Sample no S161A), context 178, fill of posthole 177 of the eastern structure	9540±55	−23.5±0.2		
SUERC-65232	Carbonised *Salix/Populus* sp. fragment (Sample S161B), context 178 fill of posthole 177 of the eastern structure	9519±31	−25.1±0.2		
SUERC-65233	Carbonised *Salix/Populus* sp. fragment (Sample S163B), context 182, fill of posthole 181 of the eastern structure	9587±32	−25.0 (assumed)		
Central Dryland Structure					
OxA-33569	Carbonised *Salix/Populus* fragment of c.20 years growth (Sample 1955), context 330 upper fill of the central depression of the central structure	9710±50	−26.1±0.2		
OxA-33701	Replicate of OxA-33569	9765±55	−24.0±0.2		
Mean	T'=0.5; T'(5%)=3.8; ν=1	9735±37			
SUERC-65238	Carbonised *Salix/Populus* fragment of c.20 years growth (Sample 1955E), context 330 upper fill of the central depression of the central structure	9221±30	−26.6±0.2		
SUERC-65239	Carbonised *Salix/Populus* fragment of c.20 years growth (Sample 1955C), context 330 upper fill of the central depression of the central structure	9754±32	−26.3±0.2		
OxA-33702	Carbonised *Salix/Populus* fragment (Sample S1989B) from context 339 fill of post-hole 338 of the central structure	9460±50	−25.2±0.2		
SUERC-65240	Carbonised *Salix/Populus* fragment (Sample S1989A), context 339 fill of posthole 338 of the central structure	9536±31	−26.4±0.2		
Western Dryland Structure					
SUERC-65231	Carbonised *Betula* sp. young twig (Sample 3491A), from context 405 fill of posthole 411 of the western structure	1.7648±0.0063	−25.6±0.2		
OxA-33598	Carbonised *Betula* sp. young twig (Sample 3491B), from context 405 fill of posthole 411 of the western structure	1.43572±0.00405	−25.6±0.2		
SUERC-65230	Carbonised *Salix/Populus* fragment of 10-15 years growth (Sample 3350A), from context 507 fill of posthole 507 of the western structure	9542±30	−26.4±0.2		
OxA-33703	Carbonised *Salix/Populus* fragment of 15-20 years growth (Sample 3350B), from context 507 fill of posthole 507 of the western structure	9585±55	−24.9±0.2		
SUERC-65222	Carbonised *Betula* sp. fragment of 15–20 years growth (Sample 3438A), from context 509 fill of posthole 515 of the western structure	9524±30	−27.3±0.2		
OxA-33571	Carbonised *Betula* sp. fragment of 25–30 years growth (Sample 3438B), from context 509 fill of posthole 515 of the western structure	9515±50	−27.3±0.2		

SC22 2006					
Hd-30192	Waterlogged *Salix* sp. roundwood (Sample 4.4), extracted from Monolith Tin 4, taken from the east-facing section of Trench SC22. Equivalent to context 34	9375±20	−29.4		
OxA-26558	Waterlogged *Salix* sp. roundwood (Sample 4.2), extracted from Monolith Tin 4, taken from the east-facing section of Trench SC22. Equivalent to context 34	9515±45	−27.1±0.2		
OxA-26559	Replicate of OxA-26558	9525±45	−27.4±0.2		
Mean	T'=0.0; T'(5%)=3.8; ν=1	9520±32			
SUERC-36356	Waterlogged *Salix* sp. roundwood (Sample 4.3), extracted from Monolith Tin 4, taken from the east-facing section of Trench SC22. Equivalent to context 34	9560±35	−28.7±0.2		
SUERC-40163	Waterlogged *Salix* sp. roundwood (Sample 4.1), extracted from Monolith Tin 4, taken from the east-facing section of Trench SC22. Equivalent to context 34	9455±30	−28.8±0.2		
OxA-16809	*Cervus elaphus* worked antler (Find 82834), from the interface between context 35 and 39, Trench SC22	9355±40	−22.1±0.3		
OxA-16810	*Cervus elaphus* antler (Find 82526) associated with a scatter of worked flint, from context 35, Trench SC22	9275±40	−22.2±0.3		
OxA-25088	Waterlogged *Populus* sp. roundwood (Find 82660), from context 35, Trench SC22	9580±45	−26.4±0.2		
SUERC-36355	Waterlogged *Salix* sp. roundwood (Find 82679), from context 35, Trench SC22	9450±35	−28.2±0.2		
Hd-30168	Waterlogged *Salix* sp. roundwood (Find 82734) from the middle of context 39, Trench SC22	9481±20	−28.1		
Hd-30190	Waterlogged *Salix* sp. roundwood (Find 82716), from the base of context 39, Trench SC22	9611±20	−28.0		
SUERC-40161	Waterlogged *Betula* sp. roundwood stem (Find 82705a), from context 39, Trench SC22	9525±30	−29.8±0.2		
OxA-26560	Replicate of SUERC-40161	9540 ±45	−28.8±0.2		
MAMS-18276	Replicate of SUERC-40161	9433±26	−28.2±0.3*		
Mean	T'=**7.3**; T'(5%)=6.0; ν=2				
SUERC-40162	Waterlogged *Salix* sp. roundwood stem (82706B.1), from context 39, Trench SC22	9505±30	−28.2±0.2		
OxA-26478	Replicate of SUERC-40162	9755 ±60	−27.3±0.2`		

Table 17.3: *Continued*

Laboratory number	Sample and context description	Radiocarbon age (BP)	$\delta^{13}C$ (‰)	$\delta^{15}N$ (‰)	C:N
Mean	T'=**14.1**; T'(5%)=3.8; ν=1				
Western Platform					
OxA-25236	Waterlogged *Corylus avellana* nutshell (Sample 201), from context 83, Trench SC24	9165±45	−26.3±0.2		
OxA-25237	Replicate of OxA-25236	9215±40	−26.1±0.2		
Mean	T'=0.7; T'5%=3.8; ν=1	9193±30			
SUERC-36347	Waterlogged *Populus* sp. roundwood (Sample 4), from context 83, Trench SC24	9275±35	−27.8±0.2		
Hd-30166	Waterlogged *Populus* sp. roundwood (Sample 215), from context 84, Trench SC24	9420±21	−29.2		
OxA-25235	Waterlogged *Salix* sp. roundwood (Sample 216), from context 84, Trench SC24	9555±45	−27.7±0.2		
Hd-30193	Waterlogged *Populus* sp. worked timber (Sample 47/402) from the western platform, context 93, Trench SC24. (10 outer rings were sampled)	9463±18	−28.7		
SUERC-40168	Waterlogged *Populus* sp. worked timber (Sample 50), from the western platform, context 93, Trench SC24). (c. 10 outer rings were sampled)	9510±30	−29.7±0.2		
OxA-X-2475-22	Replicate of SUERC-40168	9570±90	−28.6±0.2		
Hd-30200	Replicate of SUERC-40168	9359±22	−29.4		
Hd-30439	Replicate of SUERC-40168	9302±23	−29.1		
Mean	T'=**35.9**; T'(5%)=7.8; ν=3				
Hd-30440	Waterlogged *Populus* sp. worked timber (Sample 46/401) from the western platform, context 93, Trench SC24.	9606±22	−28.3		
OxA-26479	46b. Replicate of Hd-30440	9595±50	−27.2±0.2		
SUERC-40169	46a. Replicate of Hd-30440.	9585±30	−27.6±0.2		
Mean	T'=0.3; T'(5%)=6.0; ν=2	9598±17			
SUERC-40170	Waterlogged *Populus* sp. worked timber (Sample 48) from the western platform, context 93, Trench SC24.	9515±45	−29.8±0.2		
MAMS-18277	Replicate of SUERC-40170	9441±26	−29.5±0.2		
Mean	T'=2.0; T'(5%)=3.8; ν=1	9460±23			
OxA-25201	Waterlogged *Salix* sp. roundwood (Sample 453) recorded directly on top of the timbers of the western platform, context 93, Trench SC24	9550±45	−28.6±0.2		
SUERC-40164	453b. Replicate of OxA-25201	9445±30	−30.3±0.2		

Mean	T'=3.8; T'(5%)=3.8; ν=1	9478±25			
SUERC-36345	Waterlogged *Salix* sp. roundwood (Sample 455), recorded directly on top of the timbers of the western platform, context 93, Trench SC24	9485±35	−30.1±0.2		
OxA-26562	455b. Replicate of SUERC-36345	9545±55	−28.9±0.2		
Mean	T'=0.8; T'(5%)=3.8; ν=1	9502±30			
OxA-25202	Waterlogged *Populus* sp. roundwood (Sample BO344) from context 93, Trench SC24. Recovered during the micro-excavation of a sediment block (Hadley et al 2010)	9620±50	−28.1±0.2		
SUERC-36346	Waterlogged *Salix* sp. roundwood (Sample BO343), from context 93, Trench SC24. Recovered during the micro-excavation of a sediment block (Hadley et al 2010)	9590±35	−27.8±0.2		
Hd-30167	Waterlogged *Populus* sp. waterlogged plank (Find 418) of the western platform, from context 245, Trench CII. (approx. outermost 10 years sampled).	8951±18	−27.9		
Hd-30201	Waterlogged *Populus* sp. worked timber (Find 420) from the western platform from context 245, Trench CII. (c. 10 outer rings sampled).	9451±34	−28.4		
SUERC-59177	Waterlogged *Betula* sp. bark mat (Find no 99307b) from context 312/310.	9502±31	−27.2±0.2		
OxA-32057	Replicate of SUERC-59177	9650±38	−25.3±0.2		
OxA-32058	Replicate of SUERC-59177	9630±38	−25.3±0.2		
Mean	T'=**11.4**; T'(5%)=6.0; ν=2				
OxA-25199	Waterlogged *Salix* sp. twig (Sample 460.3) from context 98, Trench SC24.	9765±50	−26.9±0.2		
OxA-25200	Waterlogged *Salix* sp. twig (Sample 438.3), picked from a 50mm slice of bulk sediment immediately below timber 402 of the western platform, context 97, Trench SC24	9765±45	−28.5±0.2		
OxA-26563	Waterlogged *Salix* sp. twig (Sample 438.5) picked from a 50mm slice of bulk sediment immediately below timber 402 of the western platform, context 97, Trench SC24.	9650±45	−27.5±0.2		
SUERC-36343	Waterlogged *Salix* sp. twig (Sample 460.2) from context 98, Trench SC24.	9680±30	−28.5±0.2		
SUERC-36344	Waterlogged Salix sp. twig (Sample 438.2), picked from a 50mm slice of bulk sediment immediately below timber 402 of the western platform, context 97, Trench SC24.	9590±35	−28.4±0.2		

Table 17.3: Radiocarbon and stable isotopic measurements on samples analysed as part of this project (* indicates stable isotopic ratio measured by AMS).

number of dated samples, for example Clark's area, are proportionally weighted in our analysis as this event is represented in the overall model by only its two boundary parameters (i.e. *start Clark area* and *end Clark area*; Figure 17.15).

Within our model of human activity we have only included dates on samples with a clear anthropogenic association. These are: worked or butchered faunal material, worked wood, charcoal from cut features or forming discrete concentrations within the peat, the remains of domestic dogs, birch bark rolls, and the resin cake from Clark's excavations. As described above, because of concerns about the difficulty of accurately radiocarbon dating some materials (particularly the faunal remains), we have also dated many non-anthropogenic samples stratigraphically related to them. These have been used as constraints for dating the archaeology. We have also been able to estimate the dates of anthropogenic events that have not been directly dated by specific radiocarbon samples: for example, the dates of the three burning episodes identified by Dark (1998a) in her pollen profile M1. These have also been included as effective likelihoods in the overall model for human activity.

We have decided to use the agreement indices provided by OxCal (Bronk Ramsey 1995, 429; Bronk Ramsey 2009a, 356-7) for outlier detection in this analysis. This is because of the detailed information we have regarding, for example, sample chemistry, which means that in many cases we have information that allows us to choose an appropriate approach for modelling specific samples. However, we recognise that for the sediment profiles in particular, where we do not really have specific information that allows us to distinguish between reworked or intrusive material, an outlier approach might be more appropriate. It is not, however, possible to use a combination of these approaches in a single model and so we have judged that the advantages of using indices of agreement in this case outweigh the benefits of outlier modelling. The model presented has good overall agreement (Amodel: 65).

First, we begin by considering parts of the archaeological sequence which can be closely stratigraphically related to dated environmental profiles. This allows us to create age-depth models for the sediment sequences, which provide strong prior information for the anthropogenic and other dated samples that can be related to them. There are three such profiles, each of which has three or more radiocarbon measurements on samples that we know derive from the terrestrial biosphere. Each profile has been modelled using a Poisson-process age-depth model (Bronk Ramsey 2008, 43–7) with variable rigidity ((P_Sequence("",100,0U(-2,2))); Bronk Ramsey and Lee 2013, 723–6). This means that we assume that sedimentation was continuous but did not necessarily occur at an entirely uniform rate. The deviations from a constant accumulation rate are calculated by the model.

The first component is centred around a combined environmental profile from Dark's pollen and macrofossil profile M1 (Dark 1998a) and macrofossil profile VP85A/2010 (see Chapter 19), which can be related to the timbers of the central platform. The relative sequence of dated samples in this component is illustrated in Figure 17.3. The age-depth profile is shown in Figure 17.4. This profile includes measurements originally obtained by Dark (1998a, Table 17.1) with two additional dates from the sequence of macrofossil samples (Profile VP85-2010) taken immediately to the north (see Chapter 19). The boundaries of the Poisson-process model have been placed at the points on the environmental profile which reflect transitions to increasingly shallow and terrestrial conditions (i.e. *onset organics M1*, *start seasonal flooding M1*, and *onset fen carr M1*). This allows for the possibility that the sedimentation rate may have changed at these points. We have also estimated the dates of the burning episodes identified by Dark (1998a, 149) from the age-depth model. The start of burning episode 1 is dated by *OxA-3349*, but the other dates have been interpolated from their heights in the age-depth profile. A *terminus post quem* for the top of the profile is provided by CAR-1022, a measurement on a bulk sample of wood peat from a stratigraphically later context in pollen profile VP85A/3 recorded by Cloutman and Smith (1988, 46; Figure 6).

Parts of this environmental profile can be related to horizons in Cloutman's pollen profiles VP85A/2 and VP85A/3 (Cloutman and Smith 1988). The utility of his radiocarbon dates is limited by the fact that, perforce, he had to date bulk sediment samples, many of which came from deposits that contained aquatic material. These measurements may therefore include a component of hard-water error (Philippsen 2013), making the results anomalously old in comparison with fully terrestrial materials from the same deposits. For this reason, where it is probable that samples dated by Cloutman would contain aquatic material, these have been modelled as *termini post quos* for their deposits. *CAR-1027* and *CAR-1021* are earlier than *onset organics M1*, *CAR-1026* and *CAR-919* can be placed between *onset organics M1* and *start seasonal flooding*. Later than *start seasonal flooding M1* lie *CAR-1025* and *CAR-1024*. Above these are a date on an aurochs metatarsal 56 (OxA-1176) and

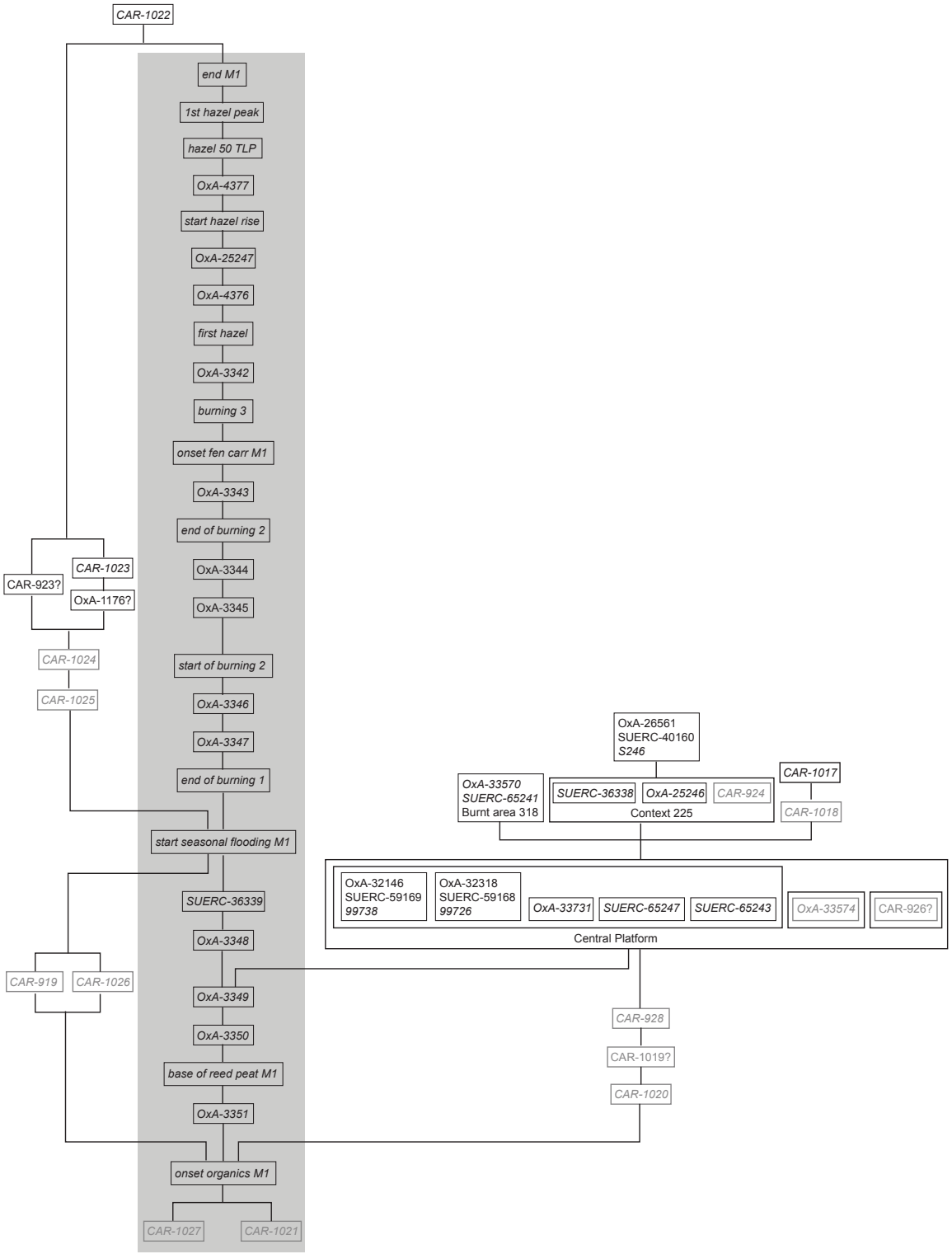

Figure 17.3: Harris matrix of dated samples from the component of the model including environmental profile M1 and VP85A 2010, the central platform, and stratigraphically related deposits (grey lettering, *termini post quos*; ?, excluded from model; grey shading, extent of age-depth model) (Copyright Historic England, CC BY-NC 4.0).

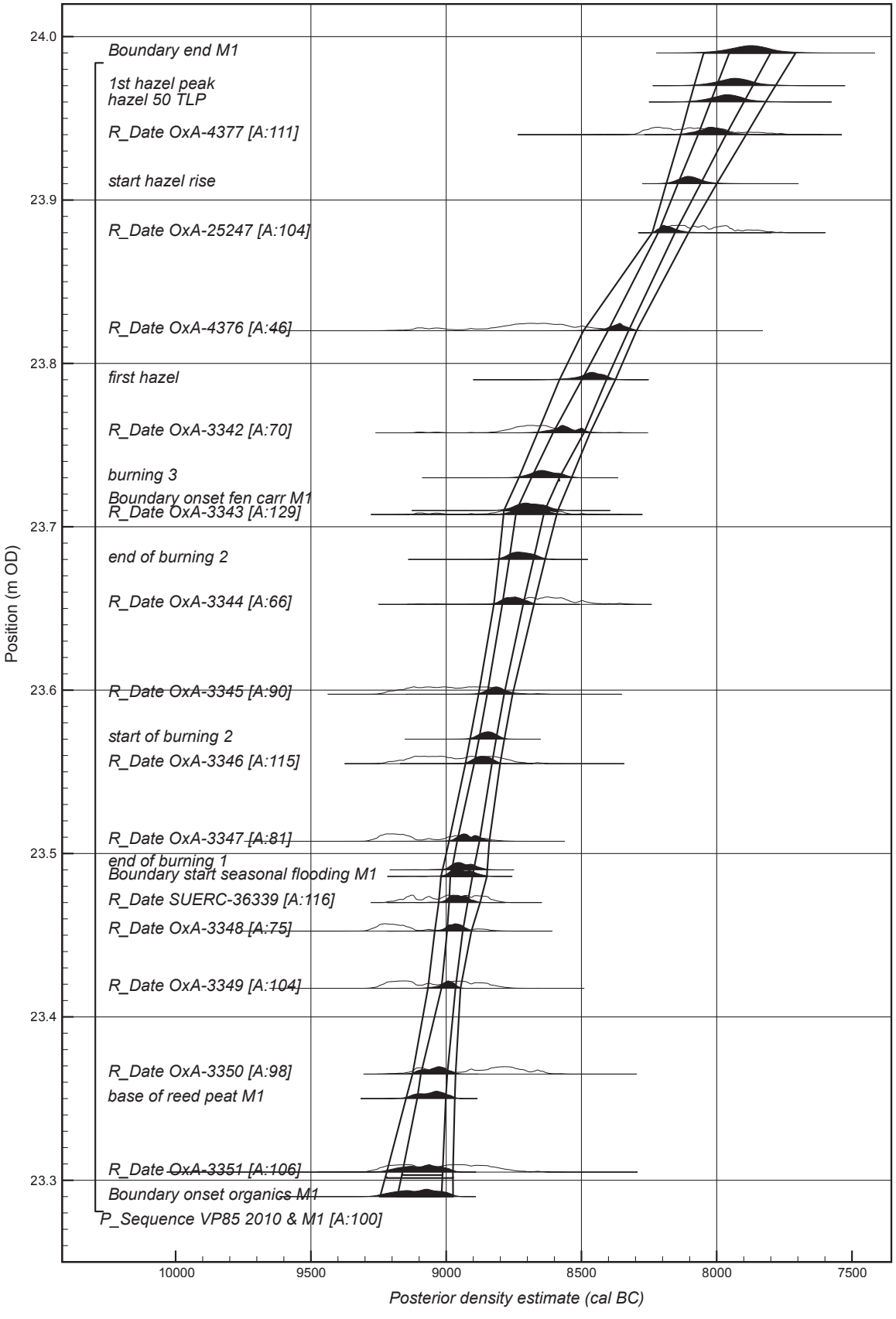
Boundary end M1
1st hazel peak
hazel 50 TLP
R_Date OxA-4377 [A:111]
start hazel rise
R_Date OxA-25247 [A:104]
R_Date OxA-4376 [A:46]
first hazel
R_Date OxA-3342 [A:70]
burning 3
Boundary onset fen carr M1
R_Date OxA-3343 [A:129]
end of burning 2
R_Date OxA-3344 [A:66]
R_Date OxA-3345 [A:90]
start of burning 2
R_Date OxA-3346 [A:115]
R_Date OxA-3347 [A:81]
end of burning 1
Boundary start seasonal flooding M1
R_Date SUERC-36339 [A:116]
R_Date OxA-3348 [A:75]
R_Date OxA-3349 [A:104]
R_Date OxA-3350 [A:98]
base of reed peat M1
R_Date OxA-3351 [A:106]
Boundary onset organics M1
P_Sequence VP85 2010 & M1 [A:100]
24.0
23.9
23.8
23.7
23.6
23.5
23.4
23.3
Position (m OD)
10000
9500
9000
8500
8000
7500
Posterior density estimate (cal BC)

the surrounding sediment (CAR-923), and a sample from an equivalent level in pollen profile VP85A/3 (*CAR-1023*). The measurements on OxA-1176 and CAR-923 diverge by more than 600 radiocarbon years. OxA-1176 is slightly too old for its stratigraphic position. It is possible that the aurochs metatarsal was reworked from an earlier deposit. However, we think that this is unlikely as contemporary assemblages of bone would have been sealed by substantial deposits of peat by this time. Given the demonstrable technical challenges of producing accurate radiocarbon dates on bone samples from Star Carr, we therefore think it is likely that this measurement is anomalously old. OxA-1176 was prepared using the gelatinisation and ion-exchange protocol (Hedges and Law 1989; Law and Hedges 1989), and it is possible that chemicals from the ion-exchange column may have contaminated the sample (Hedges and Pettitt 1998). CAR-923 seems to be anomalously recent for its position within the reed peat in comparison with SUERC-65223, which dates the top of this layer in the nearby environmental profile 3178 (see below). For this reason it has been excluded from the model. All three samples at this height are earlier than *CAR-1022*. A sequence of samples, *CAR-1020*, CAR-1019 and *CAR-928*, fall between *onset organics M1* and *central platform*. CAR-1019 is anomalously recent and has been excluded from the model. The central platform is also stratigraphically later than the level in the M1 profile dated by *OxA-3349*. This is a conservative reading that allows for uncertainties in the relationship between the platform and the dated samples in the environmental profiles.

Seven timbers have been dated from the three layers of the central platform (Chapter 6). Of these CAR-926 (a measurement obtained by Cloutman and Smith on an unidentified timber from the platform) seems to be anomalously recent and has been excluded from the model. *OxA-33574,* a measurement on timber <103111>, is slightly earlier than the other dated timbers and may have been salvaged from the surrounding swamp (and have been several hundred years old when incorporated in the platform; *reuse central*; Figure 17.19). The radiocarbon measurements on the other five timbers are statistically consistent (T'=3.4; T'(5%)=9.5; ν=4; Ward and Wilson 1978). Though it was made up of three layers, the timbers lay directly on top of one another with no intervening sediment. As such, we believe the platform was constructed as a single event, and so we have combined the dates on its timbers. This suggests that the central platform was constructed in *8985–8925 cal BC (95% probability; central platform*; Figure 17.14), probably in *8970–8940 cal BC (68% probability)*.

Stratigraphically later than the platform was a discrete concentration of charcoal (318) which appears to be associated with a dense scatter of worked flint generated through the manufacture of a number of axes (Chapters 8 and 32). Several environmental samples are also later than the platform: *SUERC-36338*, and *OxA-25246*, which were collected from deposits overlying the timbers during the 2010 excavations, and *CAR-924* from comparable deposits excavated in 1985 (Cloutman and Smith 1988). These dates are, in turn, earlier than *S246*, a twig from the overlying sediment. Also later than the central platform are *CAR-1018* and *CAR-1017*, from Cloutman's VP85A/2 pollen profile (Cloutman and Smith 1988). *CAR-924 and CAR-1018* were bulk sediment samples that could have contained a component of aquatic plant material and so, conservatively, have been incorporated in the model as *termini post quos*.

The second sediment profile that can be related stratigraphically to archaeological activity is Profile 3178, a vertical sequence of macrofossil samples taken from the north-facing section of trench SC34 and adjacent to the southern edge of the debris scatter (Chapter 19). Six radiocarbon measurements are available from four levels in this sequence, although unfortunately a further six failed in laboratory processing. The relative sequence of dated samples in this component is illustrated in Figure 17.5. The age-depth model for profile 3178 is shown in Figure 17.6 and the phase of use of the detrital wood scatter is shown in Figure 17.7.

Five samples of bone and antler (*SUERC-66181, OxA-33671, OxA-33673,* <*108967*> and <*108966*>) and two samples of waterlogged wood (*SUERC-59178–9),* from the detrital wood scatter within the fine detrital

Figure 17.4 (page 60): Probability distributions of radiocarbon dates in the age-depth model for environmental profile M1 and VP85A 2010. Each distribution represents the relative probability that an event occurs at a particular time. For each of the dates two distributions have been plotted: one in outline, which is the result of simple radiocarbon calibration, and a solid one, based on the chronological model used. Distributions other than those relating to particular samples correspond to aspects of the model. For example, the distribution '*onset organics M1'* is the estimated date when organic sedimentation began at this location. The overall model is defined exactly in Appendix 17.1 .

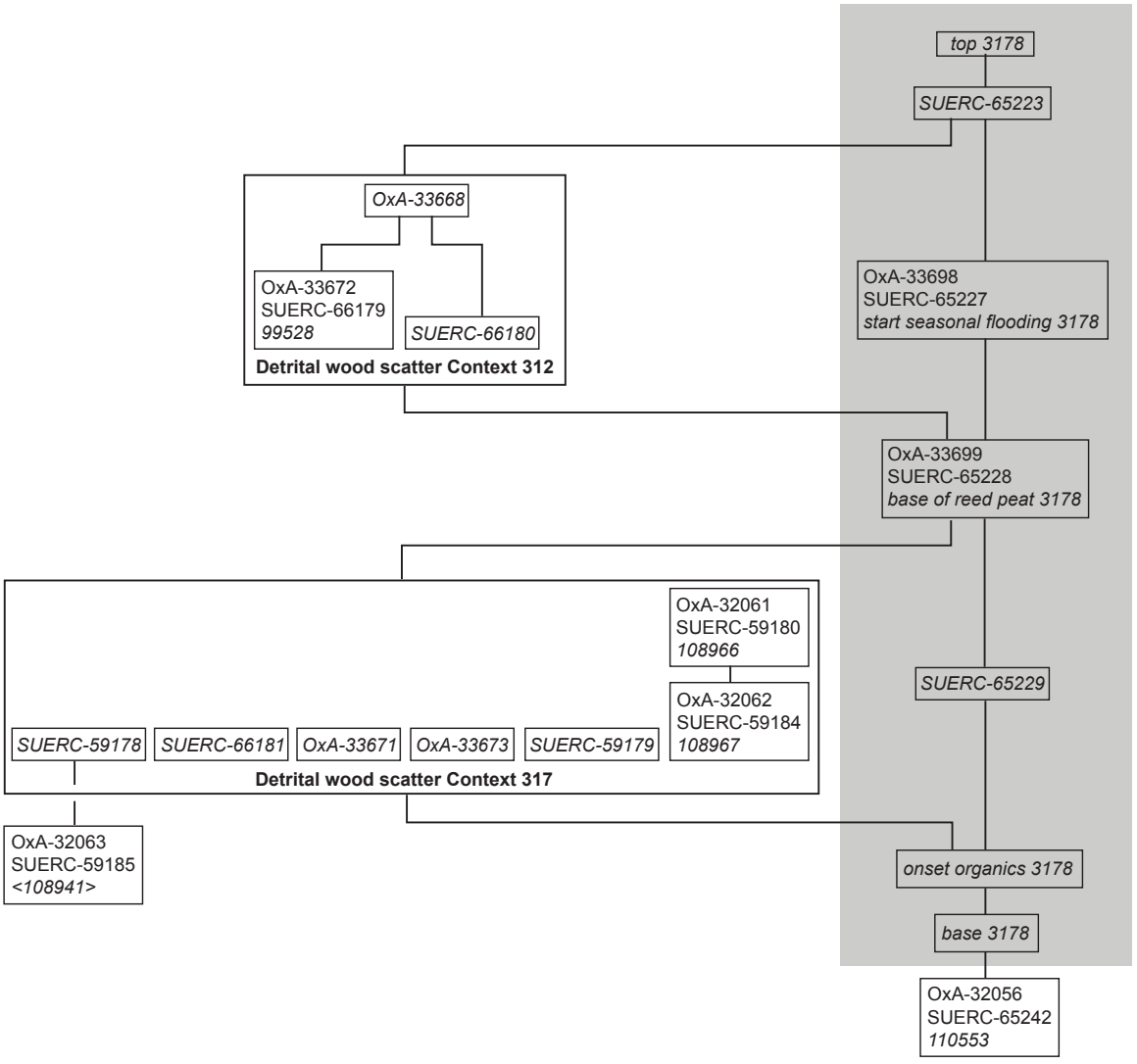

Figure 17.5: Harris matrix of dated samples from the component of the model including environmental profile 3178, the detrital wood scatter and stratigraphically related deposits (grey lettering, *termini post quos*; ?, excluded from model; grey shading, extent of age-depth model) (Copyright Historic England, CC BY-NC 4.0).

mud (317) have been dated (Chapters 6 and 7). These are stratigraphically later than *onset organics 3178* and earlier than *base of reed peat 3178*. Unshed red deer antler <*108967*> is physically below elk antler <*108966*>. Above this was recorded an unworked waterlogged timber (*SUERC-59179*), although the relevant radiocarbon measurements are incompatible with this sequence and this timber seems to have been displaced. <*108967*> is recorded as lying above a radially split timber <*110553*> from the underlying sand (320). There are two statistically consistent measurements on this timber (OxA-32056 and SUERC-65242; T'=0.4; T'(5%)=3.8; ν=1).

Figure 17.6 (page 63): Probability distributions of radiocarbon dates in the age-depth model for environmental profile 3178. The format is as Figure 17.4. The overall model is defined exactly in Appendix 17.1 (Copyright Historic England, CC BY-NC 4.0).

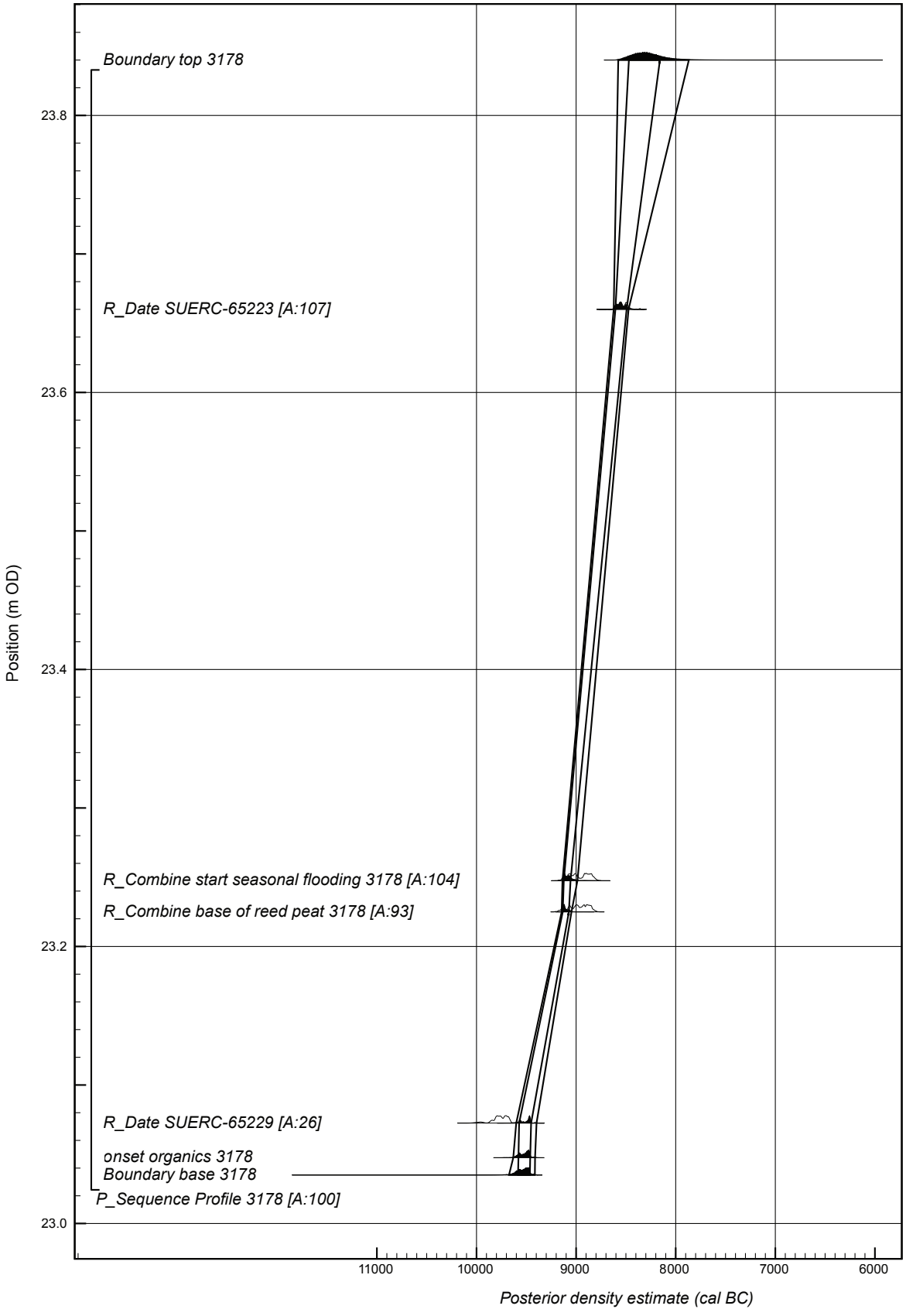
Boundary top 3178
R_Date SUERC-65223 [A:107]
R_Combine start seasonal flooding 3178 [A:104]
R_Combine base of reed peat 3178 [A:93]
R_Date SUERC-65229 [A:26]
onset organics 3178
Boundary base 3178
P_Sequence Profile 3178 [A:100]
Position (m OD)
23.8
23.6
23.4
23.2
23.0
11000
10000
9000
8000
7000
6000
Posterior density estimate (cal BC)

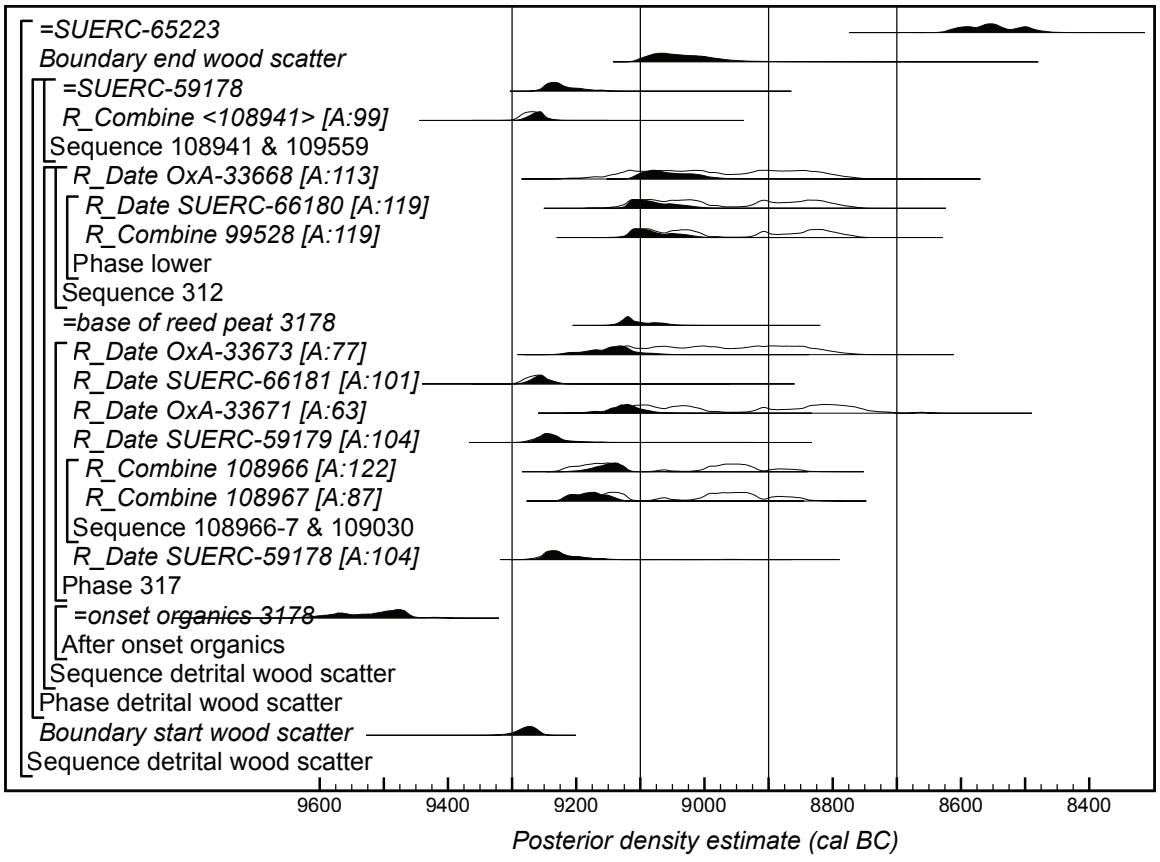

Figure 17.7: Probability distributions of radiocarbon dates from the detrital wood scatter. The format is as Figure 17.4. The overall model is defined exactly in Appendix 17.1 (Copyright Historic England, CC BY-NC 4.0).

However, their weighted mean (9989±25BP) is far earlier than any other anthropogenic sample dated from Star Carr. Given that there are two statistically consistent measurements from two different laboratories it seems unlikely that the measurements are in error, and these results are compatible with this timber being earlier than *onset organics 3178*. This makes it unlikely that the timber is part of the detrital wood scatter that has been pushed down into the underlying sand. This leaves two possibilities: either the timber was not worked and the recording is in error (which we do not think is likely), or it represents an earlier episode of human activity at the edge of the lake. One further sample has been dated from the lower part of the detrital wood scatter, an elk skull *<108941>* (Chapter 7), which lay at the interface between the basal sands (320) and the overlying fine detrital mud (317) and below the timber dated by *SUERC-59178*. *<108941>* has been included in the model for the detrital wood scatter, but we do not know its relationship to *onset organics 3178*. The detrital wood scatter continues into the overlying reed peat (312) where there are measurements on an antler frontlet and aurochs bone (*<99528>* and *SUERC-66180*) and on a birch bark roll from a higher level within the same deposit (*OxA-33668*). The detrital wood scatter ends before *top 3178*.

The third sediment profile that can be related stratigraphically to archaeological activity is Profile CII/2010, a vertical sequence of macrofossil samples taken from the west-facing section of Clark's cutting II. Five radiocarbon measurements are available from three dated levels. The relative sequence of dated samples in this component is illustrated in Figure 17.8. The age-depth model for profile CII/2010 is shown in Figure 17.9 and the model for the human activity represented by the worked material within the brushwood is shown in Figure 17.10. The earliest dated archaeological material that can be associated to this profile comes from a deposit of *Salix/Populus* sp. roundwood recorded immediately to the east of cutting II in 2013. This has been referred to as brushwood, though the deposit actually represents an accumulation of both unworked and

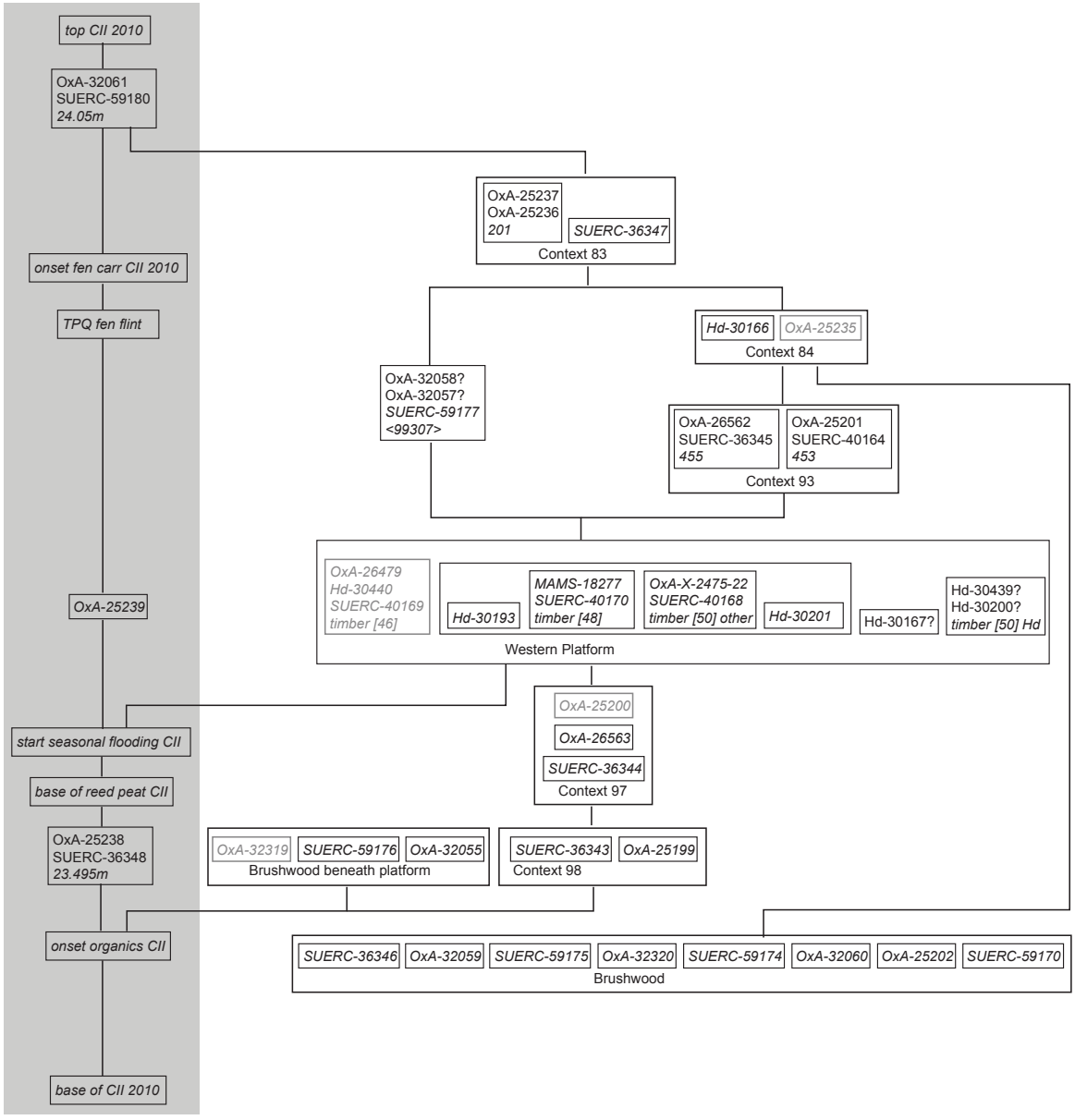

Figure 17.8: Harris matrix of dated samples from the component of the model including environmental profile CII 2010, the western platform and stratigraphically related deposits (grey lettering, *termini post quos*; ?, excluded from model; grey shading, extent of age-depth model) (Copyright Historic England, CC BY-NC 4.0).

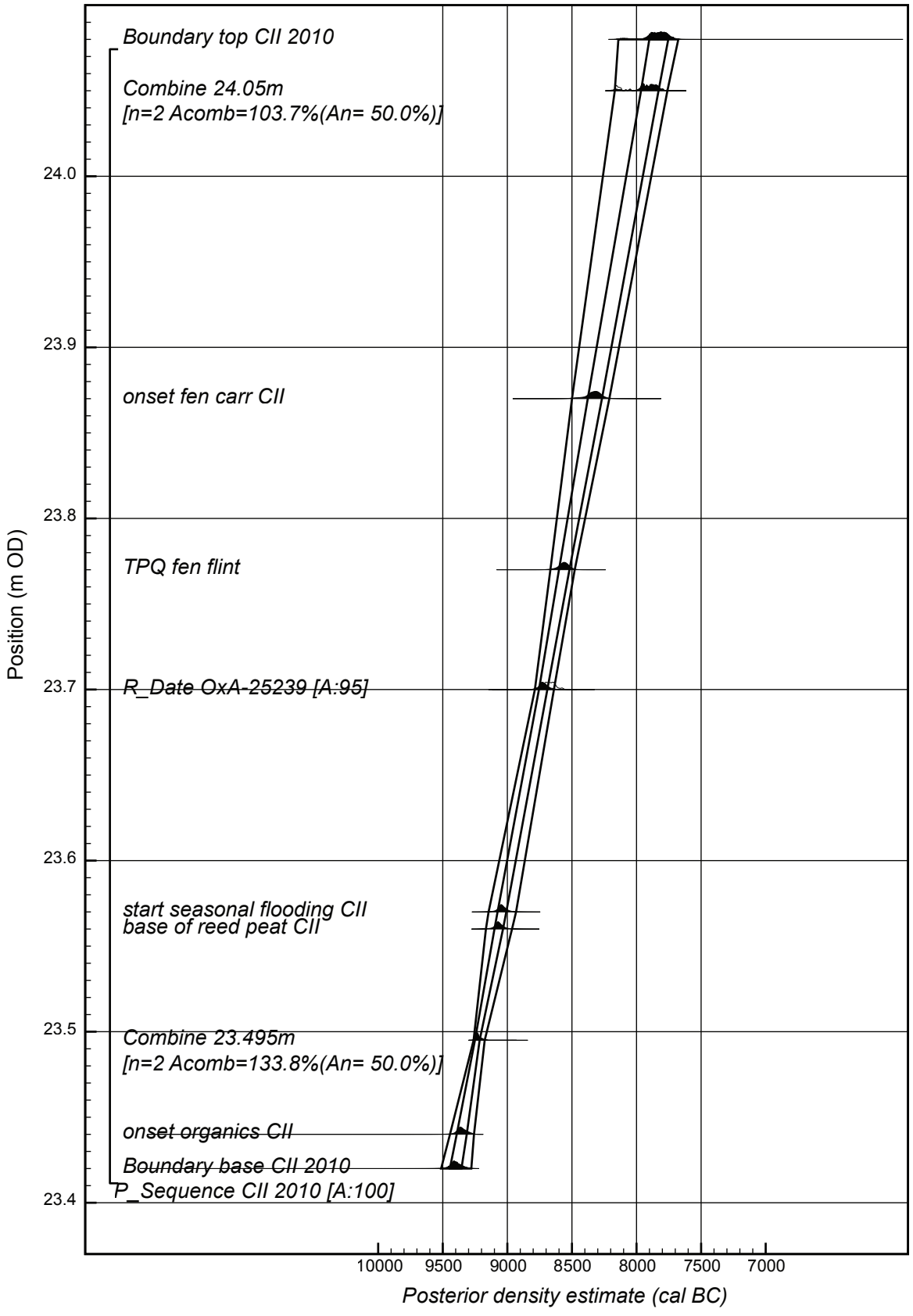
Boundary top CII 2010
Combine 24.05m
[n=2 Acomb=103.7%(An= 50.0%)]
onset fen carr CII
TPQ fen flint
R_Date OxA-25239 [A:95]
start seasonal flooding CII
base of reed peat CII
Combine 23.495m
[n=2 Acomb=133.8%(An= 50.0%)]
onset organics CII
Boundary base CII 2010
P_Sequence CII 2010 [A:100]
Position (m OD)
24.0
23.9
23.8
23.7
23.6
23.5
23.4
10000
9500
9000
8500
8000
7500
7000
Posterior density estimate (cal BC)

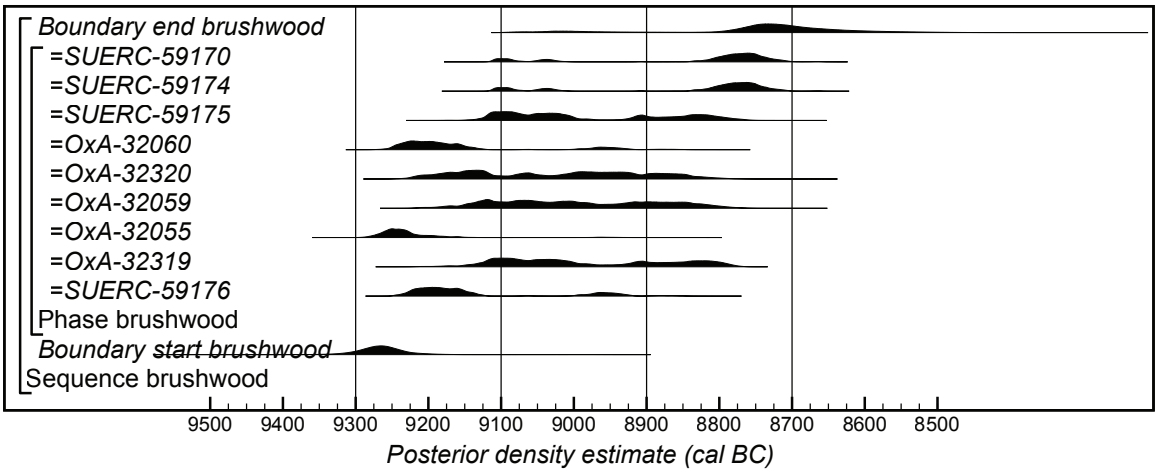

Figure 17.10: Probability distributions of radiocarbon dates from the brushwood. The format is as Figure 17.4. The overall model is defined exactly in Appendix 17.1 (Copyright Historic England, CC BY-NC 4.0).

anthropogenically modified roundwood. This material has accumulated through a combination of natural processes (falling from trees at the lake shore) and human agency. The modified material dates a phase of human activity in this area of the site that included the trimming and working of roundwood.

One sample of worked roundwood (*OxA-32319*) has been dated from the basal sand (320). This provides a *terminus post quem* for the overlying western platform. Later than *onset organics CII*, seven samples have been dated from the final detrital mud (97=317) and twiggy layer (98) beneath the platform. These comprise two further samples of worked roundwood (*SUERC-59176* and *OxA-32055*) and three waterlogged twigs (*OxA-25200, OxA-26563* and *SUERC-36344*) from the fine detrital mud and two waterlogged twigs (*OxA-25199* and *SUERC-36343*) from the twiggy layer. One of the twigs (*OxA-25200*) seems to have been reworked and has been modelled as a *terminus post quem* for the overlying deposits. The western platform is also stratigraphically later than *start seasonal flooding CII,* based on the position of the worked timbers in cutting II relative to the macrofossil profile CII/2010.

Six worked timbers have been dated from the western platform (Chapter 6). Considerable difficulties have been encountered in producing accurate radiocarbon measurements on this material. Statistically consistent groups of measurements are available from timber <46> (Hd-30440, SUERC-40169, and OxA-26479; T'=0.3, T' (5%)=6.0, ν=2) and timber <48> (MAMS-18277 and SUERC-40170; T'=2.0, T' (5%)=3.8, ν=1). The measurements on timber <50>, however, are widely divergent (SUERC-40168, OxA-X-2475-22, Hd-30200, and Hd-30439; T'=35.9, T' (5%)=7.8, ν=3). The two measurements from Heidelberg are statistically consistent (T'=3.2, T' (5%)=3.8, ν=1) as are the two measurements from Oxford and East Kilbride (T'=0.4, T' (5%)=3.8, ν=1). However, the Heidelberg dates are anomalously recent in comparison to dates from material stratified above them. It seems that the Acid-Base Acid pretreatment protocol used at Heidelberg was not always effective, and that a bleaching step was required for this material. Hd-30167 from timber <418> seems to be anomalously recent for the same reason. Excluding these three measurements we have accurate dates on five timbers from the western platform. However, timber <46> is significantly earlier than the others (T'=41.5, T' (5%)=9.5, ν=4) and appears to have been salvaged from an earlier episode of activity (and to have been some decades old when reused; *reuse western*; Figure 17.19). The remaining radiocarbon measurements on the other four

Figure 17.9 (page 66): Probability distributions of radiocarbon dates in the age-depth model for environmental profile CII 2010. The format is as Figure 17.4. The overall model is defined exactly in Appendix 17.1 (Copyright Historic England, CC BY-NC 4.0).

timbers are statistically consistent (T'=3.2, T' (5%)=7.8, ν=3). Although it was made up of several layers of wood, there was no intervening sediment and there was little vertical variation between the timbers. For these reasons we believe the platform was constructed as a single event, and so we have combined the dates on its timbers. This suggests that the western platform was constructed in *8805–8755 cal BC* (*95% probability; western platform*; Figure 17.14), probably in *8795–8765 cal BC (68% probability)*.

Lying on the surface of the platform were two pieces of roundwood (*453* and *455*) that must post-date its construction. In the overlying deposit, two samples of roundwood have been dated (*Hd-30166* and *OxA-25235*), although the latter appears to be reworked. Difficulties were also encountered in obtaining accurate measurements on the bark mat <99307> recovered from the reed peat above the platform (Chapter 30). The three measurements are not statistically consistent (T'=11.4, T' (5%)=6.0, ν=2). The Oxford measurements are anomalously old for their position in the stratigraphic sequence, but the *SUERC-59177* has good agreement with its position in the model (A: 109). Overlying all these samples are dates on a piece of waterlogged round wood (*SUERC-36347*) and a waterlogged *Corylus avellana* nut shell (*201*) from the overlying sediment. Stratigraphically later than these are the dates on macrofossils from *24.05m* at the top of Profile CII/2010.

Three more pieces of worked roundwood have been dated from brushwood recovered from the reed peat above the western platform (*OxA-32059*, *OxA-32320*, and *SUERC-59175*). However, the results are too early for this stratigraphic position and the wood appears to be reworked. They have thus been placed within the phase of human activity represented by the worked material within the brushwood (see above) and are later than *onset organics CII* and earlier than *Hd-30166* and *OxA-25235* from the overlying context. Five further samples of brushwood have been dated. Whilst these cannot be securely related stratigraphically to the western platform they must also fall within these stratigraphic boundaries. Two of these (*SUERC-36346* and *OxA-25202*) are unworked and simply provide constraints for the sequence. However, the other three have been humanly modified (*OxA-32060*, *SUERC-59170*, and *SUERC-59174*) and so, again, have been placed within the phase of human activity represented by the worked material within the brushwood.

One further sequence of natural deposits must be described before we outline the model for human activity at Star Carr. This is the sequence of samples recovered from trench SC22, the most easterly of the excavated trenches. The relative sequence of dated samples in this component is illustrated in 17.11. Four pieces of unworked roundwood have been dated from the coarse reed peat in the lower part of this trench (*Hd-30190, Hd-30168, <82705>, <82706>*). The two measurements on roundwood <82706> are statistically significantly different (T'=14.1, T' (5%)=3.8, ν=1). OxA-26478 appears to be anomalously old and has been excluded from the model. Four samples have been dated from the overlying context. Two pieces of roundwood (*SUERC-36355* and *OxA-25088*), the latter of which appears to be reworked, and two pieces of worked antler (OxA-16809–10), which produced anomalously young ages due to the incomplete removal of contaminants (see Table 17.3). Between these dated samples and those from the overlying context lay a scatter of worked flint, some of which was associated with one of the pieces of worked antler. The date of this assemblage has been estimated from the sequence of deposits and the surrounding radiocarbon dates (*SC22 scatter*). Four pieces of waterlogged wood were dated from the overlying wood peat; two of these appear to have been reworked (*SUERC-36356*; *roundwood 4.2*), whilst the others (*Hd-30192* and *SUERC-40163*) appear to provide reliable dates for this deposit.

We now return to the overall structure of the model for the chronology of human activity at Star Carr (Figure 17.2). The components of this model are either spatially discrete phases of human activity or discrete episodes. Where we have four or more effective likelihoods for a phase of activity these have been placed within boundaries so that they do not disproportionately affect the model outcomes. These likelihoods either cross-refer to the sequences already described (in which case they incorporate the constraints of those sequences) or are radiocarbon dates on anthropogenic samples (which may themselves be further constrained by limiting dates). For example, the phase of activity represented by the worked wood within the brushwood is represented by samples which cross-refer to the sequence illustrated in Figure 17.8. In contrast, Clark's area (Figure 17.15) is represented by samples which are unrelated to the stratigraphic sequences so far described. Some components, for example, that relate to the date of artefacts from VP85A (Figure 17.13) incorporate a mixture of the two.

The posterior distributions for the burning episodes identified by Dark (1998a) in her profile M1 are shown in Figure 17.12 and are derived from the age-depth sequence shown in Figure 17.4. One sample of sediment from around an artefact in VP85A (*CAR-924*) appears in the sequence illustrated in Figure 17.3. Additionally *CAR-925* dates the deposition of barbed point <245>, and *CAR-930*, which may have contained a component

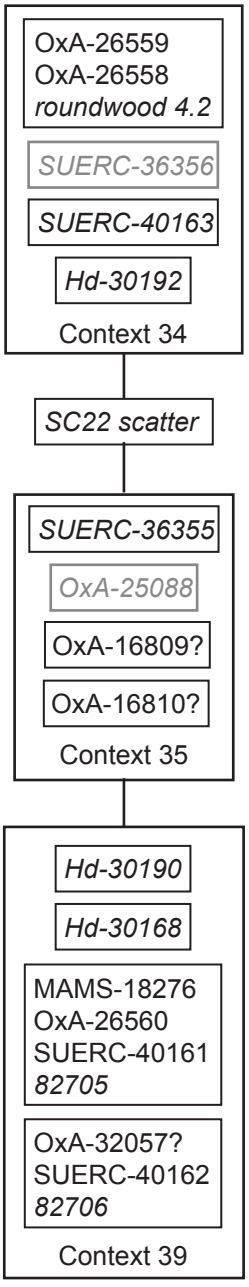

Figure 17.11: Harris matrix of dated samples from the component of the model in trench SC22 (grey lettering, *termini post quos*; ?, excluded from model; grey shading, extent of age-depth model) (Copyright Historic England, CC BY-NC 4.0).

of aquatic macrofossils, provides a *terminus post quem* for charcoal find <153>. A sequence of samples are available from around antler <216>; *CAR-922* from sediment around the artefact itself, is constrained by dates from sediment below (*CAR-1047*) and above (*CAR-1050*). This component of the model is shown in Figure 17.13.

The component for activity producing the detrital wood scatter (Figure 17.7) cross refers to dates for the onset of organic sedimentation and the base and top of the reed peat in Profile 3178 (Figure 17.6), and the

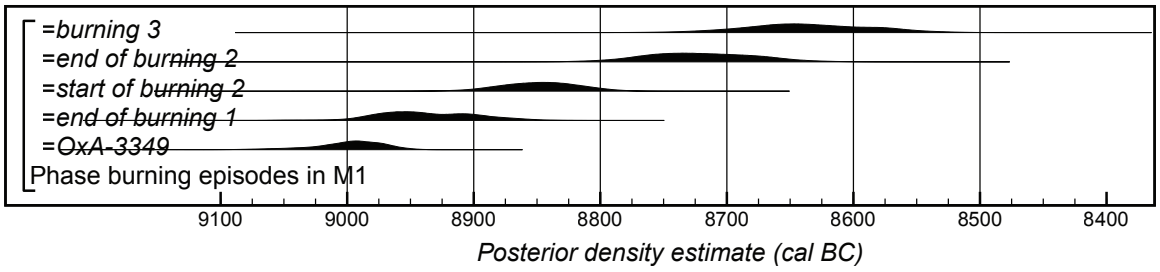

Figure 17.12: Probability distributions for the dates of the burning episodes identified in environmental profile M1 (*OxA-3349* dates the start of burning 1). The format is as Figure 17.4. The overall model is defined exactly in Appendix 17.1 (Copyright Historic England, CC BY-NC 4.0).

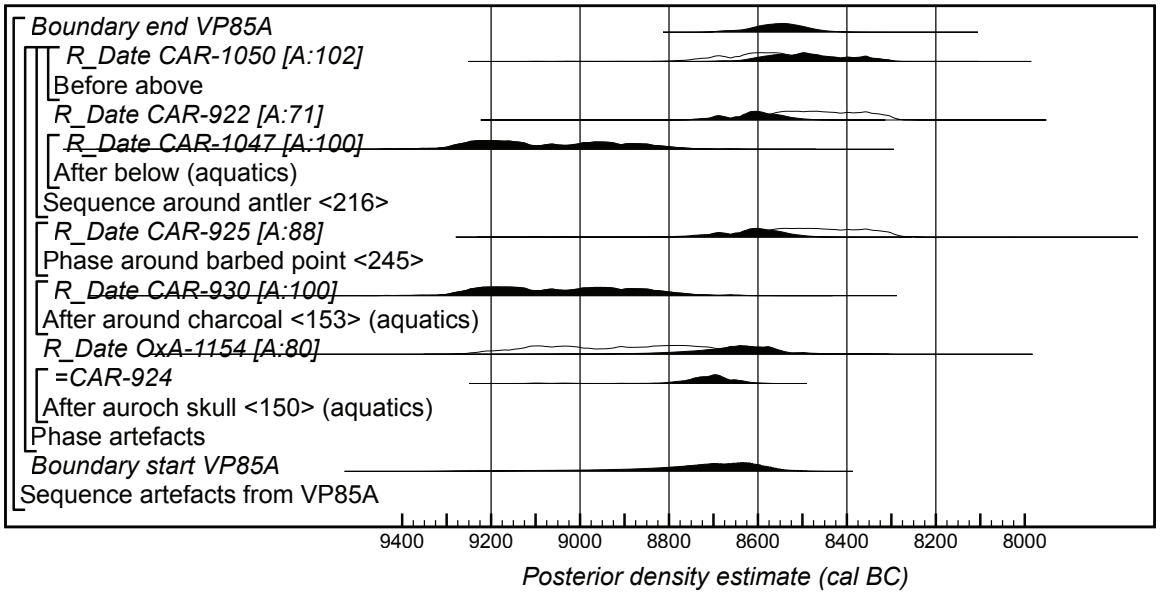

Figure 17.13: Probability distributions for the dates of artefacts found in trench VP85A. The format is as Figure 17.4. The overall model is defined exactly in Appendix 17.1 (Copyright Historic England, CC BY-NC 4.0).

component relating to activity represented by the worked wood in the brushwood layer (Figure 17.10) cross refers to the sequence illustrated in Figure 17.8.

The dates for the three platforms are shown in Figure 17.14. That for the western platform cross-refers to the sequence illustrated in Figure 17.8, and that for the central platform to the sequence illustrated in Figure 17.3. A single radiocarbon date *OxA-33662* on timber <113252> is available from the eastern platform. This timber is stratigraphically later than a bulk sample of waterlogged birch fruits and catkin scales from the underlying fine detrital mud (*SUERC-66037*). It also overlies the start of seasonal flooding recorded in the macrofossil profile taken from below this timber, which corresponds to the same dated horizon in the nearby environmental profile VP85A/2010 (Figure 17.4; *start seasonal flooding M1*). Above timber <113252> lay a waterlogged seed of *Prunus padus* and a fallen tree <113251> (*OxA-33713* and *SUERC-66036*). This suggests that the eastern platform was constructed in *8945–8760 cal BC (95% probability; OxA-33662*; Figure 17.14), probably in *8915–8895 cal BC (9% probability)* or *8880–8795 cal BC (59% probability)*.

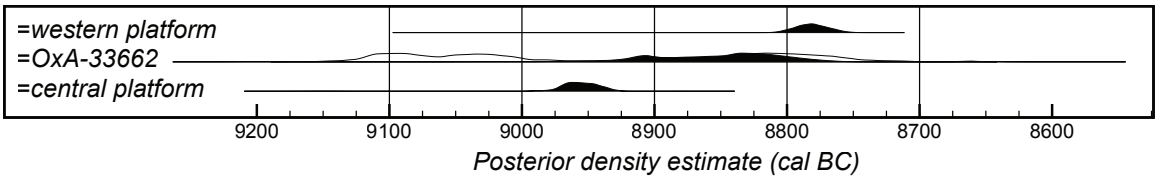

Figure 17.14: Probability distributions for the construction dates of the platforms. The format is as Figure 17.4. The overall model is defined exactly in Appendix 17.1 (Copyright Historic England, CC BY-NC 4.0).

Eight samples of worked bone and antler have been dated from the dense concentration of material culture recorded in 2015 between Clark's cuttings I and II, and the area to the south of Clark's excavations (Chapter 3) (*OxA-33674–7; SUERC-66177–8, SUERC-66182* and *SUERC-66186–7*). A further four samples have been dated from artefacts recovered by Tot Lord from the section of cutting II immediately after Clark's fieldwork (Dark et al. 2006). We believe that these derive from the same deposit of artefacts. These four artefacts were originally dated using the ion-exchange protocol at Oxford (Hedges and Law 1989; Law and Hedges 1989; OxA-4450, OxA-4451, OxA-4577–8). Replicate measurements were undertaken on these samples using the ultrafiltration protocol at Oxford described by Bronk Ramsey et al. (2000), although these samples had to be re-ultrafiltered and dated when the original protocol was found to be problematic (OxA-10808–9). All four samples were dated a third time using the improved ultrafiltration protocol at Oxford described by Bronk Ramsey et al. (2004a) (OxA-21236–9). The replicate measurements on each artefact are statistically consistent (Table 17.3), if OxA-4450 is considered to be anomalously recent. OxA-4451 is also considerably more recent than the other measurements on antler splinter <460>, and so OxA-4450 and OxA–4451 are both excluded from the model.

The radiocarbon dates on these artefacts form a very tight group, and indeed the radiocarbon ages on 11 of them are statistically consistent (T'=7.9, T'(5%)=18.3, ν=10), all but the weighted mean on frontlet <115876> (T'=22.9, T'(5%)=19.7, ν=11). This is compatible with these 11 artefacts being of exactly the same calendar date—potentially deriving from a single episode of deposition. This consistency is striking, and in our view there are two possible explanations. Either the weighted mean of the measurements on frontlet <115876> (SUERC-66177 and OxA-33674) is a statistical outlier, in which case the entire deposit is the result of one massive, very short episode of deposition, or over 90% of the material was deposited in such a concentrated period, but a small number of artefacts were deposited over the following decades. The component shown in Figure 17.15 incorporates the second reading, estimating the date of the concentrated deposition represented by the 11 artefacts with statistically consistent ages. <115876> is included separately as a discrete episode of deposition (Figure 17.17).

The model estimates that bone and antler artefacts began to be placed in Clark's deposition area in *9125–9090 cal BC (4% probability; start Clark area*; Figure 17.15) or *8915–8775 cal BC (91% probability)*, probably in *8850–8800 cal BC (68% probability)*. This deposition ended in *9100–9075 cal BC (3% probability; end Clark area;* Figure 17.15) or *8830–8710 cal BC (92% probability)*, probably in *8810–8755 cal BC (68% probability)*. It accumulated over a period of *1–145 years (95% probability; use Clark area;* Figure 17.19), probably for a period of *1–65 years (68% probability*). However, it is clear from the shape of the posterior distribution (Figure 17.19) that a very short duration is probable. It should be noted that the bone and antler artefacts were recovered from within the fine detrital mud, with many artefacts lying on the basal sand.

A macrofossil profile recorded through Clark's area shows that the assemblage lies within sediments that formed in reed swamp in permanently standing water (Environmental Zone 1). However, it is *98% probable* that *start Clark area* (Figure 17.15) post-dates the transition to the shallower (potentially seasonally flooded) swamp in the adjacent, dated macrofossil profile CII/2010 (*onset seasonal flooding CII;* Figure 17.9). This suggests that the dated artefacts (and presumably the entire assemblage) must have sunk into the deposits from which they were recorded.

Four birch bark rolls (*OxA-33667, 115195* and *SUERC-66048–9*), from the reed peat in the vicinity of Clark's area have also been dated. This clearly evidences human activity in this area both before and after the deposition

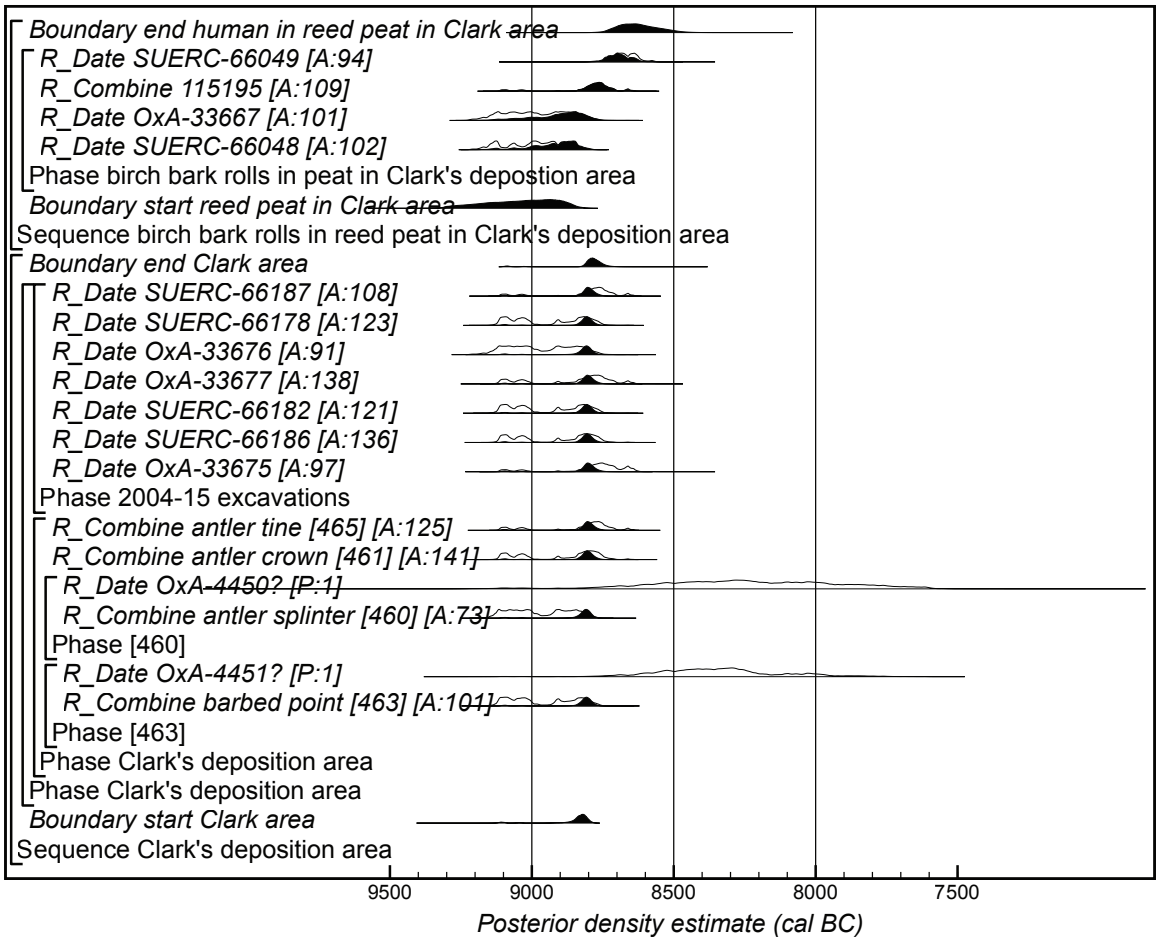

Figure 17.15: Probability distributions of dates on bone and antler artefacts in Clark's area, and carbonised birch bark rolls in reed peat in this location. The format is as Figure 17.4. The overall model is defined exactly in Appendix 17.1 (Copyright Historic England, CC BY-NC 4.0).

of Clark's area (Figure 17.15). However, these birch bark rolls were all found at or above the levels of the artefacts in Clark's area. This indicates that the lighter birch bark rolls have not sunk.

Four samples on anthropogenic materials have been dated from the peat over marl in the area to the south of the western platform (*SUERC-66044*, *SUERC-66046* and *OxA-33666* on birch bark rolls, and *OxA-33678* on a tooth from the skeleton of a domestic dog; Figure 17.16). All four samples are later than *SUERC-36349*, a fragment of burnt reed from a bulk sample of the underlying reed peat and earlier than waterlogged twigs from an overlying layer of wood peat (*SUERC-36353* and *OxA-25241*).

A sequence of four birch bark rolls have been dated from deposits to the north of Clark's cutting III (bead manufacturing area; see Chapter 33) (Figure 17.16). *SUERC-66039* and *OxA-33663* come from the reed peat at a similar height of a base of a substantial flint scatter. *OxA-33664* and *SUERC-66043* come from the lower part of the overlying wood peat, within and towards the top of the flint scatter.

Figure 17.17 shows date estimates for dispersed episodes of human activity within the wetlands. These are simply constrained to be part of the overall period of human activity at Star Carr (Figure 17.2). The estimated date for burnt area (318) has been cross referenced from the sequence illustrated in Figure 17.3. The date on the bark mat (*SUERC-59177*) and the *terminus post quem* for the deposition of the fen flint interpolated from the age-depth model for CII/2010 (Figure 17.7), have been cross referenced from the sequence illustrated in Figure 17.8. The date for the flint scatter in SC22 (*SC22 scatter*) has been cross referenced from the sequence illustrated in Figure 17.11. Samples from two domesticated dogs (*OxA-V-994-33* and *KIA-307034*) and a resin cake (*OxA-2343*) from Clark's original excavations have been dated by previous researchers (Schulting and

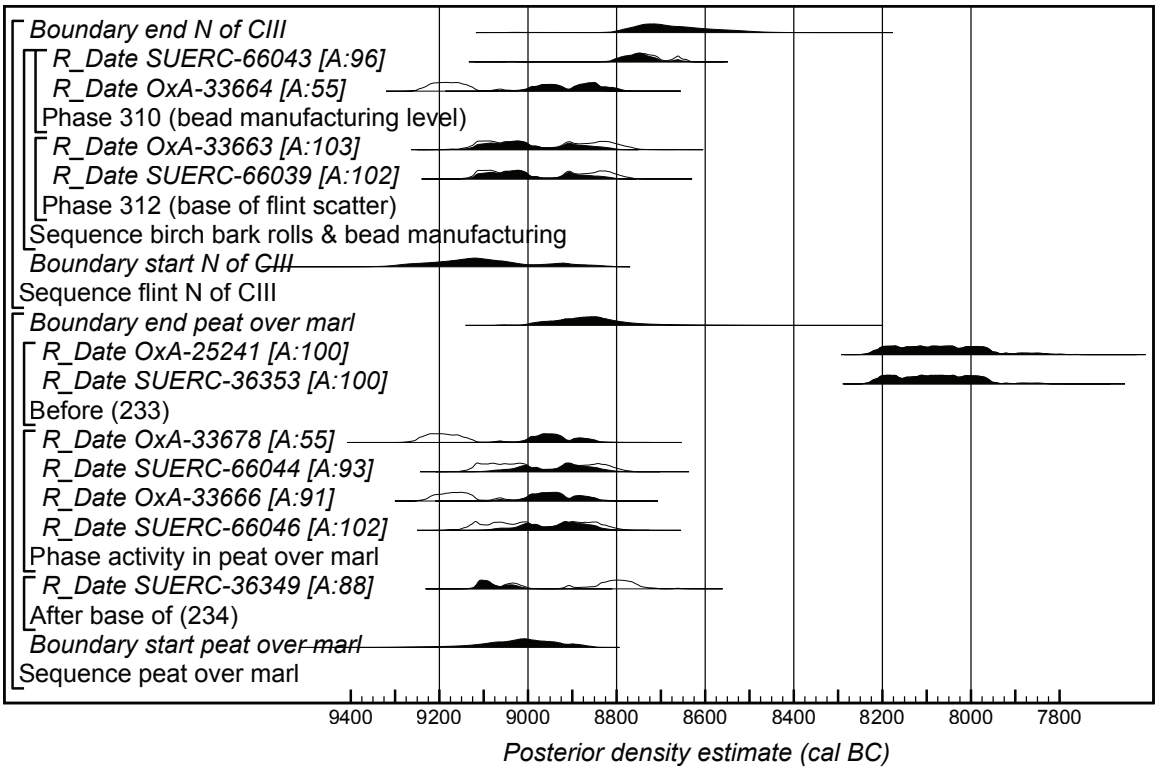

Figure 17.16: Probability distributions of dates on samples from the peat over the marl in the area south of the western platform, and from peat to the north of Clark's cutting III. The format is as Figure 17.4. The overall model is defined exactly in Appendix 17.1 (Copyright Historic England, CC BY-NC 4.0).

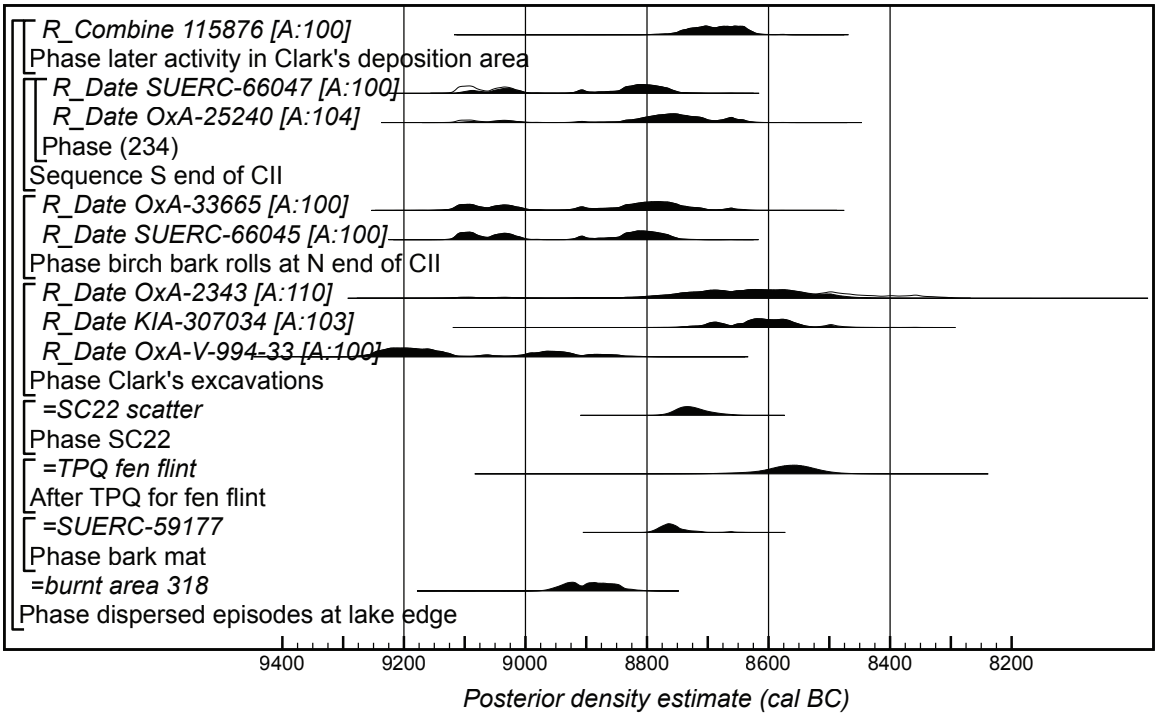

Figure 17.17: Probability distributions of dates on samples from dispersed human activities along the lake edge. The format is as Figure 17.4. The overall model is defined exactly in Appendix 17.1 (Copyright Historic England, CC BY-NC 4.0).

Richards 2009; Hedges et al. 1994; Roberts et al. 1998). Dates are also available on two birch bark rolls from the wood peat at the north end of cutting II (*SUERC-66045* and *OxA-33665*), and on a sample from the water-logged bow (*OxA-25240*) and a birch bark roll (*SUERC-66047*) from the reed peat to the south of the same trench, cross referenced from the sequence shown in Figure 17.16. Frontlet <*115876*>, which we interpret as later activity in the vicinity of Clark's deposition area is also placed in this component.

Finally, we consider the dates from the structures excavated on the dryland part of the site (Figure 17.18). Datable material was scarce, consisting of tiny fragments of carbonised wood only. Four statistically consistent measurements (T'=2.4, T'(5%)=7.8, ν=3) are available from postholes [177] and [181] and the central depression of the eastern dryland structure (*OxA-33700, SUERC-65232–3,* and *SUERC-65237).* Four statistically consistent measurements (T'=1.2, T'(5%)=7.8, ν=3) are also available from postholes [507] and [515] of the western dryland structure (*OxA-33571, OxA-33703, SUERC-65222* and *SUERC-65230).* Two intrusive, modern fragments of charcoal were dated from posthole [411] (SUERC-65231 and OxA33598; Table 17.3).

In contrast, the dates from the central dryland structure are widely scattered (Figure 17.18). Two samples from the upper fill of the central depression (*1955D* and *SUERC-65239*) have produced statistically consistent radiocarbon measurements (T'=0.2, T'(5%)=3.8, ν=1), although the third result from this deposit (*SUERC-65238*) is much later. Two statistically consistent results are also available from fragments of charcoal from posthole [338] (*SUERC-65240* and *OxA-33702*; T'=1.7, T'(5%)=3.8, ν=1). Between them, these results clearly span the entire period of human activity on the site. We consider it implausible that this structure could have stood for centuries and so must interpret the taphonomy of the dated material to come to a view on the time

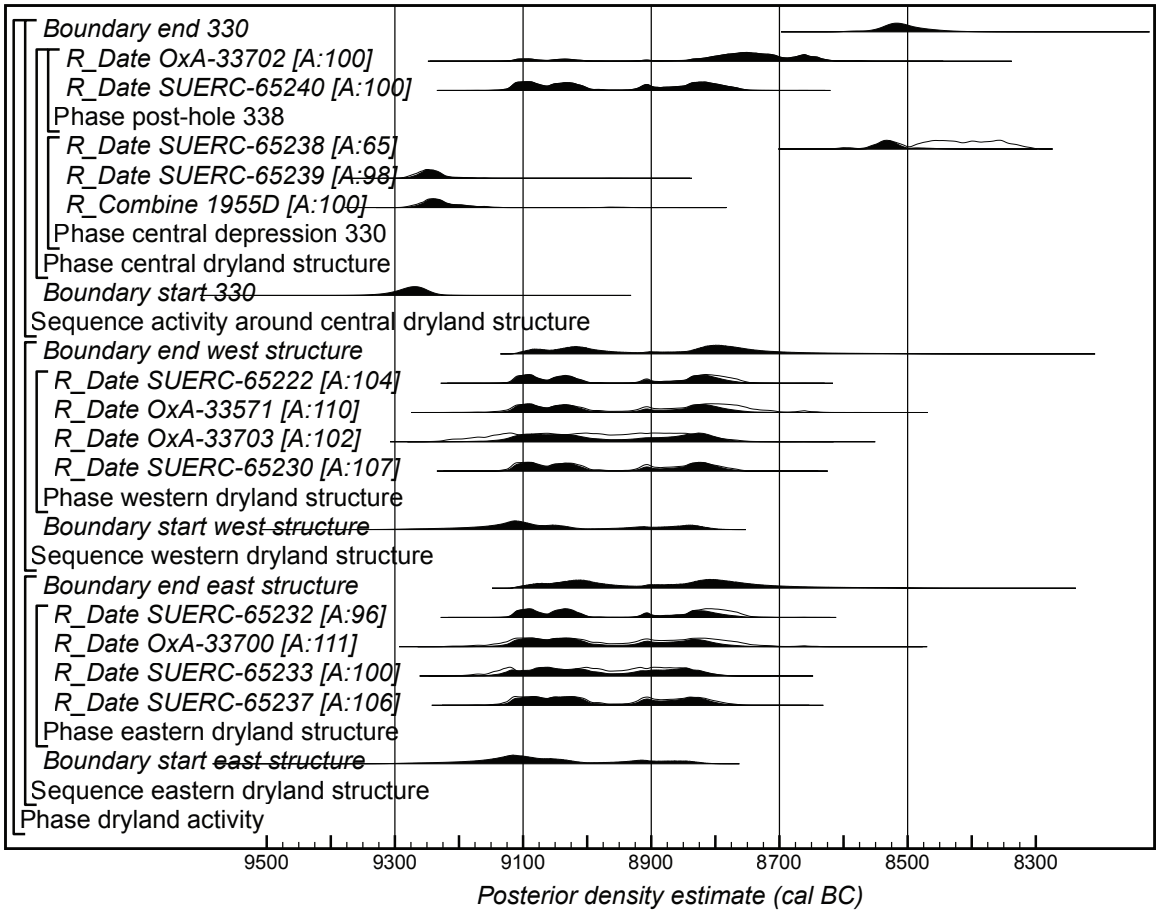

Figure 17.18: Probability distributions of dates on samples from the dryland structures. The format is as Figure 17.4. The overall model is defined exactly in Appendix 17.1 .

when it was used. The structure may have been used at the time when the charcoal which produced the two statistically consistently measurements from the hollow was deposited (*1955D* and *SUERC-65239*). Posthole [338] is part of a crescent of postholes around the edge of this hollow, and has produced two statistically consistent later results (*SUERC-65240* and *OxA-33702*). However, the presence of a scatter of burnt flint, outside the central structure centred to the west of the posthole, raises the possibility that the two samples from the posthole are dating this event rather than the structure. In addition, a pit/posthole [336], with a large concentration of burnt flint and bone, is situated less than a metre to the west of posthole [338] (see Figure 5.3): it is therefore possible that later burning events, possibly contemporary with the eastern structure, may have produced charcoal which was worked into posthole [338]. The sample from the central hollow dated by *SUERC-65238* is also, presumably, intrusive in this feature from a much later episode of activity on the site.

However, it is striking that all the radiocarbon ages from samples from the eastern and western dryland structures and posthole [338] of the central dryland structure are statistically consistent (T'=6.7, T'(5%)=16.9, ν=9). This is compatible with the suggestion that all these samples may relate to the same, relatively brief, episode of occupation. Indeed, the estimated durations for the eastern and western dryland structures (Figure 17.19) suggest a short use-life. The shape of these distributions also suggests that it is unlikely that either structure was constructed on the first peak on the probability distribution and demolished on the second.

The chronological model for human activity at Star Carr (Appendices 17.1–17.2) suggests that this began in *9385–9260 cal BC (95% probability; start Star Carr*; Figure 17.2) probably in *9335–9275 cal BC (68% probability*). This activity ended in *8555–8380 cal BC (95% probability; end Star Carr*; Figure 17.2) probably in *8525–8440 cal BC (68% probability)*. However, as described above, we are concerned that due to preservation bias we have been unable to adequately sample stratigraphically later activity in drier deposits, and so it is possible that this date estimate is slightly too early. Overall, the site was in use for *735–965 years (95% probability; use Star Carr*; Figure 17.19), probably for *775–885 years (68% probability)*.

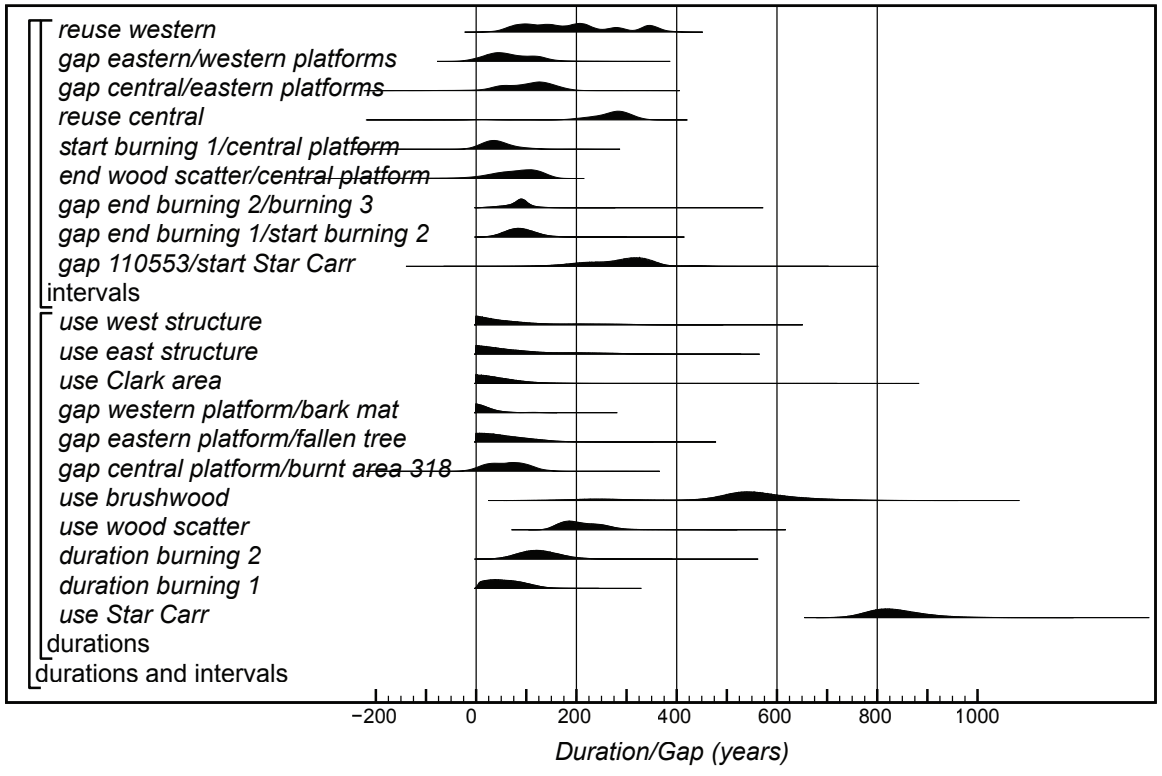

Figure 17.19: Probability distributions of key parameters for durations of archaeological activities and intervals between them, derived from the model defined exactly in Appendix 17.1 (Copyright Historic England, CC BY-NC 4.0).

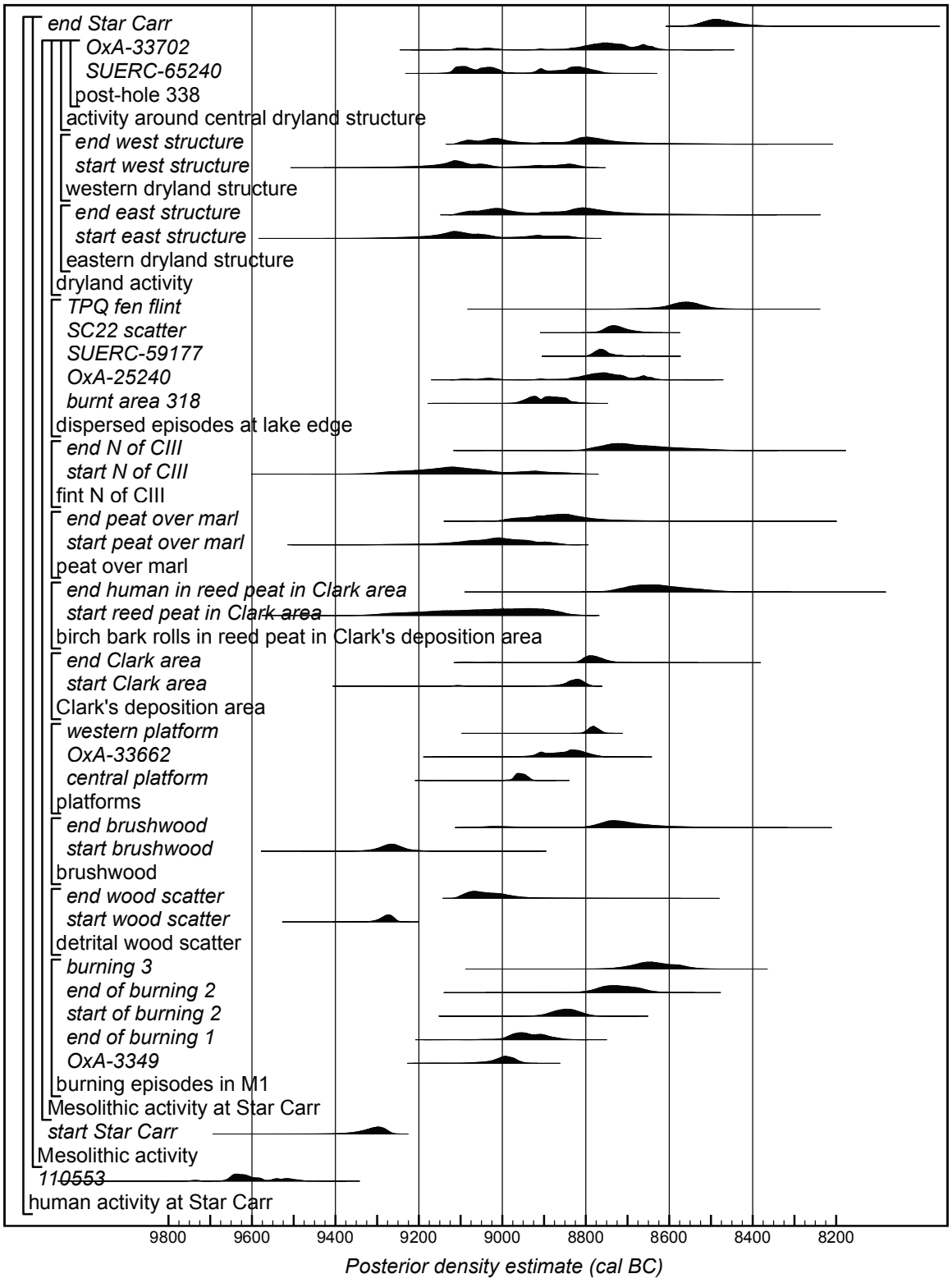

Figure 17.20: Probability distributions of key parameters of archaeological activities at Star Carr (*OxA-3349* is the start of burning 1, *OxA-33662* is the dated timber from the eastern platform, *SUERC-59177* is the bark mat, and *OxA-25240* is the bow), derived from the model defined exactly in Appendix 17.1 (Copyright Historic England, CC BY-NC 4.0).

Parameter	**Figure**	***Highest Posterior Density interval (cal BC)***	
		(95% probability)	*(68% probability)*
110553		*9745–9725 (1%)* or *9670–9475 (94%)*	*9660–9575 (65%)* or *9525–9510 (3%)*
start Star Carr	17.2	*9385–9260*	*9335–9275*
end Star Carr	17.2	*8555–8380*	*8525–8440*
OxA-3349	17.20	*9070–8945*	*9020–8965*
end of burning 1	17.20	*9015–8845*	*8980–8895*
start of burning 2	17.20	*8915–8785*	*8880–8815*
end of burning 2	17.20	*8805–8630*	*8770–8675*
burning 3	17.20	*8735–8535*	*8685–8580*
start wood scatter	17.20	*9315–9245*	*9290–9255*
end wood scatter	17.20	*9115–8915*	*9095–9000*
start brushwood	17.20	*9340–9190*	*9295–9235*
end brushwood	17.20	*9090–8920 (12%)* or *8820–8510 (83%)*	*8785–8630*
western platform	17.20	*8805–8755*	*8795–8765*
central platform	17.20	*8985–8925*	*8970–8940*
OxA-33662	17.20	*8945–8760*	*8915–8895 (9%)* or *8880–8795 (59%)*
start Clark area	17.20	*9125–9090 (4%)* or *8915–8775 (91%)*	*8850–8800*
end Clark area	17.20	*9100–9075 (3%)* or *8830–8710 (92%)*	*8810–8755*
start reed peat in Clark area	17.20	*9280–8845*	*9135–8875*
end human in reed peat in Clark area	17.20	*8745–8480*	*8710–8570*
start peat over marl	17.20	*9195–8855*	*9090–8925*
end peat over marl	17.20	*9015–8650*	*8955–8795*
start N of CIII	17.20	*9300–8850*	*9250–9025 (66%)* or *8930–8915 (2%)*
end N of CIII	17.20	*8810–8485*	*8775–8610*
TPQ fen flint	17.20	*8670–8475*	*8605–8515*
SC22 scatter	17.20	*8775–8665*	*8755–8705*
burnt area 318	17.17	*8965–8820*	*8940–8910 (22%)* or *8905–8845 (46%)*
SUERC-59177	17.17	*8800–8705 (94%)* or *8665–8655 (1%)*	*8785–8745*
OxA-25240	17.17	*9105–9070 (2%)* or *9060–9005 (6%)* or *8920–8895 (1%)* or *8865–8625 (86%)*	*8820–8700 (62%)* or *8675–8650 (6%)*
start east structure	17.20	*9250–8820*	*9180–9020 (57%)* or *8935–8895 (7%)* or *8880–8840 (4%)*
end east structure	17.20	*9115–8630*	*9090–8965 (32%)* or *8865–8735 (36%)*
start west structure	17.20	*9260–9005 (63%)* or *8985–8795 (32%)*	*9175–9025 (51%)* or *8920–8905 (2%)* or *8880–8815 (15%)*
end west structure	17.20	*9110–8625*	*9095–8975 (31%)* or *8840–8730 (37%)*

Table 17.4: Highest Posterior Density intervals for key parameters of archaeological activities at Star Carr (*OxA-3349* is the start of burning 1, *OxA-33662* is the dated timber from the eastern platform, *SUERC-59177* is the bark mat, and *OxA-25240* is the bow), derived from the model defined exactly in Appendix 17.1.

Parameter	*Highest Posterior Density interval (years)*	
	(95% probability)	*(68% probability)*
Durations		
use Star Carr	*735–965*	*775–885*
use wood scatter	*135–310*	*160–250*
use brushwood	*160–360 (12%)* or *410–765 (83%)*	*470–655*
use Clark area	*1–145*	*1–65*
use east structure	*1–275*	*1–110*
use west structure	*1–285*	*1–100*
duration burning 1	*1–130*	*10–85*
duration burning 2	*45–215*	*80–165*
gap central platform/burnt area 318	*–15–140*	*15–105*
gap eastern platform/fallen tree	*1–155*	*1–80*
gap western platform/bark mat	*1–80*	*1–30*
Intervals		
gap 110553/Star Carr	*125–395*	*230–365*
gap end burning 1/start burning 2	*25–155*	*55–120*
gap end burning 2/burning 3	*20–135*	*65–110*
reuse central	*175–350*	*240–320*
reuse western	*45–310 (81%)* or *315–380 (14%)*	*70–230 (62%)* or *335–360 (6%)*
start burning 1/central platform	*1–105*	*1–60*
end wood scatter/central platform	*–55–170*	*40–140*
gap central/eastern platforms	*–5–205*	*50–160*
gap eastern/western platforms	*–25–170*	*10–120*

Table 17.5: Highest Posterior Density intervals for key durations of archaeological activities Star Carr and of intervals between them, derived from the model defined exactly in Appendix 17.1 (*see* Figure 17.19).

The character and intensity of occupation demonstrably varied across this period. Key parameters for human activity at Star Carr are illustrated in Figure 17.20, and Highest Posterior Density intervals for these distributions are given in Table 17.4. The relative order of key parameters is provided in Table 17.8. Key parameters for the durations of archaeological activities at Star Carr and intervals between them are shown in Figure 17.19, and Highest Posterior Density intervals for these distributions are given in Table 17.5. Discussion and further analysis of these date estimates are integrated with the site narrative in Chapter 9.

The lake edge environment

Each of the environmental profiles from Star Carr documents the gradual transition from reedswamp forming in standing water to increasingly shallower and ultimately terrestrialised wetland environments. This was driven by the accumulation of organic sediments, which caused the depth of water within the lake margins to become shallower, a process known as hydroseral succession (see Chapter 19). Whilst this was a gradual, ongoing process, there are a series of comparable horizons in each of the macrofossil profiles that reflect changes in the amount of water reaching the deposits. These have been used to divide the environmental sequences into three broad phases or zones; reedswamp in standing water (Zone 1), shallower to seasonally

flooded swamp (Zone 2) and fen/carr forming above the level of the lake water (Zone 3). These horizons have been dated, along with the start of organic sedimentation in each of the profiles.

The age-depth models for Profiles M1 and VP85A 2010, 3178 and CII 2010 are described above, as these sequences can be related by stratigraphy to archaeological activity (Figures 17.3–4, 17.5–6 and 17.8–9). However, a fourth environmental profile, Dark's Clark Site Profile (Dark 1998a, 141–6) has three radiocarbon dates on reed charcoal picked from known depths in the sediment. An age-depth model for this sequence, constructed on the same basis as those previously described is shown in Figure 17.21.

The results of this model are surprisingly different from those provided by the age-depth model for CII 2010 (Figure 17.9), which is only 5 m to the north. The date estimates for *onset organics DCS* and *start seasonal flooding DCS* (Figure 17.22; Table 17.6) in particular are much later than those from CII 2010. These estimates derive from interpolation of the age-depth model below the levels from which the material that was radiocarbon dated from Dark's Clark Site Profile was taken. In these circumstances, it is possible that the accumulation

Parameter	***Highest Posterior Density interval (cal BC)***	
	(95% probability)	*(68% probability)*
Environmental Zones		
first EZ1	*9635–9445 (94%)* or *9435–9410 (1%)*	*9580–9550 (14%)* or *9535–9460 (54%)*
last EZ1	*9245–8970*	*9185–9015*
first EZ2	*9145–9010*	*9125–9055*
last EZ2	*9015–8850*	*8985–8900*
first EZ3	*8795–8605*	*8750–8655*
last EZ3	*8500–8215*	*8380–8265*
Profile M1/VP85A 2010		
onset organics M1	*9245–8970*	*9185–9015*
start seasonal flooding M1	*9020–8845*	*8985–8900*
onset fen carr M1	*8790–8585*	*8745–8635*
Profile 3178		
onset organics 3178	*9635–9445 (94%)* or *9430–9410 (1%)*	*9580–9550 (14%)* or *9535–9460 (54%)*
start seasonal flooding 3178	*9140–8985*	*9125–9055*
SUERC-65223	*8625–8470*	*8610–8530 (58%)* or *8510–8490 (10%)*
Profile CII 2010		
onset organics CII	*9445–9255*	*9395–9310*
start seasonal flooding CII	*9150–8930*	*9080–9005*
onset fen carr CII	*8500–8210*	*8380–8265*
Dark's Clark Site Profile		
onset organics DCS	*9165–8585*	*8910–8670*
start seasonal flooding DCS	*8950–8570*	*8825–8695 (56%)* or *8690–8645 (12%)*
onset fen carr DCS	*8770–8430*	*8720–8560*

Table 17.6: Highest Posterior Density intervals for the establishment of the different environmental zones around the lake edge at Star Carr (*SUERC-65223* dates the onset of fen/carr in environmental profile 3178), derived from the model defined exactly in Appendix 17.1 (*see* Figure 17.22).

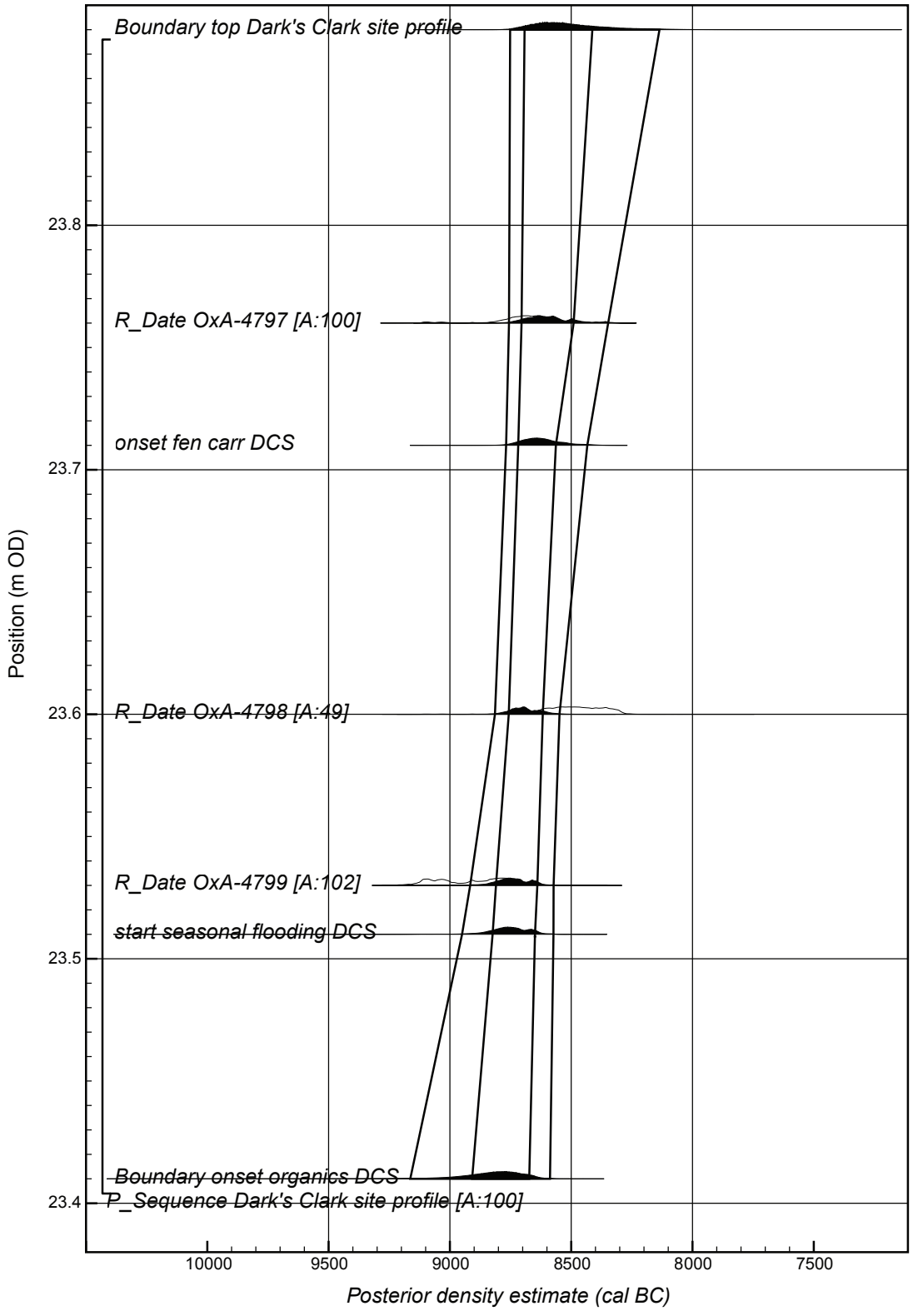

Figure 17.21: Probability distributions of radiocarbon dates in the age-depth model for Dark's Clark Site environmental profile. The format is as Figure 17.4. The overall model is defined exactly in Appendix 17.1

rate was much lower in the bottom part of this profile and so extrapolation from the faster accumulation rate higher up is invalid. Against this possibility is the near-constant accumulation rate visible in Profile CII 2010 (Figure 17.9). On balance, it seems more probable that the lower part of Dark's Clark Site Profile was subject to an episode of truncation or erosion in antiquity and so the date estimates relate to the re-establishment of organic sedimentation in this location rather than its initiation. For this reason, these two parameters have not been included in the modelling of the hydroseral succession.

Figure 17.22 shows the estimated dates for the three key hydroseric transitions in the four dated environmental profiles. In some cases, radiocarbon dates on bulk sediments which might contain an element of hard-water error are available that can provide limiting dates for the succession. By calculating the first and last event for each environmental transition, we can estimate the duration of each transition (Figure 17.23).

Onset of organic sedimentation around the lake edge began in *9635–9445 cal BC (94% probability; first EZ1*; Figure 17.22) or *9435–9410 cal BC (1% probability)*, probably in *9580–9550 cal BC (14% probability)* or *9535–9460 cal BC (54% probability)*. This is clearly (*100% probable*) earlier than the start of Mesolithic activity on the site. The start of organic sedimentation was very uneven around the shoreline, occurring first in Profile 3178, then in Profile CII 2010, and finally in Profile M1/VP85A 2010 (*98% probable*). The onset of seasonal flooding over the marl in the area south of the western platform could not be dated but must have occurred

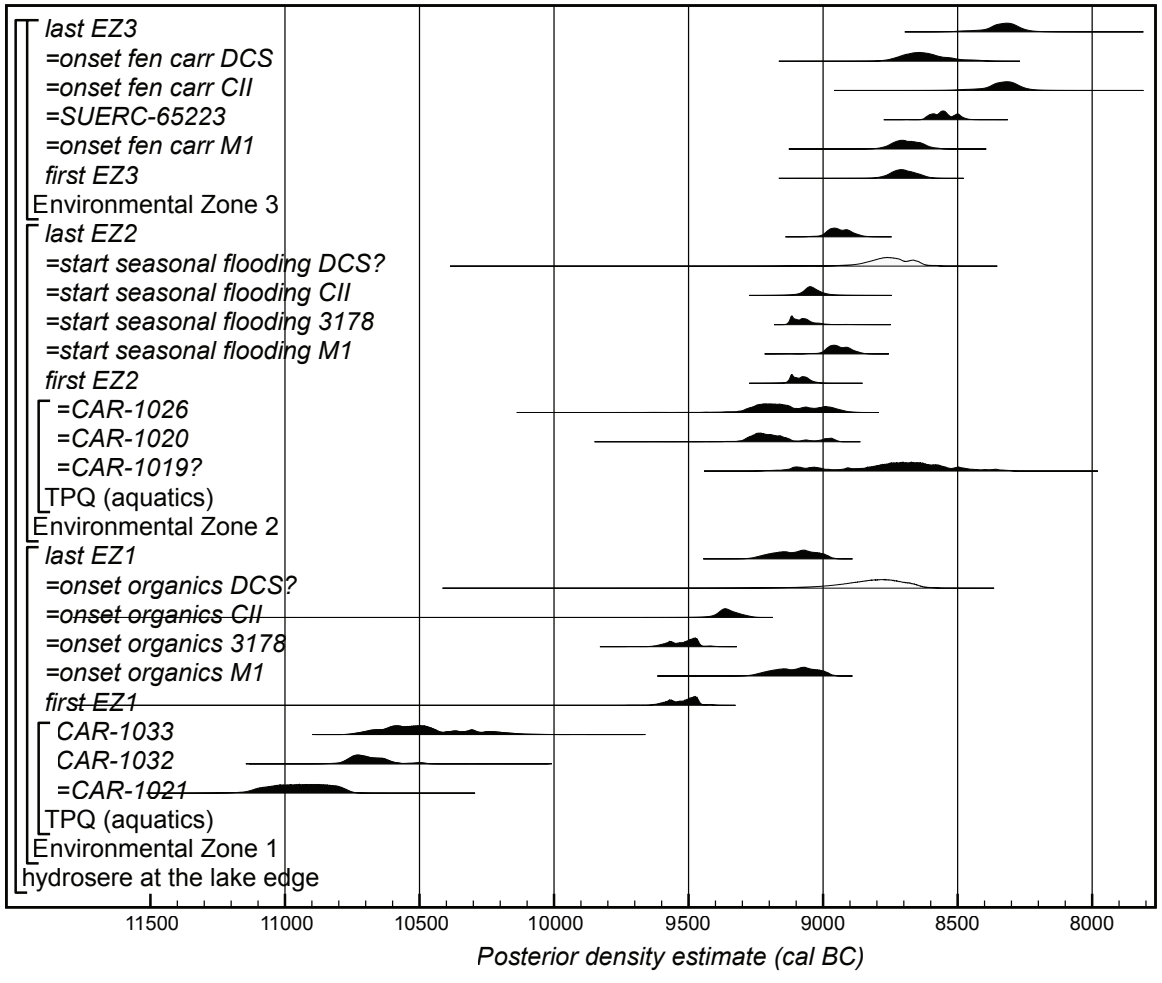

Figure 17.22: Probability distributions for the establishment of the different environmental zones around the lake edge at Star Carr (*SUERC-65223* dates on the onset of fen/carr in environmental profile 3178), derived from the model defined exactly in Appendix 17.1 (Copyright Historic England, CC BY-NC 4.0).

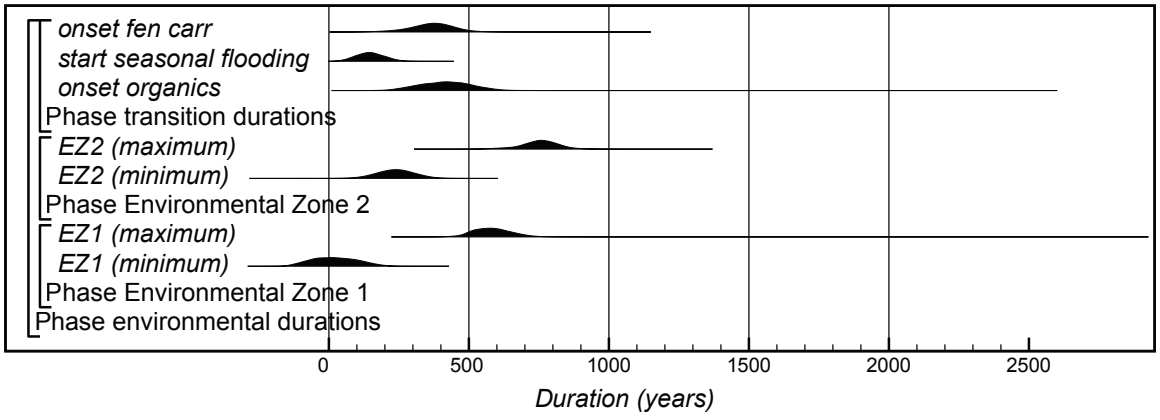

Figure 17.23: Probability distributions for the duration of the establishment of each environmental zone around the embayment and the minimum and maximum durations of each environmental zone, derived from the model defined exactly in Appendix 17.1 (Copyright Historic England, CC BY-NC 4.0).

Parameter	***Highest Posterior Density interval (years)***	
	(95% probability)	*(68% probability)*
Transition durations		
onset organics	*230–595*	*315–510*
start seasonal flooding	*45–250*	*90–200*
onset fen carr	*185–530*	*295–455*
Envionmental Zone durations		
EZ1 (minimum)	*–130–180*	*–70–105*
EZ1 (maximum)	*450–725*	*505–645*
EZ2 (minimum)	*100–375*	*170–310*
EZ2 (maximum)	*585–890*	*695–825*

Table 17.7: Highest Posterior Density intervals for the duration of the establishment of each environmental zone around the embayment and the minimum and maximum durations of each environmental zone, derived from the model defined exactly in Appendix 17.1 (*see* Figure 17.23).

before *9130–9000 cal BC (95% probability; SUERC-36349*; Figure 17.16), probably before *9120–9075 cal BC (55% probability*) or *9050–9030 cal BC (13% probability)*. Despite these variations, organic sediments were present across the lake edge by *9245–8970 cal BC (95% probability; last EZ1*; Figure 17.22), probably by *9185–9015 cal BC (68% probability)*.

Although the sequence of change in the hydrosere is the same in all locations around the lake, it is possible (*58% probable*) that the onset of organic sedimentation along some parts of the shore may have post-dated the start of seasonal flooding elsewhere. This began in *9145–9010 cal BC (95% probability; first EZ2*; Figure 17.22), probably in *9125–9055 cal BC (68% probability)*. Environmental Zone 2 was fully established, including in the area over the marl in the area south of the western platform (cf. *SUERC-36349*; Figure 17.16) by *9015–8850 cal BC (95% probability; last EZ2*; Figure 17.22), probably by *8980–8900 cal BC (68% probability)*. The transition to seasonal flooding occurred around the lake edge within a century or two and was thus much less varied than the transition to organic sedimentation, which had taken several centuries to occur (*onset organics* and *start*

seasonal flooding; Figure 17.23; Table 17.7). Environmental Zone 1 persisted for longest in Profile M1/VP85A 2010 (*90% probable*). This probably reflects relatively small variations in the rates of peat formation across the lake edge, which may have been caused by differences in local vegetation and the accumulation of plant material. Broadly speaking, Environmental Zone 2 saw the most intensive human exploitation of the lake edge.

Reed swamp persisted around the shoreline for at least several centuries, in some places for many centuries, before fen/carr became established (*EZ2 (minimum)*; *EZ2 (maximum)*; Figure 17.23; Table 17.7). This began to form in *8795–8605 cal BC (95% probability; first EZ3*; Figure 17.22), probably in *8750–8655 cal BC (68% probability)*. Again, there is considerable variability in the dates at which fen/carr replaced reed swamp around the shoreline (*onset fen carr*; Figure 17.23; Table 17.7), with the earliest fen/carr probably appearing in Profile M1/VP85A 2012 (*74% probable*), and the latest in Profile CII 2010 (*98% probable*). Fen/Carr was fully established around the lake edge by *8500–8215 cal BC* (*95% probability; last EZ3;* Figure 17.22), probably by *8380–8265 cal BC (68% probability)*. As with the transition to seasonal flooding, this was probably due to localised variations in peat accumulation and the composition of the in-situ vegetation. Mesolithic occupation at Star Carr probably ended before the reed swamp had entirely disappeared (*95% probable*).

Conclusions

Dating Star Carr has been particularly challenging because, by the time of the recent excavations, many of the organic finds were in a severely degraded state. This made making accurate radiocarbon age determinations very challenging and, in some cases, impossible.

Nonetheless, the narrative told in Chapter 9 utilises the chronology presented here to untangle the order of episodes of activity that cannot be related by direct stratigraphy (Table 17.8). For example, we do now know the order in which the three lake-edge platforms were constructed (Figure 17.14). We have also untangled the duration and intensity of different episodes of human activity. The detrital wood scatter, for example, was clearly a place of habitual deposition for 200 years or so, whereas in Clark's area artefacts were placed by a single generation of people (be it in a single afternoon or over a few decades) (Figure 17.19). The modelled chronology also allows us to assess the contemporaneity of different activities. Deposition in the area of peat over the marl to the south of the western platform, for example, was clearly over by the time the western platform was constructed *(85% probable)*, but was probably contemporary with the construction of the central platform (*67% probable)* (Table 17.8; Figure 17.20).

But this is not really a human-scale narrative. Most of the date estimates provided by the model, even at 68% probability, span over a century (Table 17.4), and so in most cases we cannot write a narrative of generations and lifetimes. It is also a partial story, as we have clearly been able to integrate only a small part of the activity on the dryland into our tale (and that very loosely). But within the chronological resolution provided by the modelling, the human story is placed within its contemporary landscape, both in terms of the changing wetland environment of the lake edge and the changing landforms and climate of the Vale (Chapter 3; Blockley et al. 2018). What is more, the resolution that we have achieved is a major development within the context of the British (and broader European) Mesolithic and provides a far more refined chronology than is usually associated with the period.

Our third objective, comparing human activity at Star Carr with contemporary activity at other sites in Britain and Northwest Europe, brings the quality and reliability of the chronology proposed here into focus. As stated above, the state of preservation of the excavated material from the site has made dating Star Carr challenging, but there are 200 radiocarbon dates from a chronological model that incorporates reliably recorded information about the relative sequence of the dated samples. And more than 150 of those samples are on short-life, single entity samples (Ashmore 1999). This is more than half the radiocarbon measurements available from the first two millennia of the British Mesolithic (Conneller et al. 2016)!

The chronology presented here has rarely reached the scale of individual human experience, but we know that the folk who built the western platform may have had grandparents who told them about their grandparents' tales of building the eastern platform. We have perhaps created a crack in the fuzzy prehistory of the Mesolithic and moved a step closer towards reclaiming the history of the Mesolithic people of the Vale.

	last EZ1	*first EZ2*	*last EZ2*	*first EZ3*	*last EZ3*	*OxA-3349*	*end of burning 1*	*start of burning 2*	*end of burning 2*	*burning 3*	*110553*	*start Star Carr*	*start wood scatter*	*end wood scatter*	*start brushwood*	*end brushwood*	*start peat over marl*
first EZ1	100%	100%	100%	100%	100%	100%	100%	100%	100%	100%	1%	100%	100%	100%	100%	100%	100%
last EZ1		58%	100%	100%	100%	100%	100%	100%	100%	100%	0%	0%	1%	78%	3%	98%	79%
first EZ2			100%	100%	100%	96%	100%	100%	100%	100%	0%	0%	0%	90%	1%	99%	79%
last EZ2				100%	100%	0%	92%	99%	100%	100%	0%	0%	0%	9%	0%	89%	20%
first EZ3					100%	0%	0%	0%	14%	100%	0%	0%	0%	0%	0%	41%	0%
last EZ3						0%	0%	0%	0%	0%	0%	0%	0%	0%	0%	0%	0%
start of burning 1 (OxA-3349)							100%	100%	100%	100%	0%	0%	0%	27%	0%	93%	44%
end of burning 1								100%	100%	100%	0%	0%	0%	9%	0%	89%	20%
start of burning 2									100%	100%	0%	0%	0%	2%	0%	85%	2%
end of burning 2										100%	0%	0%	0%	0%	0%	50%	0%
burning 3											0%	0%	0%	0%	0%	18%	0%
early worked timber (110553)												100%	100%	100%	100%	100%	100%
start Star Carr													100%	100%	100%	100%	100%
start wood scatter														100%	66%	100%	99%
end wood scatter															1%	96%	58%
start brushwood																100%	98%
end brushwood																	6%
start peat over marl																	
end peat over marl																	
central platform																	
eastern platform (OxA-33662)																	
western platform																	
start Clark area																	
end Clark area																	
start reed peat in Clark area																	
end human in reed peat in Clark area																	
start N of CIII																	
end N of CIII																	
burnt area 318																	
bow (OxA-25240)																	
bark mat (SUERC-59177)																	
SC22 scatter																	
TPQ fen flint																	
start east structure																	
end east structure																	
start west structure																	
end west structure																	

Table 17.8: Probabilities of the relative chronology of key parameters from Star Carr; the cells show the probability that the parameter listed at the left of the table is earlier than the parameter listed at the head of the table, e.g. the probability that *first EZ2* is earlier than *start Clark area* is 96%; the probability that *start Clark area* is earlier than *first EZ2* is 4% (i.e. 100% minus 96%).

end peat over marl	*central platform*	*OxA-33662*	*western platform*	*start Clark area*	*end Clark area*	*start reed peat in Clark area*	*end human in reed peat in Clark area*	*start N of CIII*	*end N of CIII*	*burnt area 318*	*OxA-25240*	*SUERC-59177*	*SC22 scatter*	*TPQ fen flint*	*start east structure*	*end east structure*	*start west structure*	*end west structure*	*end Star Carr*
100%	100%	100%	100%	100%	100%	100%	100%	100%	100%	100%	100%	100%	100%	100%	100%	100%	100%	100%	100%
99%	100%	100%	100%	97%	98%	68%	100%	51%	100%	100%	98%	100%	100%	100%	61%	93%	64%	93%	100%
100%	99%	100%	100%	96%	98%	65%	100%	42%	100%	100%	98%	100%	100%	100%	53%	95%	56%	95%	100%
81%	36%	98%	100%	91%	94%	24%	100%	13%	99%	79%	90%	100%	100%	100%	21%	62%	27%	62%	100%
7%	0%	1%	5%	1%	7%	0%	82%	0%	58%	0%	23%	15%	33%	98%	0%	11%	0%	12%	100%
0%	0%	0%	0%	0%	0%	0%	0%	0%	0%	0%	0%	0%	0%	0%	0%	0%	0%	0%	5%
96%	100%	100%	100%	93%	95%	42%	100%	22%	99%	100%	92%	100%	100%	100%	30%	73%	35%	73%	100%
81%	34%	98%	100%	92%	94%	24%	100%	14%	99%	79%	90%	100%	100%	100%	21%	62%	28%	62%	100%
42%	0%	47%	98%	65%	91%	4%	100%	3%	98%	18%	84%	100%	100%	100%	6%	46%	11%	51%	100%
8%	0%	1%	9%	1%	12%	0%	89%	0%	67%	0%	31%	24%	47%	99%	0%	13%	0%	15%	100%
3%	0%	0%	0%	0%	1%	0%	54%	0%	33%	0%	6%	2%	6%	85%	0%	5%	0%	5%	100%
100%	100%	100%	100%	100%	100%	100%	100%	100%	100%	100%	100%	100%	100%	100%	100%	100%	100%	100%	100%
100%	100%	100%	100%	100%	100%	100%	100%	100%	100%	100%	100%	100%	100%	100%	100%	100%	100%	100%	100%
100%	100%	100%	100%	100%	100%	97%	100%	96%	100%	100%	100%	100%	100%	100%	98%	100%	99%	100%	100%
96%	91%	97%	99%	93%	95%	50%	100%	28%	99%	96%	94%	100%	100%	100%	36%	83%	40%	82%	100%
100%	100%	100%	100%	100%	100%	95%	100%	93%	100%	100%	100%	100%	100%	100%	97%	100%	97%	100%	100%
19%	11%	15%	20%	14%	21%	6%	82%	3%	65%	13%	35%	30%	48%	94%	4%	20%	5%	21%	100%
100%	76%	96%	100%	94%	96%	46%	100%	29%	99%	92%	94%	100%	100%	100%	37%	78%	42%	78%	100%
	12%	56%	85%	63%	80%	10%	97%	6%	93%	36%	78%	89%	92%	99%	10%	46%	15%	49%	100%
		97%	100%	93%	94%	30%	100%	16%	99%	100%	90%	100%	100%	100%	25%	63%	31%	63%	100%
			95%	60%	88%	6%	100%	4%	98%	24%	83%	99%	100%	100%	7%	46%	12%	50%	100%
				2%	48%	0%	100%	0%	93%	0%	63%	100%	99%	100%	0%	25%	0%	29%	100%
					100%	6%	100%	4%	98%	14%	83%	100%	100%	100%	6%	46%	10%	51%	100%
						4%	99%	2%	91%	6%	63%	77%	94%	100%	3%	29%	3%	33%	100%
							100%	37%	99%	88%	94%	100%	100%	100%	45%	80%	49%	80%	100%
								0%	31%	0%	7%	2%	7%	77%	0%	5%	0%	5%	100%
									100%	93%	97%	100%	100%	100%	60%	89%	62%	89%	100%
										2%	21%	16%	30%	86%	1%	10%	1%	11%	100%
											88%	100%	100%	100%	13%	55%	20%	57%	100%
												52%	70%	99%	4%	27%	5%	29%	100%
													83%	100%	0%	19%	0%	21%	100%
														100%	0%	13%	0%	14%	100%
															0%	2%	0%	2%	100%
																100%	53%	85%	100%
																	18%	52%	100%
																		100%	100%
																			100%

Appendix 17.1: CQL2 code defining chronological model for Star Carr

```
Options()
 {
  Resolution=1;
  ConvergenceData=TRUE;
  kIterations=20000;
 };
 Phase("Star Carr")
 {
  Phase("central platform")
  {
   Sequence("M1 & VP85A 2010")
   {
    After("TPQs for onset organics")
    {
     R_Date("CAR-1027", 9800, 80);
     R_Date("CAR-1021", 11010, 120);
    };
    P_Sequence("VP85 2010 & M1",100,0,U(-2,2))
    {
     Boundary("onset organics M1")
     {
      z=23.29;
     };
     R_Date("OxA-3351", 9630, 100)
     {
      z=23.305, 0.0025;
     };
     Date("base of reed peat M1")
     {
      z=23.35;
     };
     R_Date("OxA-3350", 9500, 70)
     {
      z=23.365, 0.0025;
     };
     R_Date("OxA-3349", 9640, 70)
     {
      z=23.4175, 0.00125;
     };
     R_Date("OxA-3348", 9700, 70)
     {
      z=23.4525, 0.00125;
     };
     R_Date("SUERC-36339", 9600, 35)
     {
      z=23.47, 0.00625;
     };
     Boundary("start seasonal flooding M1")
     {
      z=23.486;
     };
```

```
Date("end of burning 1")
{
 z=23.49;
};
R_Date("OxA-3347", 9680, 70)
{
 z=23.5075, 0.00125;
};
R_Date("OxA-3346", 9560, 70)
{
 z=23.555, 0.0025;
};
Date("start of burning 2")
{
 z=23.57;
};
R_Date("OxA-3345", 9580, 70)
{
 z=23.5975, 0.00125;
};
R_Date("OxA-3344", 9360, 70)
{
 z=23.6525, 0.00125;
};
Date("end of burning 2")
{
 z=23.68;
};
R_Date("OxA-3343", 9420, 70)
{
 z=23.7075, 0.00125;
};
Boundary("onset fen carr M1")
{
 z=23.71;
};
Date("burning 3")
{
 z=23.73;
};
R_Date("OxA-3342", 9390, 70)
{
 z=23.7575, 0.00125;
};
Date("first hazel")
{
 z=23.79;
};
R_Date("OxA-4376", 9385, 115)
{
 z=23.82, 0.005;
};
R_Date("OxA-25247", 8865, 40)
```

```
 {
  z=23.88, 0.01;
 };
 Date("start hazel rise")
 {
  z=23.91;
 };
 R_Date("OxA-4377", 8940, 90)
 {
  z=23.94, 0.005;
 };
 Date("hazel 50 TLP")
 {
  z=23.96;
 };
 Date("1st hazel peak")
 {
  z=23.97;
 };
 Boundary("end M1")
 {
  z=23.99;
 };
};
 R_Date("CAR-1022", 8670, 90);
};
Sequence("between onset organics and start seasonal flooding")
{
 Date("=onset organics M1");
 After("TPQs for start seasonal flooding M1")
 {
  R_Date("CAR-919", 9510, 80);
  R_Date("CAR-1026", 9680, 110);
 };
 Date("=start seasonal flooding M1");
};
Sequence("around central platform")
{
 Date("=onset organics M1");
 After("TPQs for central platform")
 {
  R_Date("CAR-1020", 9720, 80);
  R_Date("CAR-1019", 9410, 110)
  {
   color="red";
   Outlier();
  };
  R_Date("CAR-928", 9670, 120);
  Date("=OxA-3349");
 };
 After("reused timber")
 {
  R_Date("OxA-33574", 9735, 45);
```

```
};
Combine("central platform")
{
 R_Date("SUERC-65243", 9663, 31);
 R_Date("OxA-33731", 9675, 45);
 R_Date("SUERC-65247", 9629, 30);
 R_Combine("99726")
 {
  R_Date("SUERC-59168", 9650, 31);
  R_Date("OxA-32318", 9460, 65);
 };
 R_Combine("99738")
 {
  R_Date("OxA-32146", 9660, 45);
  R_Date("SUERC-59169", 9702, 45);
 };
 R_Date("CAR-926", 9240, 90)
 {
  Outlier("red");
  color="red";
 };
};
Phase("later than central platform")
{
 Combine("burnt area 318")
 {
  R_Date("SUERC-65241", 9606, 30);
  R_Date("OxA-33570", 9580, 50);
 };
 Sequence("225 & 224")
 {
  Phase("225")
  {
   R_Date("SUERC-36338", 9555, 35);
   R_Date("OxA-25246", 9515, 40);
   After("aquatics")
   {
    R_Date("CAR-924", 9320, 80);
   };
  };
  Phase("224")
  {
   R_Combine("S246")
   {
    R_Date("OxA-26561", 9305, 45);
    R_Date("SUERC-40160", 9415, 30);
   };
  };
 };
 Sequence("VP85A/2")
 {
  After("aquatics")
  {
```

```
    R_Date("CAR-1018", 9410, 110);
   };
   R_Date("CAR-1017", 8580, 90);
  };
 };
};
Sequence("upper part of VP85A/3")
{
 Date("=start seasonal flooding M1");
 After("aquatics")
 {
  R_Date("CAR-1025", 9480, 100);
  R_Date("CAR-1024", 9540, 110);
 };
 Phase("around level of auroch metatarsal <56>")
 {
  R_Date("CAR-923", 9030, 100)
  {
   color="red";
   Outlier();
  };
  R_Date("OxA-1176", 9700, 160)
  {
   color="red";
   Outlier();
  };
  R_Date("CAR-1023", 9290, 60);
 };
 Date("=CAR-1022");
};
};
P_Sequence("Profile 3178",100,0,U(-2,2))
{
 Boundary("base 3178")
 {
  z=23.035;
 };
 After("sand (320)")
 {
  R_Combine("110553")
  {
   R_Date("SUERC-65242", 9977, 30);
   R_Date("OxA-32056", 10010, 40);
  };
 };
 Date("onset organics 3178")
 {
  z=23.0475;
 };
 R_Date("SUERC-65229", 10095, 30)
 {
  z=23.0725, 0.00625;
 };
```

```
 R_Combine("base of reed peat 3178")
 {
  z=23.225, 0.00625;
  R_Date("SUERC-65228", 9559, 31);
  R_Date("OxA-33699", 9740, 65);
 };
 R_Combine("start seasonal flooding 3178")
 {
  z=23.2475, 0.00625;
  R_Date("OxA-33698", 9555, 55);
  R_Date("SUERC-65227", 9583, 30);
 };
 R_Date("SUERC-65223", 9290, 30)
 {
  z=23.66, 0.0125;
 };
 Boundary("top 3178")
 {
  z=23.84;
 };
};
Phase("western platform")
{
 P_Sequence("CII 2010",100,0,U(-2,2))
 {
  Boundary("base CII 2010")
  {
   z=23.42;
  };
  Date("onset organics CII")
  {
   z=23.44;
  };
  Combine("23.495m")
  {
   z=23.495;
   R_Date("OxA-25238", 9735, 40);
   R_Date("SUERC-36348", 9710, 35);
  };
  Date("base of reed peat CII")
  {
   z=23.56;
  };
  Date("start seasonal flooding CII")
  {
   z=23.57;
  };
  R_Date("OxA-25239", 9400, 40)
  {
   z=23.70;
  };
  Date("TPQ fen flint")
  {
```

```
 z=23.77;
};
Date("onset fen carr CII")
{
 z=23.87;
};
Combine("24.05m")
{
 z=24.05;
 R_Date("OxA-25242", 8810, 40);
 R_Date("SUERC-36354", 8845, 35);
};
Boundary("top CII 2010")
{
 z=24.08;
};
};
Sequence("western platform area")
{
 Date("=onset organics CII");
 Phase("below western platform")
 {
  After("in basal sand")
  {
   R_Date("OxA-32319", 9540, 50);
  };
  R_Date("SUERC-59176", 9670, 31);
  R_Date("OxA-32055", 9766, 39);
  Sequence("98 & 97")
  {
   Phase("98")
   {
    R_Date("SUERC-36343", 9680, 30);
    R_Date("OxA-25199", 9765, 50);
   };
   Phase("97")
   {
    R_Date("SUERC-36344", 9590, 35);
    R_Date("OxA-26563", 9650, 45);
    After("reworked")
    {
     R_Date("OxA-25200", 9765, 45);
    };
   };
  };
  Date("=start seasonal flooding CII");
 };
 Phase("western platform timbers")
 {
  After("salvaged timbers")
  {
   R_Combine("timber [46]")
   {
```

```
  R_Date("Hd-30440", 9606, 22);
  R_Date("SUERC-40169", 9585, 30);
  R_Date("OxA-26479", 9595, 50);
 };
};
Combine("western platform")
{
 R_Combine("timber [50] other")
 {
  R_Date("SUERC-40168", 9510, 30);
  R_Date("OxA-X-2475-22", 9570, 90);
 };
 R_Combine("timber [48]")
 {
  R_Date("MAMS-18277", 9441, 26);
  R_Date("SUERC-40170", 9515, 45);
 };
 R_Date("Hd-30193", 9463, 18);
 R_Date("Hd-30201", 9451, 34);
};
Phase("innaccurate measurements")
{
 R_Combine("timber [50] Hd")
 {
  color="red";
  Outlier();
  R_Date("Hd-30439", 9302, 23);
  R_Date("Hd-30200", 9359, 22);
 };
 R_Date("Hd-30167", 8951, 18)
 {
  color="red";
  Outlier();
 };
};
};
Phase("93, bark matt & 84")
{
 Sequence("93 & 84")
 {
  Phase("93")
  {
   R_Combine("453")
   {
    R_Date("SUERC-40164", 9445, 30);
    R_Date("OxA-25201", 9550, 45);
   };
   R_Combine("455")
   {
    R_Date("OxA-26562", 9545, 55);
    R_Date("SUERC-36345", 9485, 35);
   };
  };
```

```
  Phase("84")
  {
   After("reworked")
   {
    R_Date("OxA-25235", 9555, 45);
   };
   R_Date("Hd-30166", 9420, 21);
  };
 };
 Phase("bark matt <99307>")
 {
  R_Date("OxA-32057", 9650, 38)
  {
   color="red";
   Outlier();
  };
  R_Date("OxA-32058", 9630, 38)
  {
   color="red";
   Outlier();
  };
  R_Date("SUERC-59177", 9502, 31);
 };
};
Phase("83")
{
 R_Date("SUERC-36347", 9275, 35);
 R_Combine("201")
 {
  R_Date("OxA-25236", 9165, 45);
  R_Date("OxA-25237", 9215, 40);
 };
};
Date("=24.05m");
};
Sequence("brushwood onset organics/84")
{
 Date("=onset organics CII");
 Phase("brushwood")
 {
  R_Date("SUERC-36346", 9590, 35);
  R_Date("OxA-25202", 9620, 50);
  R_Date("OxA-32320", 9615, 45);
  R_Date("OxA-32059", 9580, 40);
  R_Date("SUERC-59175", 9547, 31);
  R_Date("SUERC-59174", 9471, 31);
  R_Date("SUERC-59170", 9465, 31);
  R_Date("OxA-32060", 9696, 40);
 };
 Phase("84")
 {
  Date("=Hd-30166");
  After("reworked")
```

```
  {
   Date("=OxA-25235");
  };
 };
};
};
Sequence("SC22")
{
 Boundary("start SC22");
 Sequence("SC22")
 {
  Phase("(39)")
  {
   R_Date("Hd-30190", 9611, 20);
   R_Date("Hd-30168", 9481, 20);
   R_Combine("82705")
   {
    R_Date("SUERC-40161", 9525, 30);
    R_Date("OxA-26560", 9540, 45);
    R_Date("MAMS-18276", 9433, 26);
   };
   R_Combine("82706")
   {
    R_Date("SUERC-40162", 9505, 30);
    R_Date("OxA-26478", 9755, 60)
    {
     Outlier();
    };
   };
  };
  Phase("(35)")
  {
   R_Date("OxA-16810", 9275, 40)
   {
    color="red";
    Outlier();
   };
   R_Date("OxA-16809", 9355, 40)
   {
    color="red";
    Outlier();
   };
   After("reworked")
   {
    R_Date("OxA-25088", 9580, 45);
   };
   R_Date("SUERC-36355", 9450, 35)
   {
   };
  };
  Date("SC22 scatter");
  Phase("(34)")
  {
```

```
   R_Date("Hd-30192", 9375, 20);
   R_Date("SUERC-40163", 9455, 30);
   After("reworked")
   {
    R_Date("SUERC-36356", 9560, 35);
    R_Combine("roundwood 4.2")
    {
     R_Date("OxA-26558", 9515, 45);
     R_Date("OxA-26559", 9525, 45);
    };
   };
  };
 };
 Boundary("end SC22");
};
P_Sequence("Dark's Clark site profile",100,0,U(-2,2))
{
 Boundary("onset organics DCS")
 {
  z=23.41;
 };
 Date("start seasonal flooding DCS")
 {
  z=23.51;
 };
 R_Date("OxA-4799", 9500, 75)
 {
  z=23.53;
 };
 R_Date("OxA-4798", 9260, 100)
 {
  z=23.60;
 };
 Date("onset fen carr DCS")
 {
  z=23.71;
 };
 R_Date("OxA-4797", 9385, 80)
 {
  z=23.76;
 };
 Boundary("top Dark's Clark site profile")
 {
  z=23.88;
 };
};
Sequence("human activity at Star Carr")
{
 Boundary("start Star Carr");
 Phase("human activity at Star Carr")
 {
  Phase("burning episodes in M1")
  {
```

```
 Date("=OxA-3349");
 Date("=end of burning 1");
 Date("=start of burning 2");
 Date("=end of burning 2");
 Date("=burning 3");
};
Sequence("artefacts from VP85A")
{
 Boundary("start VP85A");
 Phase("artefacts")
 {
  After("auroch skull <150> (aquatics)")
  {
   Date("=CAR-924");
  };
  R_Date("OxA-1154", 9500, 120);
  After("around charcoal <153> (aquatics)")
  {
   R_Date("CAR-930", 9660, 110);
  };
  Phase("around barbed point <245>")
  {
   R_Date("CAR-925", 9260, 100);
  };
  Sequence("around antler <216>")
  {
   After("below (aquatics)")
   {
    R_Date("CAR-1047", 9690, 110);
   };
   R_Date("CAR-922", 9250, 80);
   Before("above")
   {
    R_Date("CAR-1050", 9310, 80);
   };
  };
 };
 Boundary("end VP85A");
};
Sequence("detrital wood scatter")
{
 Boundary("start wood scatter");
 Phase("detrital wood scatter")
 {
  Sequence("detrital wood scatter")
  {
   After("onset organics")
   {
    Date("=onset organics 3178");
   };
   Phase("317")
   {
    R_Date("SUERC-59178", 9723, 31);
```

```
    Sequence("108966-7 & 109030")
    {
     R_Combine("108967")
     {
      R_Date("OxA-32062", 9645, 45);
      R_Date("SUERC-59184", 9611, 37);
     };
     R_Combine("108966")
     {
      R_Date("OxA-32061", 9680, 45);
      R_Date("SUERC-59180", 9608, 39);
     };
    };
    R_Date("SUERC-59179", 9743, 31);
    R_Date("OxA-33671", 9520, 45);
    R_Date("SUERC-66181", 9780, 32);
    R_Date("OxA-33673", 9585, 45);
   };
   Date("=base of reed peat 3178");
   Sequence("312")
   {
    Phase("lower")
    {
     R_Combine("99528")
     {
      R_Date("SUERC-66179", 9538, 35);
      R_Date("OxA-33672", 9545, 45);
     };
     R_Date("SUERC-66180", 9553, 33);
    };
    R_Date("OxA-33668", 9570, 45);
   };
  };
  Sequence("108941 & 109559")
  {
   R_Combine("<108941>")
   {
    R_Date("OxA-32063", 9820, 45);
    R_Date("SUERC-59185", 9779, 40);
   };
   Date("=SUERC-59178");
  };
  Span("use wood scatter");
 };
 Boundary("end wood scatter");
 Date("=SUERC-65223");
};
Sequence("brushwood")
{
 Boundary("start brushwood");
 Phase("brushwood")
 {
  Date("=SUERC-59176");
```

```
 Date("=OxA-32319");
 Date("=OxA-32055");
 Date("=OxA-32059");
 Date("=OxA-32320");
 Date("=OxA-32060");
 Date("=SUERC-59175");
 Date("=SUERC-59174");
 Date("=SUERC-59170");
};
Boundary("end brushwood");
Span("use brushwood");
};
Phase("platforms")
{
Date("=western platform");
Date("=central platform");
Sequence("eastern platform")
{
 After("317")
 {
  R_Date("SUERC-66037", 9762, 29);
  Date("=start seasonal flooding M1");
 };
 Phase("eastern platform")
 {
  R_Date("OxA-33662", 9525, 45);
 };
 Before("312")
 {
  R_Date("OxA-33713", 9320, 50);
  R_Date("SUERC-66036", 9512, 29);
 };
};
};
Sequence("Clark's deposition area")
{
Boundary("start Clark area");
Phase("Clark's deposition area")
{
 Phase("Clark's deposition area")
 {
  Phase("[463]")
  {
   R_Combine("barbed point [463]")
   {
    R_Date("OxA-10808", 9505, 60);
    R_Date("OxA-21236", 9561, 38);
   };
   R_Date("OxA-4451", 9120, 150)
   {
    color="red";
    Outlier();
   };
```

```
  };
  Phase("[460]")
  {
   R_Combine("antler splinter [460]")
   {
    R_Date("OxA-21237", 9585, 39);
    R_Date("OxA-10809", 9530, 55)
    {
    };
   };
   R_Date("OxA-4450", 9060, 220)
   {
    color="red";
    Outlier();
   };
  };
  R_Combine("antler crown [461]")
  {
   R_Date("OxA-4577", 9670, 100);
   R_Date("OxA-21238", 9485, 38);
  };
  R_Combine("antler tine [465]")
  {
   R_Date("OxA-21239", 9468, 38);
   R_Date("OxA-4578", 9590, 90);
  };
 };
 Phase("2004-15 excavations")
 {
  R_Date("OxA-33675", 9465, 45);
  R_Date("SUERC-66186", 9518, 35);
  R_Date("SUERC-66182", 9531, 35);
  R_Date("OxA-33677", 9490, 45);
  R_Date("OxA-33676", 9560, 45);
  R_Date("SUERC-66178", 9529, 35);
  R_Date("SUERC-66187", 9479, 35);
 };
};
Boundary("end Clark area");
Span("use Clark area");
};
Sequence("birch bark rolls in reed peat in Clark's deposition area")
{
 Boundary("start reed peat in Clark area");
 Phase("birch bark rolls in peat in Clark's depostion area")
 {
  R_Date("SUERC-66048", 9600, 28);
  R_Date("OxA-33667", 9580, 45);
  R_Combine("115195")
  {
   R_Date("OxA-33669", 9465, 45);
   R_Date("OxA-33670", 9490, 45);
  };
```

```
 R_Date("SUERC-66049", 9389, 29);
 };
 Boundary("end human in reed peat in Clark area");
};
Sequence("peat over marl")
{
 Boundary("start peat over marl");
 After("base of (234)")
 {
  R_Date("SUERC-36349", 9510, 35);
 };
 Phase("activity in peat over marl")
 {
  R_Date("SUERC-66046", 9577, 28);
  R_Date("OxA-33666", 9640, 40);
  R_Date("SUERC-66044", 9562, 29);
  R_Date("OxA-33678", 9680, 50);
 };
 Before("(233)")
 {
  R_Date("SUERC-36353", 8890, 35);
  R_Date("OxA-25241", 8883, 39);
 };
 Boundary("end peat over marl");
};
Sequence("flint N of CIII")
{
 Boundary("start N of CIII");
 Sequence("birch bark rolls & bead manufacturing")
 {
  Phase("312 (base of flint scatter)")
  {
   R_Date("SUERC-66039", 9552, 30);
   R_Date("OxA-33663", 9550, 40);
  };
  Phase("310 (bead manufacturing level)")
  {
   R_Date("OxA-33664", 9660, 45);
   R_Date("SUERC-66043", 9448, 27);
  };
 };
 Boundary("end N of CIII");
};
Phase("dispersed episodes at lake edge")
{
 Date("=burnt area 318");
 Phase("bark mat")
 {
  Date("=SUERC-59177");
 };
 After("TPQ for fen flint")
 {
  Date("=TPQ fen flint");
```

```
 };
 Phase("SC22")
 {
  Date("=SC22 scatter");
  Date("=OxA-16810")
  {
   Outlier();
   color="red";
  };
  Date("=OxA-16809")
  {
   Outlier();
   color="red";
  };
 };
 Phase("Clark's excavations")
 {
  R_Date("OxA-V-994-33", 9680, 55);
  R_Date("KIA-307034", 9342, 41);
  R_Date("OxA-2343", 9350, 90);
 };
 Phase("birch bark rolls at N end of CII")
 {
  R_Date("SUERC-66045", 9519, 29);
  R_Date("OxA-33665", 9500, 45);
 };
 Sequence("S end of CII")
 {
  After("base of (234)")
  {
   Date("=SUERC-36349");
  };
  Phase("(234)")
  {
   R_Date("OxA-25240", 9470, 45);
   R_Date("SUERC-66047", 9518, 29);
  };
  Before("(233)")
  {
   Date("=SUERC-36353");
   Date("=OxA-25241");
  };
 };
 Phase("later activity in Clark's deposition area")
 {
  R_Combine("115876")
  {
   R_Date("SUERC-66177", 9431, 32);
   R_Date("OxA-33674", 9345, 50);
  };
 };
};
Phase("dryland activity")
```

```
{
 Sequence("eastern dryland structure")
 {
  Boundary("start east structure");
  Phase("eastern dryland structure")
  {
   R_Date("SUERC-65237", 9556, 30);
   R_Date("SUERC-65233", 9587, 32);
   R_Date("OxA-33700", 9540, 55);
   R_Date("SUERC-65232", 9519, 31);
   Span("use east structure");
  };
  Boundary("end east structure");
 };
 Sequence("western dryland structure")
 {
  Boundary("start west structure");
  Phase("western dryland structure")
  {
   R_Date("SUERC-65230", 9542, 30);
   R_Date("OxA-33703", 9585, 55);
   R_Date("OxA-33571", 9515, 50);
   R_Date("SUERC-65222", 9524, 30);
   Span("use west structure");
  };
  Boundary("end west structure");
 };
 Sequence("activity around central dryland structure")
 {
  Boundary("start 330");
  Phase("central dryland structure")
  {
   Phase("central depression 330 ")
   {
    R_Combine("1955D")
    {
     R_Date("OxA-33569", 9710, 50);
     R_Date("OxA-33701", 9765, 55);
    };
    R_Date("SUERC-65239", 9754, 32);
    R_Date("SUERC-65238", 9221, 30);
   };
   Phase("post-hole 338 ")
   {
    R_Date("SUERC-65240", 9536, 31);
    R_Date("OxA-33702", 9460, 50);
   };
  };
  Boundary("end 330");
 };
};
Boundary("end Star Carr");
```

```
 Span("use Star Carr");
};
Order("archaeological summary")
{
 Phase("lake edge environment")
 {
  Date("=first EZ1");
  Date("=last EZ1");
  Date("=first EZ2");
  Date("=last EZ2");
  Date("=first EZ3");
  Date("=last EZ3");
  Date("=onset organics M1");
  Date("=onset organics 3178");
  Date("=onset organics CII");
  Date("=start seasonal flooding 3178");
  Date("=start seasonal flooding CII");
  Date("=start seasonal flooding M1");
  Date("=onset fen carr M1");
  Date("=SUERC-65223");
  Date("=onset fen carr CII");
 };
 Phase("burning events")
 {
  Date("=OxA-3349");
  Date("=end of burning 1");
  Date("=start of burning 2");
  Date("=end of burning 2");
  Date("=burning 3");
 };
 Date("=110553");
 Date("=start Star Carr");
 Date("=start 330");
 Date("=start wood scatter");
 Date("=end wood scatter");
 Date("=start brushwood");
 Date("=end brushwood");
 Date("=start peat over marl");
 Date("=end peat over marl");
 Date("=CAR-930");
 Date("=OxA-33678");
 Date("=OxA-33574");
 Date("=central platform");
 Date("=OxA-V-994-33");
 Date("=start east structure");
 Date("=end east structure");
 Date("=start west structure");
 Date("=end west structure");
 Phase("post-hole 338 ")
 {
  Date("=OxA-33702");
  Date("=SUERC-65240");
 };
```

```
 Date("=burnt area 318");
 Date("=OxA-33662");
 Date("=start N of CIII");
 Date("=end N of CIII");
 Date("=start reed peat in Clark area");
 Date("=end human in reed peat in Clark area");
 Date("=timber [46]");
 Date("=western platform");
 Date("=OxA-25240");
 Date("=start Clark area");
 Date("=end Clark area");
 Date("=115876");
 Date("=SUERC-59177");
 Date("=SC22 scatter");
 Date("=TPQ fen flint");
 Date("=end 330");
 Date("=CAR-922");
 Date("=CAR-923");
 Date("=OxA-1154");
 Date("=CAR-925");
 Date("=CAR-924")
 {
  color="gray";
 };
 Date("=OxA-2343");
 Date("=KIA-307034");
 Date("=end Star Carr");
};
Phase("archaeological differences")
{
 Difference("gap 110553", "start Star Carr", "110553");
};
Phase("archaeological intervals")
{
 Sequence("burning")
 {
  Date("=OxA-3349");
  Interval("duration burning 1");
  Date("=end of burning 1");
  Interval("gap end burning 1/start burning 2");
  Date("=start of burning 2");
  Interval("duration burning 2");
  Date("=end of burning 2");
  Interval("gap end burning 2/burning 3");
  Date("=burning 3");
 };
 Sequence("central platform/burnt area 318")
 {
  Date("=OxA-3349");
  Interval("start burning 1/central platform");
  Date("=central platform");
  Interval("central platform/burnt area 318");
  Date("=burnt area 318");
```

```
 };
 Sequence("western platform and bark mat")
 {
  Date("=western platform");
  Interval("gap western platform/bark mat");
  Date("=SUERC-59177");
 };
 Sequence("eastern platform and overlying tree")
 {
  Date("=OxA-33662");
  Interval("gap eastern platform/fallen tree");
  Date("=SUERC-66036");
 };
};
Phase("Lake edge environment")
{
 Phase("hydrosere at the lake edge")
 {
  Phase("Environmental Zone 1")
  {
   After("TPQ (aquatics)")
   {
    Date("=CAR-1021")
    {
     color="gray";
    };
    R_Date("CAR-1032", 10710, 90)
    {
     color="gray";
    };
    R_Date("CAR-1033", 10520, 90)
    {
     color="gray";
    };
   };
   First("first EZ1");
   Date("=onset organics M1");
   Date("=onset organics 3178");
   Date("=onset organics CII");
   Date("=onset organics DCS")
   {
    color="red";
    Outlier();
   };
   Last("last EZ1");
  };
  Phase("Environmental Zone 2")
  {
   After("TPQ (aquatics)")
   {
    Date("=CAR-1019")
    {
     color="red";
```

```
  Outlier();
 };
 Date("=CAR-1020")
 {
  color="gray";
 };
 Date("=CAR-1026")
 {
  color="gray";
 };
};
First("first EZ2");
Date("=start seasonal flooding M1");
Date("=start seasonal flooding 3178");
Date("=start seasonal flooding CII");
Date("=start seasonal flooding DCS")
{
 Outlier();
 color="red";
};
Last("last EZ2");
};
Phase("Environmental Zone 3")
{
First("first EZ3");
Date("=onset fen carr M1");
Date("=SUERC-65223");
Date("=onset fen carr CII");
Date("=onset fen carr DCS");
Last("last EZ3");
};
};
Phase("hydrosere at the lake edge (orders)")
{
Order("Environmental Zone 1")
{
Date("=onset organics M1");
Date("=onset organics 3178");
Date("=onset organics CII");
Date("=onset organics DCS");
};
Order("Environmental Zone 2")
{
Date("=start seasonal flooding M1");
Date("=start seasonal flooding 3178");
Date("=start seasonal flooding CII");
Date("=start seasonal flooding DCS");
};
Order("Environmental Zone 3")
{
Date("=onset fen carr M1");
Date("=SUERC-65223");
Date("=onset fen carr CII");
```

```
  Date("=onset fen carr DCS");
  };
  Order("overlaps")
  {
   Date("=last EZ1");
   Date("=first EZ2");
   Date("=last EZ2");
   Date("=first EZ3");
  };
 };
};
Phase("environmental calculations")
{
 Phase("Zone durations within profiles")
 {
  Phase("M1")
  {
   Difference("EZ1 M1", "=start seasonal flooding M1", "=onset organics M1");
   Difference("EZ2 M1", "=onset fen carr M1", "=start seasonal flooding M1");
  };
  Phase("3178")
  {
   Difference("EZ1 3178", "=start seasonal flooding 3178", "=onset organics 3178");
   Difference("EZ2 3178", "=SUERC-65223", "=start seasonal flooding 3178");
  };
  Phase("CII")
  {
   Difference("EZ1 CII", "=start seasonal flooding CII", "=onset organics CII");
   Difference("EZ2 CII", "=onset fen carr CII", "=start seasonal flooding CII");
  };
  Phase("DCS")
  {
   Difference("EZ1 DCS", "=start seasonal flooding DCS", "=onset organics DCS");
   Difference("EZ2 DCS", "=onset fen carr DCS", "=start seasonal flooding DCS");
  };
 };
 Phase("variations within transitions")
 {
  Phase("onset organics (start Environmental Zone 1)")
  {
   Difference("OO M1 3178", "=onset organics 3178", "=onset organics M1");
   Difference("OO M1 CII", "=onset organics CII", "=onset organics M1");
   Difference("OO M1 DCS", "=onset organics DCS", "=onset organics M1");
   Difference("OO 3178 CII", "=onset organics CII", "=onset organics 3178");
   Difference("OO 3178 DCS", "=onset organics DCS", "=onset organics 3178");
   Difference("OO CII DCS", "=onset organics DCS", "=onset organics CII");
  };
  Phase("start seasonal flooding (start Environmental Zone 2)")
  {
   Difference("SSF M1 3178", "=start seasonal flooding 3178", "=start seasonal flooding M1");
   Difference("SSF M1 CII", "=start seasonal flooding CII", "=start seasonal flooding M1");
   Difference("SSF M1 DCS", "=start seasonal flooding DCS", "=start seasonal flooding M1");
   Difference("SSF 3178 CII", "=start seasonal flooding CII", "=start seasonal flooding 3178");
```

```
  Difference("SSF 3178 DCS", "=start seasonal flooding DCS", "=start seasonal flooding 3178");
  Difference("SSF CII DCS", "=start seasonal flooding DCS", "=start seasonal flooding CII");
 };
 Phase("start fen carr (start Environmental Zone 3)")
 {
  Difference("SFC M1 3178", "=SUERC-65223", "=onset fen carr M1");
  Difference("SFC M1 CII", "=onset fen carr CII", "=onset fen carr M1");
  Difference("SFC M1 DCS", "=onset fen carr DCS", "=onset fen carr M1");
  Difference("SFC 3178 CII", "=onset fen carr CII", "=SUERC-65223");
  Difference("SFC 3178 DCS", "=onset fen carr DCS", "=SUERC-65223");
  Difference("SFC CII DCS", "=onset fen carr DCS", "=onset fen carr CII");
 };
};
Phase("Environmental Zone 1")
{
 Difference("EZ1 (minimum)", "first EZ2", "last EZ1");
 Difference("EZ1 (maximum)", "last EZ2", "first EZ1");
};
Phase("Environmental Zone 2")
{
 Difference("EZ2 (minimum)", "first EZ3", "last EZ2");
 Difference("EZ2 (maximum)", "last EZ3", "first EZ2");
};
Phase("transition durations")
{
 Difference("onset organics", "last EZ1", "first EZ1");
 Difference("start seasonal flooding", "last EZ2", "first EZ2");
 Difference("onset fen carr", "last EZ3", "first EZ3");
};
};
Order("onset reed peat")
{
 Date("=SUERC-36349");
 Date("=base of reed peat 3178");
 Date("=base of reed peat M1");
 Date("=base of reed peat CII");
};
Phase("base reed peat differences")
{
 Difference("SUERC-36349/CII", "base of reed peat CII", "SUERC-36349");
 Difference("SUERC-36349/3178", "base of reed peat 3178", "SUERC-36349");
 Difference("SUERC-36349/M1", "base of reed peat M1", "SUERC-36349");
};
};
```

Appendix 17.2: CQL2 code calculating additional parameters for Star Carr (using prior distributions calculated by the model defined in Appendix 17.1)

```
Options()
 {
  Resolution=1;
  kIterations=20000;
 };
 Phase("Star Carr additional calculations")
 {
  Phase("invoke priors")
  {
   Sequence("dummy")
   {
    R_Simulate("a", -9000, 50);
    R_Simulate("b", -9000, 50);
   };
   Prior("timber_46_","/timber_46_.prior");
   Prior("OxA_33574","/OxA_33574.prior");
   Difference("gap central platform/burnt area 318", "burnt_area_318", "central_platform");
   Difference("gap end wood scatter/central platform", "central_platform", "end_wood_scatter");
   Difference("start burning 1/central platform", "central_platform", "OxA_3349");
   Difference("reuse central", "central_platform", "OxA_33574");
   Difference("gap central/eastern platforms", "OxA_33662", "central_platform");
   Difference("gap eastern/western platforms", "western_platform", "OxA_33662");
   Difference("reuse western", "western_platform", "timber_46_");
  };
  Order("EZ3")
  {
   Prior("onset_fen_carr_CII","/onset_fen_carr_CII.prior");
   Prior("onset_fen_carr_DCS","/onset_fen_carr_DCS.prior");
   Prior("onset_fen_carr_M1","/onset_fen_carr_M1.prior");
   Prior("SUERC_65223","/SUERC_65223.prior");
  };
  Phase("human activity at Star Carr")
  {
   Prior("110553","/110553.prior");
   Phase("Mesolithic activity")
   {
    Prior("start_Star_Carr","/start_Star_Carr.prior");
    Phase("Mesolithic activity at Star Carr")
    {
     Phase("burning episodes in M1")
     {
      Prior("OxA_3349","/OxA_3349.prior");
      Prior("end_of_burning_1","/end_of_burning_1.prior");
      Prior("start_of_burning_2","/start_of_burning_2.prior");
      Prior("end_of_burning_2","/end_of_burning_2.prior");
      Prior("burning_3","/burning_3.prior");
     };
     Phase("detrital wood scatter")
     {
      Prior("start_wood_scatter","/start_wood_scatter.prior");
```

```
 Prior("end_wood_scatter","/end_wood_scatter.prior");
};
Phase("brushwood")
{
 Prior("start_brushwood","/start_brushwood.prior");
 Prior("end_brushwood","/end_brushwood.prior");
};
Phase("platforms")
{
 Prior("central_platform","/central_platform.prior");
 Prior("OxA_33662","/OxA_33662.prior");
 Prior("western_platform","/western_platform.prior");
};
Phase("Clark's deposition area")
{
 Prior("start_Clark_area","/start_Clark_area.prior");
 Prior("end_Clark_area","/end_Clark_area.prior");
};
Phase("birch bark rolls in reed peat in Clark's deposition area")
{
 Prior("start_reed_peat_in_Clark_area","/start_reed_peat_in_Clark_area.prior");
 Prior("end_human_in_reed_peat_in_Clark_area","/end_human_in_reed_peat_in_Clark_area.prior");
};
Phase("peat over marl")
{
 Prior("start_peat_over_marl","/start_peat_over_marl.prior");
 Prior("end_peat_over_marl","/end_peat_over_marl.prior");
};
Phase("fint N of CIII")
{
 Prior("start_N_of_CIII","/start_N_of_CIII.prior");
 Prior("end_N_of_CIII","/end_N_of_CIII.prior");
};
Phase("dispersed episodes at lake edge")
{
 Prior("burnt_area_318","/burnt_area_318.prior");
 Prior("OxA_25240","/OxA_25240.prior");
 Prior("SUERC_59177","/SUERC_59177.prior");
 Prior("SC22_scatter","/SC22_scatter.prior");
 Prior("TPQ_fen_flint","/TPQ_fen_flint.prior");
};
Phase("dryland activity")
{
 Phase("eastern dryland structure")
 {
  Prior("start_east_structure","/start_east_structure.prior");
  Prior("end_east_structure","/end_east_structure.prior");
 };
 Phase("western dryland structure")
 {
  Prior("start_west_structure","/start_west_structure.prior");
  Prior("end_west_structure","/end_west_structure.prior");
 };
```

```
    Phase("activity around central dryland structure")
    {
     Phase("post-hole 338")
     {
      Prior("SUERC_65240","/SUERC_65240.prior");
      Prior("OxA_33702","/OxA_33702.prior");
     };
    };
   };
  };
  Prior("end_Star_Carr","/end_Star_Carr.prior");
 };
};
Phase("durations and intervals")
{
 Phase("durations")
 {
  Prior("use Star Carr","/use_Star_Carr.prior");
  Prior("duration_burning_1","/duration_burning_1.prior");
  Prior("duration_burning_2","/duration_burning_2.prior");
  Prior("use_wood_scatter","/use_wood_scatter.prior");
  Prior("use_brushwood","/use_brushwood.prior");
  Date("=gap central platform/burnt area 318");
  Prior("gap_eastern_platform_fallen_tree","/gap_eastern_platform_fallen_tree.prior");
  Prior("gap_western_platform_bark_mat","/gap_western_platform_bark_mat.prior");
  Prior("use_Clark_area","/use_Clark_area.prior");
  Prior("use_east_structure","/use_east_structure.prior");
  Prior("use_west_structure","/use_west_structure.prior");
 };
 Phase("intervals")
 {
  Prior("gap_110553","/gap_110553.prior");
  Prior("end_burning_1_start_burning_2","/end_burning_1_start_burning_2.prior");
  Prior("end_burning_2_burning_3","/end_burning_2_burning_3.prior");
  Date("=gap end wood scatter/central platform");
  Date("=start burning 1/central platform");
  Date("=reuse central");
  Date("=gap central/eastern platforms");
  Date("=gap eastern/western platforms");
  Date("=reuse western");
 };
};
};
```